



**INSTITUTO POTOSINO DE INVESTIGACIÓN
CIENTÍFICA Y TECNOLÓGICA, A.C.**

POSGRADO EN CIENCIAS APLICADAS

**Métodos Matemáticos de Factorización y una Aproximación por
Retroalimentación para Sistemas Biológicos (Mathematical Methods
of Factorization and a feedback approach for biological systems)**

Tesis que presenta

Octavio Cornejo Pérez

Para obtener el grado de

Doctor en Ciencias Aplicadas

En la opción de

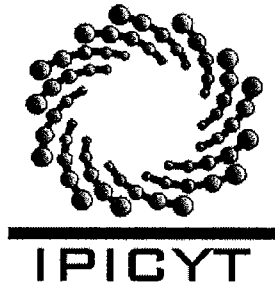
Control y Sistemas Dinámicos

Codirectores de la Tesis:

Dr. Alejandro Ricardo Femat Flores

Dr. Haret-Codratian Rosu Barbus

San Luis Potosí, S.L.P., Septiembre de 2005.



Instituto Potosino de Investigación Científica y Tecnológica, A.C.

Acta de Examen de Grado

COPIA CERTIFICADA

El Secretario Académico del Instituto Potosino de Investigación Científica y Tecnológica, A.C., certifica que en el Acta 001 del Libro Primero de Actas de Exámenes de Grado del Programa de Doctorado en Ciencias Aplicadas en la opción de Control y Sistemas Dinámicos está asentado lo siguiente:

En la ciudad de San Luis Potosí a los 20 días del mes de septiembre del año 2005, se reunió a las 15:00 horas en las instalaciones del Instituto Potosino de Investigación Científica y Tecnológica, A.C., el Jurado integrado por:

Dr. José Socorro García Díaz	Presidente	UGTO
Dr. Alejandro Ricardo Femat Flores	Secretario	IPICYT
Dr. Haret-Codratian Rosu Barbus	Sinodal	IPICYT
Dr. José Elías Pérez López	Sinodal externo	UASLP
Dr. Marco Antonio Reyes Santos	Sinodal externo	UGTO
Dr. Román López Sandoval	Sinodal	IPICYT

a fin de efectuar el examen, que para obtener el Grado de:

**DOCTOR EN CIENCIAS APLICADAS
EN LA OPCIÓN DE CONTROL Y SISTEMAS DINÁMICOS**

sustentó el C.

Octavio Cornejo Pérez

sobre la Tesis intitulada:

Métodos Matemáticos de Factorización y una Aproximación por Retroalimentación para Sistemas Biológicos (Mathematical Methods of Factorization and a feedback approach for biological systems)

que se desarrolló bajo la dirección de

Dr. Alejandro Ricardo Femat Flores
Dr. Haret-Codratian Rosu Barbus

El Jurado, después de deliberar, determinó

APROBARLO

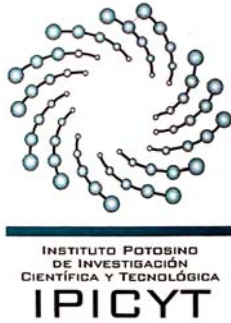
Dándose por terminado el acto a las 17:35 horas, procediendo a la firma del Acta los integrantes del Jurado. Dando fé el Secretario Académico del Instituto.

A petición del interesado y para los fines que al mismo convengan, se extiende el presente documento en la ciudad de San Luis Potosí, S.L.P., México, a los 20 días del mes septiembre de 2005.


Dr. Marcial Bernal Marín
Secretario Académico




Mtra. Ma. Elisa Lucio Aguilar
Jefa del Departamento de Asuntos Escolares



Instituto Potosino de Investigación Científica y Tecnológica, A.C.

División de Matemáticas Aplicadas y Sistemas Computacionales

Doctorado en Ciencias Aplicadas, Opción Terminal: Control y Sistemas Dinámicos

M. F. Octavio Cornejo Pérez

Jurado Examinador:

Dr. J. Socorro García Díaz
Presidente

Dr. A. Ricardo Femat Flores
Secretario

Dr. Haret C. Rosu Barbus
Sinodal

Dr. Marco A. Reyes Santos
Sinodal

Dr. J. Elías Pérez López
Sinodal

Dr. Román López Sandoval
Sinodal

San Luis Potosí, S. L. P., 20 de Septiembre de 2005.



INSTITUTO POTOSINO
DE INVESTIGACIÓN
CIENTÍFICA Y TECNOLÓGICA, A.C.

IPICYT

Núm. 001

Nombre del Sustentante:

OCTAVIO

CORNEJO

PEREZ



Octavio Cornejo Pérez
Firma

Acta de Examen de Grado

En la ciudad de San Luis Potosí, a los 20 días, del mes de SEPTIEMBRE del año 2005, se reunió a las 15:00 horas, en las instalaciones del Instituto Potosino de Investigación Científica y Tecnológica, A.C., el Jurado integrado por:

<u>DR. JOSE SOCORRO GARCIA DIAZ</u>	<u>PRESIDENTE</u>
<u>DR. ALEJANDRO RICARDO FEMAT FLORES</u>	<u>SECRETARIO</u>
<u>DR. HARET-CODRATIAN ROSU BARBUS</u>	<u>SINODAL</u>
<u>DR. JOSE ELIAS PEREZ LOPEZ</u>	<u>SINODAL</u>
<u>DR. MARCO ANTONIO REYES SANTOS</u>	<u>SINODAL</u>
<u>DR. ROMAN LOPEZ SANDOVAL</u>	<u>SINODAL</u>

a fin de efectuar el examen, que para obtener el Grado de Doctor (a) en Ciencias Aplicadas en la opción de Control y Sistemas Dinámicos, sustentó el (la)

c. OCTAVIO CORNEJO PEREZ

sobre la Tesis intitulada: MÉTODOS MATEMÁTICOS DE FACTORIZACIÓN Y UNA APROXIMACIÓN POR RETROALIMENTACIÓN PARA SISTEMAS BIOLÓGICOS

que se desarrolló bajo la dirección de:

DR. ALEJANDRO RICARDO FEMAT FLORES
DR. HARET-CODRATIAN ROSU BARBUS

El Jurado, después de deliberar, determinó:

A PROBARLO

Dándose por terminado el acto a las 17:35 horas, procediéndose a la firma del Acta por los integrantes del Jurado. Dando fe el Secretario Académico del Instituto.

Presidente

Secretario

Sinodal

Sinodal

Sinodal

Acknowledgments

I am grateful to my parents, brothers and close relatives for their permanent support not only during my doctoral studies but also during all my life till now.

I am also very grateful to my thesis advisors, Dr. Haret C. Rosu Barbus and Dr. Ricardo Femat for everything I have learned from them and for their support, collaboration and friendship.

I thank Drs. J. Socorro García-Díaz, Román López-Sandoval, Elías Pérez-López and Marco A. Reyes-Santos, for their kindness and availability for reviewing this document, as well as for their comments and useful remarks on the present work that helped me to improve it.

I would like to acknowledge the authorities of IPICYT for the excellent working conditions that allowed me to achieve good progress in my doctoral investigations.

Last but not the least, I would like to thank all my IPICYT friends from all the areas of research. Special mentions go to Eugenia (Maru), Luis Adolfo (my Brother), Pánfilo (the Sevillian Panfilote) and Vrani (the Dane).

And of course nothing would have been possible without the financial support from CONACYT.

To all the people and institutions I mentioned here, once again Thank You.

Octavio

Abstract

This thesis presents the original results I have obtained during the three-year doctoral period in the División de Matemáticas Aplicadas y Sistemas Computacionales (DMASC) of the Instituto Potosino de Investigación Científica y Tecnológica (IPICYT), in San Luis Potosí, México. These results have been obtained under supervision and collaboration of Dr. Haret C. Rosu in what refers to the first part of the thesis, and of Dr. Ricardo Femat for the second part.

The first part deals with some types of factorization methods that we were able to develop and that lead us to particular solutions of travelling kink type for reaction-diffusion equations and also to more general nonlinear differential equations of interest in biology and nonlinear physics. We also applied supersymmetric approaches in the context of biological dynamics of microtubules and the related transport properties associated to their domain walls. In addition, a complex supersymmetric extension of the classical harmonic oscillator by which we obtain new oscillatory modes has been developed; results that could be extended to physical optics and the physics of cavities. Moreover, an application to chemical physics of diatomic molecules using supersymmetric and factorization procedures is developed.

The second part contains a detailed study on the synchronization of the chaotic dynamics of two Hodgkin-Huxley neurons, by means of the mathematical tools belonging to the geometrical control theory. Despite using different parameters for each of the two neurons our analysis shows that synchronization states are achieved. The synchronization is attained by the feedback structure of the interconnection (coupling). Numerical results for the obtained neuronal dynamical states are displayed.

Resumen

Esta tesis presenta los resultados originales que he obtenido durante los tres años de periodo doctoral en la División de Matemáticas Aplicadas y Sistemas Computacionales (DMASC) del Instituto Potosino de Investigación Científica y Tecnológica (IPICYT), en San Luis Potosí, México. Estos resultados se han obtenido bajo la supervisión y colaboración del Dr. Haret C. Rosu en lo referente a la primera parte de tesis, y del Dr. Ricardo Femat para la segunda parte.

La primera parte trata con algunos métodos de factorización que fuimos capaces de desarrollar y que nos condujeron a soluciones particulares del tipo *kink* viajeras para ecuaciones de reacción-difusión y también para ecuaciones diferenciales no lineales más generales de interés en biología y física no lineal. Se aplicaron también técnicas de supersimetría en el contexto de dinámica biológica de microtúbulos y las propiedades de transporte asociadas a sus paredes de dominio. En adición, se desarrolló una extensión supersimétrica compleja del oscilador armónico clásico por el cual obtuvimos nuevos modos de oscilación; resultados que pueden extenderse a óptica física y la física de cavidades. Además, se desarrolló una aplicación a la fisico-química de moléculas diatómicas usando procedimientos de supersimetría y de factorización.

La segunda parte contiene un estudio referente a sincronización de la dinámica caótica de dos neuronas Hodgkin-Huxley, en donde se han aplicado los métodos matemáticos pertenecientes a la teoría de control geométrico. Aunque se han utilizado diferentes parámetros para cada una de las dos neuronas, nuestro estudio muestra que se obtienen estados dinámicos de sincronización. La sincronización se logra por la estructura de retroalimentación de la interconexión (acoplamiento). Se muestran los resultados numéricos para los estados de dinámica neuronal obtenidos.

Preface

Scientific research and technological progress are important characteristics of the modern world. They represent fundamental activities that can help mankind to understand and transform nature with the purpose of improving standards of life. Almost three years have past since I started my doctoral degree activity with the hope to contribute myself to the worldwide scientific knowledge. The lines of research I chose were on the border between mathematics and biology because I was convinced that the interdisciplinary activity is very rewarding and could give me better perspectives.

The doctoral thesis consists of four parts, of which the first contains five chapters and is devoted to factorization methods of differential equations and their applications in biology and physics, whereas the second part is divided in two chapters and deals with the synchronization phenomena as studied in neuronal ensembles. The thesis ends up with a final conclusion and the bibliography presented in Parts III and IV, respectively.

The first chapter is a general presentation of the factorization methods for linear second order differential equations. Also, the organization for Part I of the thesis is presented.

The second chapter contains an original result for performing factorizations of second order differential equations with polynomial nonlinearities that has been reported in a paper published in Physical Review E in 2005. At the same time the novel procedure allows to obtain particular solutions of travelling kink type in a very efficient way.

The third chapter presents more applications of the method to more complicated nonlinear differential equations. The results of this chapter are published in Progress of Theoretical Physics in 2005.

In the fourth chapter, I included the results of a supersymmetric factorization model

in the context of microtubules that we published in Physics Letters A in 2003.

The fifth chapter refers to the original results that have been published in Journal of Physics A in December of 2004. A complex extension to the classical harmonic oscillator based on a supersymmetric factorization procedure that has been applied before in particle physics is introduced in this chapter. The application of the same method to the case of Morse potential, a well-known exactly solvable problem in quantum mechanics with many applications in the physics and chemistry of diatomic molecules is also included here; these results are published in Revista Mexicana de Física, 2005.

With the sixth chapter starts the second part of the thesis. Some remarks on the kink type results obtained through factorization methods in the first part for pulse propagation along neuron axons, and the connection with the synchronization dynamics of a minimal ensemble of two neurons, employing nonlinear control theory are presented.

In the seventh chapter, we focus first on synchronization phenomena from the standpoint of their role and importance in natural and technical systems. The concept of chaos and the presence of chaotic behavior in nature are also described. Next, synchronization methods for the control of chaos and their applications in biological systems are shortly reviewed. The problem of the synchronization of two Hodgkin-Huxley (HH) neurons is emphasized because of its possible implications in the dynamical processes of the brain. A brief discussion of the widely known HH mathematical model of the neuron is given. Also, in the Introduction section, the organization of Chapters 7 and 8 belonging to Part II of the thesis is presented.

In the eighth chapter, numerical results for the synchronized dynamics of two HH neurons are presented. The mathematical methods employed belong to the theory of geometrical nonlinear control and are used with the goal of studying the synchronization of two HH neurons that are unidirectionally coupled. These results are published in Chaos, Solitons and Fractals in July 2005.

The order of published papers in this thesis is the following:

Chapter 2. H.C. Rosu, O. Cornejo-Pérez, *Supersymmetric pairing of kinks for polynomial nonlinearities*, Phys. Rev. E **71**, 046607 (2005).

Chapter 3. O. Cornejo-Pérez, H.C. Rosu, *Nonlinear second order ODE's: factorizations and particular solutions*, Prog. Theor. Phys. **114**, 533 (2005).

Chapter 4. H.C. Rosu, J.M. Morán-Mirabal, O. Cornejo, *One-parameter nonrelativistic supersymmetry for microtubules*, Phys. Lett. A **310**, 353 (2003).

Chapter 5. H.C. Rosu, O. Cornejo-Pérez, R. López-Sandoval, *Classical harmonic oscillator with Dirac-like parameters and possible applications*, J. Phys. A **37**,

11699 (2004). O. Cornejo-Pérez, R. López-Sandoval, H.C. Rosu, *Riccati nonhermiticity with application to the Morse potential*, Rev. Mex. Fís. **51**, 316 (2005).

Chapter 8. O. Cornejo-Pérez, R. Femat, *Unidirectional synchronization of Hodgkin-Huxley neurons*, Chaos, Solitons and Fractals **25**, 43 (2005).

Contents

I	FACTORIZATION METHODS	5
1	Factorization techniques for linear second order differential equations	6
1.1	Introduction	6
1.2	Darboux covariance	9
1.3	The Mielnik construction	11
1.4	The connection with intertwining	12
2	A new factorization technique for differential equations with polynomial nonlinearity	14
2.1	Introduction	14
2.2	Generalized Fisher equation	17
2.3	Equations of the Dixon-Tuszyński-Otwinowski type	22
2.4	FitzHugh-Nagumo equation	23
2.5	Conclusion of the chapter	25
3	Application to more general nonlinear differential equations	26
3.1	Introduction	26
3.2	Modified Emden equation	27
3.3	Generalized Lienard equation	30
3.4	Convective Fisher equation	32
3.5	Generalized Burgers-Huxley equation	33
3.6	Conclusion of the chapter	37
4	One-parameter supersymmetry for microtubules	38
4.1	Introduction	38

4.2	Caticha's supersymmetric model as applied to MTs	39
4.3	The Mielnik extension	40
4.4	Conclusion of the chapter	41
5	Supersymmetric method with Dirac parameters	46
5.1	Introduction	46
5.2	Classical harmonic oscillator: The Riccati approach	47
5.3	Matrix formulation	48
5.4	Extension through parameter K	49
5.5	More K parameters	50
5.6	Possible applications of the K -modes	52
5.7	Quantum mechanics with Riccati nonhermiticity	57
5.8	Complex extension with a single K parameter	58
5.9	Complex extension with parameters K and K'	59
5.10	Application to the Morse potential	59
5.11	Conclusion of the chapter	62
II	SYNCHRONIZATION METHODS	64
6	Preliminary remarks on Part II	65
7	Synchronization of chaotic dynamics and neuronal systems	66
7.1	Introduction	66
7.2	Synchronization methods for the control of chaos	67
7.3	Applications of synchronization methods in biological systems . .	68
7.4	Synchronized dynamics of neurons	68
7.5	The Hodgkin-Huxley model of the neuron	69
8	Unidirectional synchronization of Hodgkin-Huxley neurons	71
8.1	Introduction	71
8.2	The Hodgkin-Huxley system redefined	72
8.3	Synchronization problem statement	73
8.4	Synchronizing the Hodgkin-Huxley neurons	75
8.5	Generalized and robust synchronization	78
8.6	Conclusion of the chapter	82
III	CONCLUSION	85
9	Final conclusion	86
IV	BIBLIOGRAPHY	87

List of Figures

Fig. 2.1: The front of mutant genes (Fisher's wave of advance) in a population and the partner susy kink propagating with the same velocity. The axis are in arbitrary units.

Fig. 2.2: The polymerization kink of Portet, Tuszyński and Dixon [20] and the susy kink propagating with the same velocity.

Fig. 3.1: Real part for the factorization curve of the parameter $a_{1+} = a_{1+}(\alpha, \beta)$ that allows the factorization of Eq. (3.8). $a_1 \neq 0$. $\alpha \in [-10, 10]$ and $\beta \in [-10, 10]$.

Fig. 3.2: Imaginary part for the factorization curve of the parameter $a_{1+} = a_{1+}(\alpha, \beta)$ that allows the factorization of Eq. (3.8). $a_1 \neq 0$. $\alpha \in [-10, 10]$ and $\beta \in [-10, 10]$.

Fig. 3.3: Real part for the factorization curve of the parameter $E_+ = E_+(G, A)$ that allows the factorization of Eq. (3.23). Note that $a_1 = -\frac{E}{3}$; $E \neq 0$. $G \in [-10, 10]$ and $A \in [-10, 10]$.

Fig. 3.4: Imaginary part for the factorization curve of the parameter $E_+ = E_+(G, A)$ that allows the factorization of Eq. (3.23). $E \neq 0$. $G \in [-10, 10]$ and $A \in [-10, 10]$.

Fig. 3.5: Factorization curve of the parameter $v = v(\mu)$ that allows the factorization of Eq. (3.30). $a_1 = -\frac{\mu}{\sqrt{2}}$.

Fig. 3.6: Real part for the factorization curve of the parameter $a_{1+} = a_{1+}(\alpha, \beta, \delta = 1)$ that allows factorization of Eq. (3.35) with $\delta = 1$. $a_1 \neq 0$. $\alpha \in [-20, 20]$ and

$\beta \in [-20, 20]$.

Fig. 3.7: Imaginary part for the factorization curve of the parameter $a_{1+} = a_{1+}(\alpha, \beta, \delta = 1)$ that allows factorization of Eq. (3.35) with $\delta = 1$. $a_1 \neq 0$. $\alpha \in [-20, 20]$ and $\beta \in [-20, 20]$.

Fig. 3.8: Real part for the factorization curve of the parameter $e_{1+} = e_{1+}(\alpha, \beta, \delta = 1)$ that allows factorization of Eq. (3.35) with $\delta = 1$. $e_1 \neq 0$. $\alpha \in [-20, 20]$ and $\beta \in [-20, 20]$.

Fig. 3.9: Imaginary part for the factorization curve of the parameter $e_{1+} = e_{1+}(\alpha, \beta, \delta = 1)$ that allows factorization of Eq. (3.35) with $\delta = 1$. $e_1 \neq 0$. $\alpha \in [-20, 20]$ and $\beta \in [-20, 20]$.

Fig. 4.1: The Montroll asymmetric double-well potential (MDWP) calculated using Eq. (4.11) for $\varepsilon_0 = 0$. In all figures $\alpha_1 = 1$, $\alpha_2 = -1.5$, $\beta = -2.5/\sqrt{2}$, $\gamma = -0.5$, $\varepsilon = 0.1$.

Fig. 4.2: The Montroll ground state wave function of Eq. (4.9) for $\phi_0(0) = 1$.

Fig. 4.3: The one-parameter Darboux modified MDWP for $\lambda = 1$.

Fig. 4.4: The low-scale left hand side of the singularity.

Fig. 4.5: The low-scale right hand side of the singularity.

Fig. 4.6: The wave functions for $\lambda = 1$.

Fig. 4.7: One parameter Darboux-modified MDWP for $\lambda = 10$.

Fig. 4.8: The bottom of the potential at the right hand side.

Fig. 4.9: The ground state wave function corresponding to $\lambda = 10$.

Fig. 4.10: Plot of the integral $I_M(\xi)$ that produces the deformation of the potential and wave functions.

Fig. 5.1: The real part of the bosonic mode $w_2^+(y; \frac{1}{2}, \frac{1}{2})$ for $t \in [0, 10]$ and $K \in [0, 4]$.

Fig. 5.2: The imaginary part of the bosonic mode $w_2^+(y; \frac{1}{2}, \frac{1}{2})$ for $t \in [0, 10]$ and $K \in [0, 4]$.

Fig. 5.3: The real part of the bosonic mode $w_2^+(y; \frac{1}{2}, \frac{1}{2})$ for $t \in [0, 20]$ and $K = 0.01$.

Fig. 5.4: The imaginary part of the bosonic mode $w_2^+(y; \frac{1}{2}, \frac{1}{2})$ for $t \in [0, 20]$ and $K = 0.01$.

Fig. 5.5: The real part of the bosonic mode $w_2^+(y; \frac{1}{2}, \frac{1}{2})$ for $t \in [0, 20]$ and $K = 2$.

Fig. 5.6: The real part of the bosonic mode $w_2^+(y; \frac{1}{2}, \frac{1}{2})$ for $t \in [0, 20]$ and $K = 2$ in the vertical strip $[-0.5, 0.5]$.

Fig. 5.7: The imaginary part of the bosonic mode $w_2^+(y; \frac{1}{2}, \frac{1}{2})$ for $t \in [0, 20]$ and $K = 2$.

Fig. 5.8: The fermionic zero mode $-1/\cos t$, (red curve), and the real part of $-1/w_2^+$, (blue curve), for $K = 0.01$.

Fig. 5.9: The fermionic zero mode $-1/\cos t$, (red curve), and the imaginary part of $-1/w_2^+$, (blue curve), for $K = 2$.

Fig. 5.10: Real part of the bosonic wave function w_2 in the range $x \in [0, 3]$ and $K \in [0, 2]$.

Fig. 5.11: Imaginary part of the bosonic wave function w_2 in the range $x \in [0, 3]$ and $K \in [0, 2]$.

Fig. 5.12: Real part of the fermionic wave function w_1 in the range $x \in [0, 3]$ and $K \in [0, 2]$.

Fig. 5.13: Imaginary part of the fermionic wave function w_1 in the range $x \in [0, 3]$ and $K \in [0, 2]$.

Fig. 8.1: Spiking patterns of the master (solid line) and slave (dashed line) systems for the action potentials in desynchronized and synchronized states. The forcing functions amplitud and frequency parameters as specified in the text: $I_{ext_M}(t) = -2.58\sin(.245t)$, $I_{ext_S}(t) = -3.15\sin(.715t)$.

Fig. 8.2: Dynamical response of the implemented control action of Fig 8.1.

Fig. 8.3: Phase locking of the synchronized action potentials of Fig 8.1.

Fig. 8.4: Spiking patterns of the master (solid line) and slave (dashed line) systems for the action potentials in desynchronized state and the transition to a robust synchronization state when the modified feedback control law is implemented. The forcing functions are $I_{ext_M}(t) = -2.58\sin(.245t)$, $I_{ext_S}(t) = -3.15\sin(.715t)$.

Fig. 8.5: Dynamical response of the implemented modified control law of Fig 8.4.

Fig. 8.6: Phase locking of the action potentials in robust synchronization state of Fig 8.4.

Part I

FACTORIZATION METHODS

Factorization techniques for linear second order differential equations

1.1 Introduction

Factorization methods are powerful yet simple algebraic procedures to find eigenspectra and eigenfunctions of differential operators that avoid "cumbersome transformations, recourse to the ready-made equipment of the mathematical warehouse or expansion into power series", to cite from the very first paragraph of the 1940's papers of Schrödinger [1]. At the present time, one can find in the literature very good informative review papers on the factorization topics [2, 3]. It is now well known that for second-order linear differential operators, the factorizations are equivalent to their Darboux isospectrality (or covariance) and also they represent a simple form of intertwining [3]. In this introduction, we will touch upon both these issues.

In the case of Sturm-Liouville operators, E. Schrödinger first developed a factorization method he called "that of adjoint first order operators" in 1940-1941 [1], during the period he lived in Dublin. In his very first paper on the method, Schrödinger deals with four cases: the Planck (harmonic) oscillator, the nonrelativistic hydrogen atom, the spherical harmonics in the three-dimensional hypersphere, and the Kepler motion in the hypersphere.

For the quantum harmonic oscillator, he wrote the amplitude equation

$$\frac{d^2\psi}{dx^2} - x^2\psi + \lambda\psi = 0, \quad (1.1)$$

and noticed that it can be written in two different factorized forms

$$\begin{aligned} \left(\frac{d}{dx} - x\right) \left(\frac{d}{dx} + x\right) \psi + (\lambda - 1)\psi &= 0, \\ \left(\frac{d}{dx} + x\right) \left(\frac{d}{dx} - x\right) \psi + (\lambda + 1)\psi &= 0. \end{aligned}$$

Operating on one of these equations with the second of the two first order differential operators which occur in it, one gets for the function which results from ψ by applying that operator an equation of the *other* type, but with $\lambda + 2$ or $\lambda - 2$, respectively, instead of λ . The mutual adjointness of the two first order linear operators maintains the quadratic integrability of the solutions and furthermore the whole spectrum can be obtained by repeated application of the adjoint operator to the $\lambda = 1$ solutions of the partner operators, e.g.,

$$\left(\frac{d}{dx} + x\right) \psi_v^+ = 0 \quad \Rightarrow \quad \psi_v^+ = e^{-\frac{x^2}{2}} \quad (1.2)$$

leads to the odd eigenfunctions in the form

$$\psi_{2n-1} = \left(\frac{d}{dx} - x\right)^n \psi_v^+, \quad (1.3)$$

whereas the even eigenfunctions are obtained similarly from the function ψ_v^- . In his last paper on the method [4], Schrödinger factorized the hypergeometric equation, finding that there are several ways of factorizing it. His factorization procedure originated "from a, virtually, well-known treatment of the oscillator", i.e., an approach that can be traced back to Dirac's creation and annihilation operators for the harmonic oscillator [5] and to older factorization ideas in a paper of Pauli [6] and in Weyl's treatment of spherical harmonics with spin [7]. It should be noted that whereas Dirac's first-order operators were considered only as a trick (or 'stratagem'), too insignificant to replace the Sturm-Liouville theory, Schrödinger speaks neatly about a method and applies it in a systematic way. However, Schrödinger's works were not very much taken into account perhaps because of the war years.

A decade later, in 1951, Infeld and Hull [8] wrote an influential paper in which they introduced a different factorization method that became widely known. They studied equations of the form

$$[\hat{M}(x, m) + \lambda_n^0] y_{n-m}^m(x) = 0,$$

where $\hat{M}(x, m)$ is an operator of the form

$$\hat{M}(x, m) = \frac{d^2}{dx^2} + r(x, m)$$

and $m = 1, 2, \dots, n$ plays the role of a parameter in the potential, whereas the specific feature of their method is that the eigenvalue λ_n^0 is the same for all values of m . Infeld and Hull noticed that such equations can be written in two factorized forms

$$[-\hat{O}_+(m, m+1)\hat{O}_-(m+1, m) - L(m+1) + \lambda_n^0] y_{n-m}^m(x) = 0$$

and

$$[-\hat{O}_-(m, m-1)\hat{O}_+(m-1, m) - L(m) + \lambda_n^0] y_{n-m}^m(x) = 0.$$

The eigenfunctions of the neighboring operators $\hat{M}(x, m)$ and $\hat{M}(x, m \pm 1)$ are connected by the following relations

$$\hat{O}_+(m-1, m)y_{n-m}^m(x) = [\lambda_n^0 - L(m+1)]y_{n-m}^m(x)$$

and

$$\hat{O}_-(m+1, m)y_{n-m}^m(x) = y_{n-m+1}^{m-1}(x) .$$

In addition, the condition

$$\hat{O}_-(n+1, n)y_0^n(x) = 0$$

is satisfied leading to

$$\lambda_n^0 = L(n+1) .$$

The eigenfunctions $y_n^0(x)$ of the operator $\hat{M}(x, 0)$ can be obtained from $y_0^n(x)$ multiplicatively

$$y_n^0(x) = \hat{O}_+(0, 1)\hat{O}_+(1, 2)\dots\hat{O}_+(n-1, n)y_0^n(x) .$$

Nothing noteworthy happened for thirty years until Witten [9] wrote a paper on dynamical breaking of supersymmetry, in which supersymmetric quantum mechanics (SUSYQM) was introduced as a toy model for supersymmetry breaking in quantum field theories.

The SUSY breaking is presented by Witten as a sort of "phase transition" with the order parameter being the Witten index, defined as the grading operator $\tau = (-1)^{\hat{N}_f}$, where \hat{N}_f is the fermion number operator. For the case of one-dimensional SUSYQM, Witten's index operator is the third Pauli matrix σ_3 , which is +1 for the bosonic sector and -1 for the fermionic sector of the one dimensional quantum problem at hand. It became also quite common to call a particular Riccati solution as a (Witten) "superpotential". Papers that now are standard references are published during 1982-1984. For example, a breakthrough algebraic result has been obtained in 1983 by Gendenshtein [10] who introduced the important concept of *shape invariance* (SI) in SUSYQM. The SI property is displayed by some classes of potentials with respect to their parameter(s), say a_n , and reads

$$V_{n+1}(x, a_n) = V_n(x, a_{n+1}) + R(a_n) ,$$

where R should be a remainder independent of x . This property assures a fully algebraic scheme for the spectrum and wave functions. Fixing $E_0 = 0$, the excited spectrum is given by the algebraic formula

$$E_n = \sum_{k=2}^{n+1} R(a_k) ,$$

and the wave functions are obtained from

$$\psi_n(x, a_1) = \prod_{k=1}^n A^+(x, a_k)\psi_0(x, a_{n+1}) .$$

Another remarkable result of that period is due to Mielnik [11], who provided the first application of the *general* Riccati solution to the harmonic oscillator, obtaining a harmonic potential with an additive tail of the type $D^2[\text{Inerf} + \text{const.}]$ similar to the Abraham-Moses class of isospectral potentials in the area of inverse scattering. D. Fernández gave a second application to the atomic hydrogen spectrum, whereas M.M. Nieto clarified further the inverse scattering aspects of Mielnik's construction. Mielnik's procedure may be seen as a double Darboux transformation in which the general Riccati (superpotential) solution is involved. In addition, Andrianov and his collaborators [12] discovered the relation between SUSYQM and Darboux Transformations (DT) or Darboux covariance while playing with matrix Hamiltonians in SUSYQM.

1.2 Darboux covariance

The *Darboux covariance* of a Sturm-Liouville equation is clearly stated by Matveev and Salle [13]. Consider the equation

$$-\psi_{xx} + u\psi = \lambda \psi ,$$

and perform the following DT (denoted by $\psi[1], u[1]$)

$$\psi \rightarrow \psi[1] = (D - \sigma_1)\psi = \psi_x - \sigma_1\psi = \frac{W(\psi_1, \psi)}{\psi_1} ,$$

$$u \rightarrow u[1] = u - 2\sigma_{1x} = u - 2D^2 \ln \psi_1 ,$$

where

$$\sigma_1 = \psi_{1x} \psi_1^{-1}$$

is the sigma notation of Matveev and Salle for the logarithmic derivative, and W is the Wronskian determinant. Then, the Darboux-transformed equation becomes

$$-\psi_{xx}[1] + u[1]\psi[1] = \lambda \psi[1] ,$$

i.e., the spectral parameter λ does not change (a result known as Darboux isospectrality). When DTs are applied iteratively one gets Crum's result. One can also say that the two SL equations are related by a DT.

Following Matveev and Salle, in order to demonstrate the equivalence of SUSYQM with a single DT we consider two Schrödinger equations

$$-D^2\psi + u\psi = \lambda \psi ,$$

$$-D^2\phi + v\phi = \lambda \phi ,$$

related by DT, i.e., $v = u[1]$ and $\phi = \psi[1]$, and notice that the function $\phi_1 = \psi_1^{-1}$ satisfies the Darboux-transformed equation for $\lambda = \lambda_1$.

If now one uses the second (transformed) equation as initial one and perform the DT with the generating function ϕ_1 , one just goes back to the initial u equation. That is why one can think of the latter procedure as a sort of *inverse DT* that can be obtained from the direct one as follows:

$$u = v - 2D^2 \ln \phi_1 = v[-1] = v - 2D^2 \ln \psi_1^{-1} ,$$

$$\psi = \left(\phi_x - \frac{\phi_{1x}}{\phi_1} \phi \right) (\lambda_1 - \lambda) = \left(\phi_x + \frac{\psi_{1x}}{\psi_1} \phi \right) (\lambda_1 - \lambda) .$$

Using the sigma notation,

$$\sigma = \frac{\psi_{1x}}{\psi_1} = -\frac{\phi_{1x}}{\phi_1}$$

the Riccati (SUSYQM) representation of the Darboux pair of Schrödinger potentials is obtained

$$u = v[-1] = \sigma_x + \sigma^2 + \lambda_1 ,$$

$$v = u[1] = -\sigma_x + \sigma^2 + \lambda_1 .$$

It is now easy to enter the issue of SUSYQM concept of supercharge operators. For that, one employs the factorization operators

$$B^+ = -D + \sigma, \quad B^- = D + \sigma .$$

They effect the wave function part of the direct and inverse DT, respectively. Moreover,

$$B^+ B^- = -D^2 + v - \lambda_1 ,$$

$$B^- B^+ = -D^2 + u - \lambda_1 .$$

Thus, the commutator $[B^+, B^-] = v - u = -2D^2 \ln \psi_1$ gives the Darboux difference in the shape of the Darboux-related potentials. Introducing the Hamiltonian operators

$$H^+ = B^- B^+ + \lambda_1 ,$$

$$H^- = B^+ B^- + \lambda_1 ,$$

one can also interpret the B operators as factorization ones and write the famous matrix representation of SUSYQM, as well as the simplest possible superalgebra. The factorizing operators in matrix representation are called *supercharges* in SUSYQM, and are nilpotent operators

$$Q^- = A_- \sigma_+ = \begin{pmatrix} 0 & 0 \\ A^- & 0 \end{pmatrix}, \quad (Q^-)^2 = 0 ,$$

and

$$Q^+ = A_+ \sigma_- = \begin{pmatrix} 0 & A^+ \\ 0 & 0 \end{pmatrix}, \quad (Q^+)^2 = 0 .$$

$\sigma_- = \begin{pmatrix} 0 & 1 \\ 0 & 0 \end{pmatrix}$ and $\sigma_+ = \begin{pmatrix} 0 & 0 \\ 1 & 0 \end{pmatrix}$ are Pauli matrices. In this realization, the matrix form of the Hamiltonian operator reads

$$\mathcal{H} = \begin{pmatrix} A^+A^- & 0 \\ 0 & A^-A^+ \end{pmatrix} = \begin{pmatrix} H_- & 0 \\ 0 & H_+ \end{pmatrix},$$

defining the partner Hamiltonians as diagonal elements of \mathcal{H} . They are partners in the sense that they are isospectral, apart from the ground state $\phi_{gr,-}$ of H_- , which is not included in the spectrum of H_+ .

1.3 The Mielnik construction

An interesting possibility to build families of potentials *strictly* isospectral with respect to the initial (bosonic) one arises if one asks for the most general superpotential (i.e., the general Riccati solution) such that $V_+(x) = w_g^2 + \frac{dw_g}{dx}$, where V_+ is the fermionic partner potential. It is easy to see that one particular solution to this equation is $w_p = w(x)$, where $w(x)$ is the common Witten superpotential. One is led to consider the following Riccati equation $w_g^2 + \frac{dw_g}{dx} = w_p^2 + \frac{dw_p}{dx}$, whose general solution can be written in the form $w_g(x) = w_p(x) + \frac{1}{v(x)}$, where $v(x)$ is an unknown function. Using this ansatz, one obtains for the function $v(x)$ the following Bernoulli equation

$$\frac{dv(x)}{dx} - 2v(x)w_p(x) = 1, \quad (1.4)$$

that has the solution

$$v(x) = \frac{\mathcal{I}_0(x) + \mu}{u_0^2(x)}, \quad (1.5)$$

where $\mathcal{I}_0(x) = \int_c^x u_0^2(y) dy$, ($c = -\infty$ for full line problems and $c = 0$ for half line problems, respectively), and μ is an integration constant thereby considered as a free parameter. Thus, $w_g(x)$ can be written as follows

$$\begin{aligned} w_g(x; \mu) &= w_p(x) + \frac{d}{dx} \left[\ln(\mathcal{I}_0(x) + \mu) \right] \\ &= w_p(x) + \sigma_0(\lambda) \\ &= -\frac{d}{dx} \left[\ln \left(\frac{u_0(x)}{\mathcal{I}_0(x) + \mu} \right) \right]. \end{aligned} \quad (1.6)$$

Finally, one easily gets the $V_-(x; \mu)$ family of potentials

$$\begin{aligned}
V_-(x; \mu) &= w_g^2(x; \mu) - \frac{dw_g(x; \mu)}{dx} \\
&= V_-(x) - 2 \frac{d^2}{dx^2} \left[\ln(\mathcal{I}_0(x) + \mu) \right] \\
&= V_-(x) - 2\sigma_{0,x}(\mu) \\
&= V_-(x) - \frac{4u_0(x)u_0'(x)}{\mathcal{I}_0(x) + \mu} + \frac{2u_0^4(x)}{(\mathcal{I}_0(x) + \mu)^2}. \tag{1.7}
\end{aligned}$$

All $V_-(x; \mu)$ have the same supersymmetric partner potential $V_+(x)$ obtained by deleting the ground state. They are asymmetric double-well potentials that may be considered as a sort of intermediates between the bosonic potential $V_-(x)$ and the fermionic partner $V_+(x) = V_-(x) - 2\sigma_{0,x}(x)$. From the last rhs of Eq. (1.6) one can infer the ground state wave functions for the potentials $V_-(x; \mu)$ as follows

$$u_0(x; \mu) = f(\mu) \frac{u_0(x)}{\mathcal{I}_0(x) + \mu}, \tag{1.8}$$

where $f(\mu)$ is a normalization factor that can be shown to be of the form $f(\mu) = \sqrt{\mu(\mu + 1)}$. One can now understand the double Darboux feature of this construction by writing the parametric family in terms of their unique "fermionic" partner potential

$$V_-(x; \mu) = V_+(x) - 2 \frac{d^2}{dx^2} \ln \left(\frac{1}{u_0(x; \mu)} \right), \tag{1.9}$$

which shows that the Mielnik transformation is of the inverse Darboux type, allowing at the same time a two-step (double Darboux) interpretation, namely, in the first step one goes to the fermionic system and in the second step one returns to a deformed bosonic system.

An application of this construction to microtubules is presented in Chapter 4.

1.4 The connection with intertwining

Intertwining has been introduced by the French mathematician J. Delsarte in 1938 [14] as an operatorial relationship involving so-called transformation (or transmutation) operators but the second World War delayed the detailed mathematical studies that came only in the 1950's. By definition, two operators L_0 and L_1 are said to be intertwined by an operator T if

$$L_1 T = T L_0. \tag{1.10}$$

If the eigenfunctions φ_0 of L_0 are known, then from the intertwining relation one can show that the (unnormalized) eigenfunctions of L_1 are given by $\varphi_1 = T \varphi_0$. The

main problem in the intertwining transformations is to construct the transformation operator T . One-dimensional quantum mechanics is one of the simplest examples of intertwining relations since Witten's transformation operator $T_{qm} = T_1$ is just a first spatial derivative plus a differentiable coordinate function (the superpotential) that should be a logarithmic derivative of the true bosonic zero mode (if it exists), but of course higher-order transformation operators can be constructed without much difficulty.

Thus, within the realm of the one-dimensional quantum mechanics, writing $T_1 = D - \frac{u'}{u}$, where u is a true bosonic zero mode, one can infer that the adjoint operator $T_1^\dagger = -D - \frac{u'}{u}$ intertwines in the opposite direction, taking solutions of L_1 to those of L_0

$$\varphi_0 = T_1^\dagger \varphi_1 . \quad (1.11)$$

In particular, for standard one-dimensional quantum mechanics, $L_0 = H_-$ and $L_1 = H_+$ and although the true zero mode of H_- is annihilated by T_1 , the corresponding (unnormalized) eigenfunction of H_+ can nevertheless be obtained by applying T_1 to the other independent zero energy solution of H_- . It is only in the last decade or so, that the intertwining approach becomes well-known to the SUSYQM factorization community and some authors start to play with higher-order generalizations. But, as always, the most important (at least for standard quantum mechanics) are the simplest cases, namely the Darboux first-order intertwining operators.

The first part of this thesis deals with factorization methods, among which an original factorization of nonlinear second order ordinary differential equations (ODE) and supersymmetric techniques, as applied to some biological and physical systems. Chapters 2 and 3 contain explicitly the new factorization procedure developed by us to obtain kink type solutions for nonlinear second order ODE that describe several important processes, for instance, the tubulin polymerization in microgravity conditions and the pulse propagation along nerve axons. In Chapter 4, supersymmetric approaches are applied in the framework of biological dynamics of microtubules (MTs); the latter results are related to transport properties associated to the MT domain walls. In Chapter 5, applications of supersymmetric factorization procedures in some physical systems are presented. A complex extension for the classical harmonic oscillator by means of a direct relationship between the Dirac and Schrödinger equations is obtained. In addition, the same procedure is applied to a molecular physics problem in connection with the dissociation of diatomic molecules.

A new factorization technique for differential equations with polynomial nonlinearity

Abstract. In this chapter, it is shown how one can obtain kink solutions of ordinary differential equations with polynomial nonlinearities by an efficient factorization procedure *directly* related to the factorization of their nonlinear polynomial part. This is different of previous factorization procedures of differential equations of this type that have been performed by only a few authors, most notably by Berkovich [17]. Of main interest here because of their numerous applications are the reaction-diffusion equations in the travelling frame and the damped-anharmonic-oscillator equations. In addition, interesting pairing of the kink solutions, a result obtained by reversing the factorization brackets in the supersymmetric quantum mechanical style, are reported. In this way, one gets ordinary differential equations with a different polynomial nonlinearity possessing kink solutions of different width but propagating at the same velocity as the kinks of the original equation. This pairing of kinks could have many applications. The mathematical procedure is illustrated with several important cases, among which the generalized Fisher equation, the FitzHugh-Nagumo equation, and the polymerization fronts of microtubules (MTs). In the latter case, a new polymerization front is predicted that can show up in solutions containing MTs borne on satellites. Because of the microgravity conditions the polymerization rates could deviate from the normal ones and this could lead to a change of the width of the polymerization front.

2.1 Introduction

Factorization of second-order linear differential equations, such as the Schrödinger equation, is a well established method to get solutions in an algebraic manner [4, 8, 15]. We are interested in factorizations of ordinary differential equations (ODE) of the type

$$u'' + \gamma u' + F(u) = 0, \quad (2.1)$$

where $F(u)$ is a given polynomial in u . If the independent variable is the time then γ is a damping constant and we are in the case of nonlinear damped oscillator equations. Many examples of this type are collected in the Appendix of a paper of Tuszyński et al. [16]. However, the coefficient γ can also play the role of the constant velocity of a travelling front if the independent variable is a travelling coordinate used to reduce a reaction-diffusion (RD) equation to the ordinary differential form as briefly sketched in the following. These RD travelling fronts or kinks are important objects in low dimensional nonlinear phenomenology describing topologically-switched configurations in many areas of biology, ecology, chemistry and physics.

Consider a scalar RD equation for $u(x, t)$

$$\frac{\partial u}{\partial t} = \mathcal{D} \frac{\partial^2 u}{\partial x^2} + sF(u), \quad (2.2)$$

where \mathcal{D} is the diffusion constant and s is the strength of the reaction process. Eq (2.2) can be rewritten as

$$\frac{\partial u}{\partial t} = \frac{\partial^2 u}{\partial x^2} + F(u), \quad (2.3)$$

where the coefficients have been eliminated by the rescalings $\tilde{t} = st$ and $\tilde{x} = (s/\mathcal{D})^{1/2}x$, and dropping the tilde. Usually, the scalar RD equation possesses travelling wave solutions $u(\xi)$ with $\xi = x - vt$, propagating at speed v . For this type of solutions the RD equation turns into the ODE

$$u'' + vu' + F(u) = 0, \quad (2.4)$$

where $' = D = \frac{d}{d\xi}$. Eq. (2.4) has the same form as nonlinear damped oscillator equations with the velocity playing the role of the friction constant.

For applications in physical optics and acoustics it is convenient to write the travelling coordinate in the form $\xi = kx - \omega t = k(x - vt)$ with $k v = \omega$. This is a simple scaling by k of the previous coordinate turning Eq. (2.4) into the form

$$u'' + \frac{v}{k}u' + \frac{1}{k^2}F(u) = 0 \quad (2.5)$$

that can be changed back to the form of Eq. (2.1) by redefining $\tilde{\gamma} = \frac{v}{k}$ and $\tilde{F}(u) = \frac{1}{k^2}F(u)$.

In general, performing the factorization of Eq. (2.1) means the following

$$\left[D - f_2(u) \right] \left[D - f_1(u) \right] u = 0. \quad (2.6)$$

This leads to the equation

$$u'' - \frac{df_1}{du}uu' - f_1u' - f_2u' + f_1f_2u = 0. \quad (2.7)$$

The following groupings of terms are possible related to different factorizations:

a) *Berkovich grouping*: In 1992, Berkovich [17] proposed to group the terms as follows

$$u'' - (f_1 + f_2)u' + \left(f_1 f_2 - \frac{df_1}{du} u' \right) u = 0, \quad (2.8)$$

and furthermore discussed a theorem according to which any factorization of an ODE of the form given in Eq. (2.6) allows to find a class of solutions that can be obtained from solving the first-order differential equation

$$u' - f_1(u)u = 0. \quad (2.9)$$

Substituting the first-order ODE (2.9) in the Berkovich grouping one gets

$$u'' - (f_{1b} + f_{2b})u' + \left(f_{1b} f_{2b} - \frac{df_{1b}}{du} f_{1b} u \right) u = 0, \quad (2.10)$$

where we redefined $f_1(u) = f_{1b}(u)$ and $f_2(u) = f_{2b}(u)$ to distinguish this case from our proposal following next. For the specific form of the ODEs we consider here, Berkovich's conditions read

$$f_{1b} \left(-\gamma - f_{1b} - \frac{df_{1b}}{du} u \right) = \frac{F(u)}{u}, \quad (2.11)$$

$$f_{1b} + f_{2b} = -\gamma. \quad (2.12)$$

b) *Grouping of this work*: We propose here the different grouping of terms

$$u'' - \left(\frac{d\phi_1}{du} u + \phi_1 + \phi_2 \right) u' + \phi_1 \phi_2 u = 0 \quad (2.13)$$

that can be considered the result of changing the Berkovich factorization by setting $f_{1b}(u) = \phi_1(u)$ and $f_{2b}(u) \rightarrow \phi_2(u)$ under the conditions

$$\phi_1 \phi_2 = \frac{F(u)}{u}, \quad (2.14)$$

$$\phi_1 + \phi_2 + \frac{d\phi_1}{du} u = -\gamma. \quad (2.15)$$

The following simple relationship exists between the factoring functions:

$$\phi_2(u) = f_{2b}(u) - \frac{df_{1b}(u)}{du} u$$

and further (third, and so forth) factorizations can be obtained through linear combinations of the functions f_{1b} , f_{2b} and ϕ_2 .

Based on our experience, we think that the grouping we propose is more convenient than that of Berkovich and also of other people employing more difficult procedures. The main advantage resides in the fact that whereas in

Berkovich's scheme Eq. (2.11) is still a differential equation to be solved, in our scheme we make a choice of the factorization functions by merely factoring polynomial expressions according to Eq. (2.14) and then imposing Eq. (2.15) leads easily to an n -depending γ coefficient for which the factorization works. This fact makes our approach extremely efficient in finding particular solutions of the kink type as one can see in the following.

In the next section, it is shown on the explicit case of the generalized Fisher equation all the mathematical constructions related to the factorization brackets and their supersymmetric quantum mechanical like reverse factorization. In less detail, but within the same approach, damped nonlinear oscillators of Dixon-Tuszyński-Otwinowski type and the FitzHugh-Nagumo equation, are studied in Sections 2.3 and 2.4, respectively.

2.2 Generalized Fisher equation

Let us consider the generalized Fisher equation given by

$$u'' + \gamma u' + u(1 - u^n) = 0, \quad (2.16)$$

The case $n = 1$ refers to the common Fisher equation and it will be shortly discussed as a subcase. Eq. (2.14) allows to factorize the polynomial function

$$\phi_1 \phi_2 = \frac{F(u)}{u} = (1 - u^n) = (1 - u^{n/2})(1 + u^{n/2}),$$

Now, by choosing

$$\phi_1 = a_1(1 - u^{n/2}), \quad \phi_2 = \frac{1}{a_1}(1 + u^{n/2}), \quad a_1 \neq 0,$$

the explicit forms of a_1 and γ can be obtained from Eq. (2.15)

$$\frac{d\phi_1}{du} u + \phi_1 + \phi_2 = -\frac{n}{2} a_1 u^{n/2} + a_1(1 - u^{n/2}) + (1/a_1)(1 + u^{n/2}) = -\gamma.$$

Introducing the notation $h_n = (\frac{n}{2} + 1)^{1/2}$ one gets: $a_1 = \pm h_n^{-1}$, $\gamma = \mp (h_n + h_n^{-1})$. Then Eq. (2.16) becomes

$$u'' \pm (h_n + h_n^{-1}) u' + u(1 - u^n) = 0 \quad (2.17)$$

and the corresponding factorization is

$$\left[D \pm h_n(u^{n/2} + 1) \right] \left[D \mp h_n^{-1}(u^{n/2} - 1) \right] u = 0. \quad (2.18)$$

It follows that Eq. (2.17) is compatible with the first-order differential equation

$$u' \mp h_n^{-1} (u^{n/2} - 1) u = 0. \quad (2.19)$$

Integration of Eq. (2.19) gives for $\gamma > 0$

$$u_{>}^{\pm} = \left(1 \pm \exp \left[(h_n - h_n^{-1}) (\xi - \xi_0) \right]\right)^{-2/n}. \quad (2.20)$$

Rewritten in the hyperbolic form, we get

$$\begin{aligned} u_{>}^{+} &= \left(\frac{1}{2} - \frac{1}{2} \tanh \left[\frac{1}{2} (h_n - h_n^{-1}) (\xi - \xi_0) \right] \right)^{2/n}, \\ u_{>}^{-} &= \left(\frac{1}{2} - \frac{1}{2} \coth \left[\frac{1}{2} (h_n - h_n^{-1}) (\xi - \xi_0) \right] \right)^{2/n}. \end{aligned} \quad (2.21)$$

The $\tanh(\cdot)$ form is precisely the solution obtained long ago by Wang [18] and Hereman and Takaoka [19] by more complicated means.

Moreover, a different solution is possible for $\gamma < 0$

$$u_{<}^{\pm} = \left(1 \pm \exp \left[- (h_n - h_n^{-1}) (\xi - \xi_0) \right]\right)^{-2/n}, \quad (2.22)$$

or

$$\begin{aligned} u_{<}^{+} &= \left(\frac{1}{2} + \frac{1}{2} \tanh \left[-\frac{1}{2} (h_n - h_n^{-1}) (\xi - \xi_0) \right] \right)^{2/n}, \\ u_{<}^{-} &= \left(\frac{1}{2} + \frac{1}{2} \coth \left[-\frac{1}{2} (h_n - h_n^{-1}) (\xi - \xi_0) \right] \right)^{2/n}, \end{aligned} \quad (2.23)$$

respectively.

2.2.1 Reversion of factorization brackets without the change of the scaling factors

Choosing now $\phi_1 = a_1(1 + u^{n/2})$ and $\phi_2 = \frac{1}{a_1}(u^{n/2} - 1)$ leads to the same equation (2.17) but now with the factorization

$$\left[D \mp h_n(u^{n/2} - 1) \right] \left[D \pm h_n^{-1}(u^{n/2} + 1) \right] u = 0, \quad (2.24)$$

and therefore the compatibility is with the different first-order equation

$$u' \pm h_n^{-1}(u^{n/2} + 1) u = 0. \quad (2.25)$$

However, the direct integration gives the solution (for $\gamma > 0$)

$$\begin{aligned} u &= \left(-\frac{1}{1 \pm \exp[(h_n - h_n^{-1}) (\xi - \xi_0)]} \right)^{2/n} \\ &= (-1)^{2/n} \left(1 \pm \exp \left[(h_n - h_n^{-1}) (\xi - \xi_0) \right] \right)^{-2/n}, \end{aligned} \quad (2.26)$$

which are similar to the known solution Eq. (2.20). For $\gamma < 0$, solutions of the type given by Eq. (2.22) are obtained.

2.2.2 Direct reversion of factorization brackets

Let us perform now a direct inversion of the factorization brackets in (2.18) similar to what is done in supersymmetric quantum mechanics in order to enlarge the class of exactly solvable quantum hamiltonians

$$\left[D \mp h_n^{-1}(u^{n/2} - 1) \right] \left[D \pm h_n(u^{n/2} + 1) \right] u = 0. \quad (2.27)$$

Doing the product of differential operators the following RD equation is obtained

$$u'' \pm (h_n + h_n^{-1}) u' + u \left[1 + u^{n/2} \right] \left[1 - h_n^4 u^{n/2} \right] = 0. \quad (2.28)$$

Eq. (2.28) is compatible with the equation

$$u' \pm h_n \left(u^{n/2} + 1 \right) u = 0, \quad (2.29)$$

and integration of the latter gives the kink solution of Eq. (2.28)

$$u_{>}^{\pm} = \left(-\frac{1}{1 \pm \exp[(h_n^3 - h_n)(\xi - \xi_0)]} \right)^{\frac{2}{n}} = \left(1 \pm \exp \left[(h_n^3 - h_n)(\xi - \xi_0) \right] \right)^{-\frac{2}{n}} \quad (2.30)$$

for $\gamma > 0$. On the other hand, for $\gamma < 0$ the exponent is the same but of opposite sign. Hyperbolic forms of the latter solutions are easy to write down and are similar up to widths to Eqs. (2.21) and (2.23), respectively.

Thus, a different RD equation given by (2.28) with modified polynomial terms and its solution have been found by reverting the factorization terms of Eq. (2.17). Although the reaction polynomial is different the velocity parameter remains the same. The main result, which is a general one, that we find here is the following: *At the velocity corresponding to the travelling kink of a given RD equation there is another propagating kink corresponding to a different RD equation that is related to the original one by reverse factorization.* We can call this kink as the supersymmetric (susy) kink because of the mathematical construction.

Finally, one can ask if the process of reverse factorization can be continued with Eq. (2.28). It can be shown that this is not the case because Eq. (2.28) has already a discretized (polynomial-order-dependent) γ and this fact prevents further solutions of this type. Suppose we consider the following factorization functions

$$\tilde{\phi}_1 = \tilde{a}_1^{-1} \left[1 - h_n^4 u^{n/2} \right], \quad \tilde{\phi}_2 = \tilde{a}_1 \left(1 + u^{n/2} \right). \quad (2.31)$$

Then, one gets $\tilde{a}_1 = \pm h_n^3$ and solve $\tilde{a}_1^{-1} + \tilde{a}_1 = h_n^{-1} + h_n$. The solutions are: $n = 0$, which implies linearity, and $n = -4$, which leads to a Milne-Pinney equation. On the other hand, Eq. (2.28) with an arbitrary γ can be treated by the inverse factorization procedure to get the susy partner RD equation and its susy kink.

2.2.3 Subcase $n = 1$

This subcase is the original Fisher equation describing the propagation of mutant genes

$$\frac{\partial u}{\partial t} = \frac{\partial^2 u}{\partial x^2} + u(1 - u). \quad (2.32)$$

In the travelling frame, the Fisher equation has the form

$$u'' + \gamma u' + u(1 - u) = 0. \quad (2.33)$$

When the γ parameter takes the value $\gamma_1 = \frac{5}{6}\sqrt{6}$ (i.e., $h_1 = \frac{\sqrt{6}}{2}$) one can factor Fisher's equation and employing our method leads easily to the known kink solution

$$u_F = \frac{1}{4} \left(1 - \tanh \left[\frac{\sqrt{6}}{12} (\xi - \xi_0) \right] \right)^2 \quad (2.34)$$

that was first obtained by Ablowitz and Zeppetella [21] with a series solution method. On the other hand, the susy kink for this case reads

$$u_{F,\text{susy}} = \frac{1}{4} \left(1 - \tanh \left[\frac{\sqrt{6}}{8} (\xi - \xi_0) \right] \right)^2, \quad (2.35)$$

i.e., it has a width one and a half times greater than the common Fisher kink and is a solution of the partner equation

$$u'' + \frac{5\sqrt{6}}{6} u' + u \left(1 - \frac{5}{4} u^{1/2} - \frac{9}{4} u \right) = 0. \quad (2.36)$$

A plot of the kinks u_F and $u_{F,\text{susy}}$ is displayed in Fig. 1.

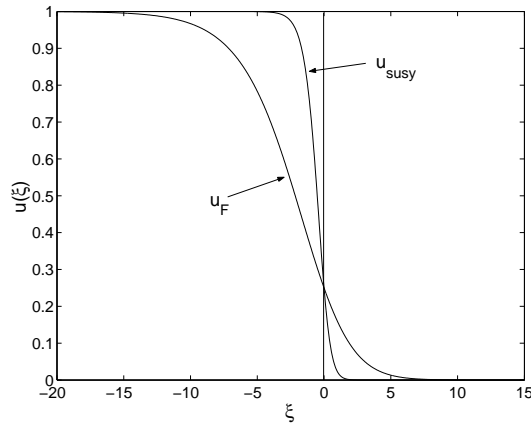


Fig. 2.1: The front of mutant genes (Fisher's wave of advance) in a population and the partner susy kink propagating with the same velocity. The axis are in arbitrary units.

2.2.4 Subcase $n = 6$

This subcase is of interest in the light of experiments on polymerization patterns of MTs in centrifuges. It has been discovered that the polymerization of the tubulin dimers proceeds in a kink-switching fashion propagating with a constant velocity within the sample. Portet, Tuszyński and Dixon [20] used RD equations to discuss the modification of self-organization patterns of MTs as well as the tubulin polymerization under the influence of reduced gravitational fields. They used the value $n = 6$ for the mean critical number of tubulin dimers at which the polymerization process starts and showed that the same nucleation number enters the polynomial term of the RD process for the number concentration c of tubulin dimers

$$c'' + \frac{5}{2}c' + c(1 - c^6) = 0. \quad (2.37)$$

The polymerization kink in their work reads

$$c_{\text{PTD}} = 2^{-\frac{1}{3}} \left(1 - \tanh \left[\frac{3}{4}(\xi - \xi_0) \right] \right)^{1/3}. \quad (2.38)$$

On the other hand, the susy polymerization kink (see Fig. (2.2)) of the form

$$c_{\text{susy}} = 2^{-\frac{1}{3}} \left(1 - \tanh[3(\xi - \xi_0)] \right)^{1/3} \quad (2.39)$$

can be taken into account according to the hyperbolic form of Eq. (2.30). It propagates with the same speed and corresponds to the equation

$$c'' \pm \frac{5}{2}c' + c(1 - 15c^3 - 16c^6) = 0. \quad (2.40)$$

In principle, this equation could be obtained as a consequence of modifying the kinetics steps in the microtubule polymerization process.

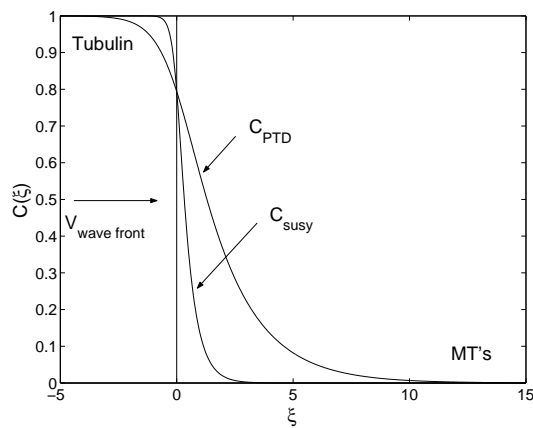


Fig. 2.2: The polymerization kink of Portet, Tuszyński and Dixon [20] and the susy kink propagating with the same velocity.

2.3 Equations of the Dixon-Tuszyński-Otwinowski type

In the context of damped anharmonic oscillators, Dixon et al. [22] studied equations of the type (in this section, we use $' = D_\tau = \frac{d}{d\tau}$)

$$u'' + u' + Au - u^{n-1} \equiv u'' + u' + u(\sqrt{A} - u^{\frac{n}{2}-1})(\sqrt{A} + u^{\frac{n}{2}-1}) = 0 \quad (2.41)$$

and gave solutions for the cases $A = \frac{2}{9}$ and $A = \frac{3}{16}$, with $n = 4$ and $n = 6$, respectively. For this case, time is the independent variable. The factorization method works nicely if one uses $g_n = \sqrt{n/2}$ and dealing with the more general equation

$$u'' \pm \sqrt{A}(g_n + g_n^{-1})u' + u(A - u^{n-2}) = 0, \quad (2.42)$$

for which we can employ either the factorization functions

$$\phi_1 = \mp g_n^{-1}(\sqrt{A} - u^{\frac{n}{2}-1}), \quad \phi_2 = \mp g_n(\sqrt{A} + u^{\frac{n}{2}-1})$$

or

$$\phi_1 = \mp g_n^{-1}(\sqrt{A} + u^{\frac{n}{2}-1}), \quad \phi_2 = \mp g_n(\sqrt{A} - u^{\frac{n}{2}-1}).$$

Then, Eq. (2.42) can be factored in the forms

$$\left[D_\tau \pm g_n(u^{\frac{n}{2}-1} + \sqrt{A}) \right] \left[D_\tau \mp g_n^{-1}(u^{\frac{n}{2}-1} - \sqrt{A}) \right] u = 0 \quad (2.43)$$

and

$$\left[D_\tau \mp g_n(u^{\frac{n}{2}-1} - \sqrt{A}) \right] \left[D_\tau \pm g_n^{-1}(u^{\frac{n}{2}-1} + \sqrt{A}) \right] u = 0. \quad (2.44)$$

Thus, Eq. (2.42) is compatible with the equations

$$u' \mp g_n^{-1}(u^{\frac{n}{2}-1} - \sqrt{A})u = 0, \quad (2.45)$$

$$u' \pm g_n^{-1}(u^{\frac{n}{2}-1} + \sqrt{A})u = 0 \quad (2.46)$$

that follows from Eq. (2.43) and Eq. (2.44). Integration of Eqs. (2.45), (2.46) gives the solution of Eq. (2.42)

$$u_{>} = \left(\frac{\sqrt{A}}{1 \pm \exp \left[\sqrt{A}(g_n - g_n^{-1})(\tau - \tau_0) \right]} \right)^{\frac{2}{n-2}}, \quad \gamma > 0 \quad (2.47)$$

and

$$u_{<} = \left(\frac{\sqrt{A}}{1 \pm \exp \left[-\sqrt{A}(g_n - g_n^{-1})(\tau - \tau_0) \right]} \right)^{\frac{2}{n-2}}, \quad \gamma < 0. \quad (2.48)$$

The solutions obtained by Dixon et al. are particular cases of the latter formulas. Reversing now the factorization brackets in (2.43)

$$\left[D_\tau \mp g_n^{-1} \left(u^{\frac{n}{2}-1} - \sqrt{A} \right) \right] \left[D_\tau \pm g_n \left(u^{\frac{n}{2}-1} + \sqrt{A} \right) \right] u = 0 \quad (2.49)$$

leads to the following equation

$$u'' \pm \sqrt{A} (g_n + g_n^{-1}) u' + u \left(\sqrt{A} + u^{\frac{n}{2}-1} \right) \left(\sqrt{A} - \frac{n^2}{4} u^{\frac{n}{2}-1} \right) = 0, \quad (2.50)$$

which is compatible with the equation

$$u' \pm g_n \left(u^{\frac{n}{2}-1} + \sqrt{A} \right) u = 0 \quad (2.51)$$

whose integration gives the solution of Eq. (2.50)

$$u_{>} = \left(\frac{\sqrt{A}}{1 \pm \exp[\sqrt{A} g_n (\tau - \tau_0)]} \right)^{\frac{2}{n-2}}, \quad \gamma > 0 \quad (2.52)$$

and

$$u_{<} = \left(\frac{\sqrt{A}}{1 \pm \exp[-\sqrt{A} g_n (\tau - \tau_0)]} \right)^{\frac{2}{n-2}}, \quad \gamma < 0. \quad (2.53)$$

2.4 FitzHugh-Nagumo equation

Let us consider the FitzHugh-Nagumo equation, which is a common approximation to describe nerve fiber propagation,

$$\frac{\partial u}{\partial t} - \frac{\partial^2 u}{\partial x^2} + u(1-u)(a-u) = 0, \quad (2.54)$$

where a is a real constant. Moreover, if $a = -1$, one gets the real Newell-Whitehead equation describing the dynamical behavior near the bifurcation point for the Rayleigh-Bénard convection of binary fluid mixtures. The travelling frame form of (2.54) has been discussed in detail by Hereman and Takaoka [19]

$$u'' + \gamma u' + u(u-1)(a-u) = 0. \quad (2.55)$$

The FitzHugh-Nagumo polynomial function allows the following factorizations:

$$\phi_1 = \pm(\sqrt{2})^{-1}(u-1), \quad \phi_2 = \pm\sqrt{2}(a-u)$$

when the γ parameter is equal to $\gamma_{a1} = \pm \frac{-2a+1}{\sqrt{2}}$ that we also write as $\gamma_{a,1} = \pm\sqrt{a}(g_{a1} - g_{a1}^{-1})$, where $g_{a1} = -\sqrt{2a}$.

In addition, we can employ the factorization functions

$$\phi_1 = \pm(\sqrt{2})^{-1}(a-u), \quad \phi_2 = \pm\sqrt{2}(u-1)$$

when $\gamma_{a,2} = \pm\frac{-a+2}{\sqrt{2}}$, or written again in the more symmetric form $\gamma_{a,2} = \pm\sqrt{a}(g_{a2} - g_{a2}^{-1})$, where $g_{a2} = -\sqrt{a/2}$. Thus, Eq. (2.55) can be factored in the two cases

$$u'' \pm \gamma_{a,1}u' + u(u-1)(a-u) = 0, \quad (2.56)$$

and

$$u'' \pm \gamma_{a,2}u' + u(u-1)(a-u) = 0. \quad (2.57)$$

In passing, we notice that for the Newell-Whitehead case $a = -1$ the two equations coincide and are the same as the generalized Fisher equation for $n = 2$.

In factorization bracket forms, Eqs. (2.56) and (2.57) are written as follows

$$\left[D \mp \sqrt{2}(a-u) \right] \left[D \pm (\sqrt{2})^{-1}(1-u) \right] u = 0 \quad (2.58)$$

and

$$\left[D \mp \sqrt{2}(u-1) \right] \left[D \mp (\sqrt{2})^{-1}(a-u) \right] u = 0, \quad (2.59)$$

and are compatible with the first order differential equations

$$u' \pm (\sqrt{2})^{-1}(1-u)u = 0, \quad \text{for } \gamma_{a,1}, \quad (2.60)$$

$$u' \mp (\sqrt{2})^{-1}(a-u)u = 0, \quad \text{for } \gamma_{a,2}. \quad (2.61)$$

Integration of Eqs. (2.60) and (2.61) gives the solution of Eq. (2.55) for the two different values of the wave front velocity $\gamma_{a,1}$ and $\gamma_{a,2}$.

For Eq. (2.56) we get

$$u_{>} = \frac{1}{1 \pm \exp[(\sqrt{2})^{-1}(\xi - \xi_0)]}, \quad u_{<} = \frac{1}{1 \pm \exp[-(\sqrt{2})^{-1}(\xi - \xi_0)]}, \quad (2.62)$$

for $\gamma_{a,1}$ positive and negative, respectively.

As for Eq. (2.57), the solutions are

$$u_{>} = \frac{a}{1 \pm \exp[-(\sqrt{2})^{-1}a(\xi - \xi_0)]}, \quad u_{<} = \frac{a}{1 \pm \exp[(\sqrt{2})^{-1}a(\xi - \xi_0)]}, \quad (2.63)$$

for $\gamma_{a,2}$ positive and negative, respectively.

Considering now the factorizations (2.58) and (2.59), the change of order of the factorization brackets gives

$$\left[D \pm (\sqrt{2})^{-1}(1-u) \right] \left[D \mp \sqrt{2}(a-u) \right] u = 0 \quad (2.64)$$

and

$$\left[D \mp (\sqrt{2})^{-1}(a-u) \right] \left[D \mp \sqrt{2}(u-1) \right] u = 0. \quad (2.65)$$

Doing the product of differential operators (and considering the factorization term $u' - \phi_2 u = 0$) gives the following RD equations

$$u'' \pm \gamma_{a1} u' + u(4u - 1)(a - u) = 0, \quad (2.66)$$

and

$$u'' \pm \gamma_{a2} u' + u(u - 1)(a - u - 3u^2) = 0, \quad (2.67)$$

Eqs. (2.66) and (2.67) are compatible with the equations

$$u' \mp \sqrt{2}(a - u)u = 0 \quad (2.68)$$

and

$$u' \mp \sqrt{2}(u - 1)u = 0, \quad (2.69)$$

respectively. Integrations of Eqs. (2.68) and (2.69) give the solutions of Eqs. (2.66) and (2.67), respectively. The explicit forms are the following:

(i) for (2.66)

$$u_{>} = \frac{a}{1 \pm \exp[-\sqrt{2}a(\xi - \xi_0)]}, \quad u_{<} = \frac{a}{1 \pm \exp[\sqrt{2}a(\xi - \xi_0)]}. \quad (2.70)$$

(ii) for (2.67)

$$u_{>} = \frac{1}{1 \pm \exp[\sqrt{2}(\xi - \xi_0)]}, \quad u_{<} = \frac{1}{1 \pm \exp[-\sqrt{2}(\xi - \xi_0)]}. \quad (2.71)$$

2.5 Conclusion of the chapter

In this chapter, we have been concerned with stating an efficient factorization scheme of ODE with polynomial nonlinearities that leads to an easy finding of analytical solutions of the kink type that previously have been obtained by far more cumbersome procedures. The main result is an interesting pairing between equations with different polynomial nonlinearities, which is obtained by applying the susy quantum mechanical reverse factorization. The kinks of the two nonlinear equations are of different widths but they propagate at the same velocity, or if we deal with damped polynomial nonlinear oscillators the two kink solutions correspond to the same friction coefficient. Several important cases, such as the generalized Fisher and the FitzHugh-Nagumo equations, have been shown to be simple mathematical exercises for this factorization technique. The physical prediction is that for commonly occurring propagating fronts, there are two kink fronts of different widths at a given propagating velocity. Moreover, the reverse factorization procedure can be also applied to the Berkovich scheme with similar results. It will be interesting to apply the approach of this work to the discrete case in which various exact results have been obtained in recent years [23]. More general cases in which the coefficient γ is an arbitrary function are also of much interest because of possible applications. The same factorization scheme as it works for more complicated ordinary differential equations is described in the next chapter.

Application to more general nonlinear differential equations

Abstract. In the previous chapter we considered the coefficient in front of the first derivative as a constant quantity. However, the employed factorization technique can be used almost unchanged for the more general case when the condition of constancy of this coefficient is relaxed. In this chapter, we obtain more kink type solutions through the same factorization procedure for a number of more general nonlinear ordinary second order differential equations with important applications in biology and physics.

3.1 Introduction

Considering the following type of differential equation

$$u'' + g(u)u' + F(u) = 0 \quad (3.1)$$

where again as in the previous chapter ' means the derivative $D = \frac{d}{d\xi}$ and $\xi = x - vt$; one can factorize Eq. (3.1) in the following form

$$[D - \phi_2(u)][D - \phi_1(u)]u = 0. \quad (3.2)$$

Performing now the product of differential operators leads to the equation

$$u'' - \frac{d\phi_1}{du}uu' - \phi_1u' - \phi_2u' + \phi_1\phi_2u = 0, \quad (3.3)$$

for which one way of grouping the terms is as follows

$$u'' - \left(\phi_1 + \phi_2 + \frac{d\phi_1}{du}u \right)u' + \phi_1\phi_2u = 0. \quad (3.4)$$

Eqs. (3.1) and (3.4) are lead to the conditions

$$g(u) = - \left(\phi_1 + \phi_2 + \frac{d\phi_1}{du} u \right) \quad (3.5)$$

and

$$F(u) = \phi_1 \phi_2 u . \quad (3.6)$$

If $F(u)$ is a polynomial function, then $g(u)$ will have the same order as the bigger of the factorizing functions $\phi_1(u)$ and $\phi_2(u)$, and will also be a function of the constant parameters provided by the function $F(u)$.

In the context of classical mechanics, Eq. (3.1) could be seen as an anharmonic oscillator with nonlinear damping. The case $g(u) = v$ where v is a constant value has been presented in the previous chapter. There, by means of a simple factorization method exact particular solutions of the kink type for reaction-diffusion equations and damped-anharmonic oscillators with polynomial nonlinearities have been obtained. In addition, SUSYQM-like reversing of factorization brackets has been performed providing new kink solutions for equations with different polynomial nonlinearities.

Based on the given grouping in Eq. (3.4) for Eq. (3.1), a simple mathematical procedure is proposed by which one gets particular solutions through factorization methods that allows finding solutions satisfying a compatible (nonlinear) first order differential equation.

The purpose of this chapter is to further apply this mathematical scheme to a wealth of important cases for which explicit particular solutions are not easy to find in the literature or are obtained by more involved techniques. The examples we present herein are the modified Emden equation, the Generalized Lienard equation, the convective Fisher equation, the generalized Burgers-Huxley equation, all of whom have significant applications in nonlinear physics. Explicit particular solutions are presented.

3.2 Modified Emden equation

Let us consider the following modified Emden equation

$$u'' + \alpha uu' + \beta u^3 = 0 . \quad (3.7)$$

The polynomial $F(u) = \beta u^3$ allows the following factorizing functions

$$\phi_1(u) = a_1 \sqrt{\beta} u , \quad \text{and} \quad \phi_2(u) = \frac{1}{a_1} \sqrt{\beta} u , \quad a_1 \neq 0 ,$$

where a_1 is an arbitrary constant. Eq. (3.5) is used to obtain the function $g(u)$,

$$g(u) = - \left(2a_1 \sqrt{\beta} u + \frac{1}{a_1} \sqrt{\beta} u \right) = -\sqrt{\beta} \left(\frac{2a_1^2 + 1}{a_1} \right) u ,$$

then identifying $\alpha = -\sqrt{\beta} \left(\frac{2a_1^2+1}{a_1} \right)$ (or $a_{1+,-} = \frac{-\alpha \pm \sqrt{\alpha^2 - 8\beta}}{4\sqrt{\beta}}$), where we use a_1 as a fitting parameter providing that $a_1 < 0$ for $\alpha > 0$. We note that $g(u) = g(\beta, a_1; u)$. Eq. (3.7) is now rewritten in the following form

$$u'' - \sqrt{\beta} \left(\frac{2a_1^2+1}{a_1} \right) uu' + \beta u^3 = 0, \quad (3.8)$$

the equation can be factorized as follows

$$\left(D - \frac{1}{a_1} \sqrt{\beta} u \right) \left(D - a_1 \sqrt{\beta} u \right) u = 0 \quad (3.9)$$

and therefore the compatible first order differential equation is

$$u' - a_1 \sqrt{\beta} u^2 = 0. \quad (3.10)$$

Integration of Eq. (3.10) gives the particular solution of Eq. (3.8)

$$u = -\frac{1}{a_1 \sqrt{\beta} (\xi - \xi_0)}, \quad (3.11)$$

where ξ_0 is an integration constant. If we consider the quadratic equation for a_1 , then Eq. (3.11) is expressed as a function of α ,

$$u = \frac{4}{(\alpha \pm \sqrt{\alpha^2 - 8\beta})(\xi - \xi_0)}. \quad (3.12)$$

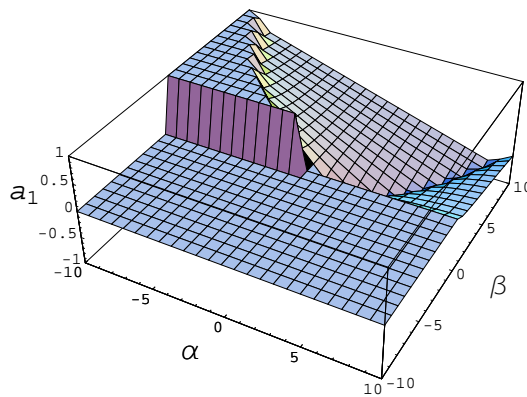


Fig. 3.1: Real part for the factorization curve of the parameter $a_{1+} = a_{1+}(\alpha, \beta)$ that allows the factorization of Eq. (3.8). $a_1 \neq 0$. $\alpha \in [-10, 10]$ and $\beta \in [-10, 10]$.

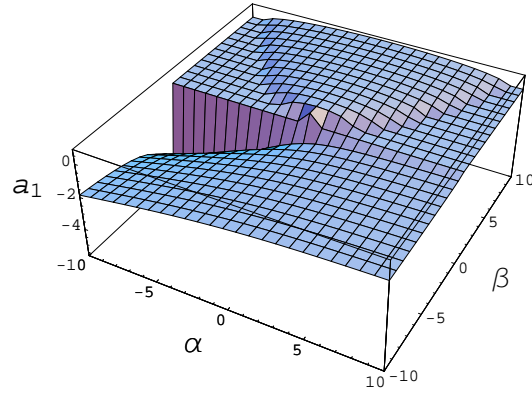


Fig. 3.2: Imaginary part for the factorization curve of the parameter $a_{1+} = a_{1+}(\alpha, \beta)$ that allows the factorization of Eq. (3.8). $a_1 \neq 0$. $\alpha \in [-10, 10]$ and $\beta \in [-10, 10]$.

Let us consider now another pair of factorizing functions

$$\phi_1(u) = a_1 \sqrt{\beta} u^2, \quad \phi_2(u) = \frac{1}{a_1} \sqrt{\beta},$$

then, using Eq. (3.5), the function $g(u) = -\sqrt{\beta} \left(\frac{1}{a_1} + 3a_1 u^2 \right)$ is easily obtained. Therefore, the original modified Emden equation (3.7) becomes

$$u'' - \sqrt{\beta} \left(\frac{1}{a_1} + 3a_1 u^2 \right) u' + \beta u^3 = 0. \quad (3.13)$$

This equation allows the factorization

$$\left(D - \frac{1}{a_1} \sqrt{\beta} \right) \left(D - a_1 \sqrt{\beta} u^2 \right) u = 0, \quad (3.14)$$

where from we obtain the compatible first order differential equation

$$u' - a_1 \sqrt{\beta} u^3 = 0 \quad (3.15)$$

with the solution

$$u = \frac{1}{[-2a_1 \sqrt{\beta} (\xi - \xi_0)]^{1/2}}. \quad (3.16)$$

The above example shows that different factorizations of $F(u)$ would yield different forms for the function $g(u)$. This is an important consequence of applying this mathematical technique to the case $g(u) \neq \text{const}$.

3.3 Generalized Lienard equation

Let us consider now the following generalized Lienard equation with a cubic polynomial function $F(u)$

$$u'' + g(u)u' + Au + Bu^2 + Cu^3 = 0. \quad (3.17)$$

The polynomial function $F(u)$ can be factorized in several ways, we consider first the factorization $F(u) = u(a + b + Cu)(d - e + u)$ where

$$a = B/2, \quad b = \sqrt{B^2 - 4AC}/2, \quad d = B/2C, \quad e = \sqrt{B^2 - 4AC}/2C,$$

and the condition $B^2 - 4AC > 0$ holds. If we consider the factorizing functions as

$$\phi_1(u) = a_1(a + b + Cu) \quad \text{and} \quad \phi_2(u) = \frac{1}{a_1}(d - e + u),$$

where again a_1 is an arbitrary constant that can be used as a fitting parameter, the function $g(u) = \left[\frac{a_1^2(a+b)+(d-e)}{a_1} + \left(\frac{2a_1^2C+1}{a_1} \right) u \right]$ will be obtained. Then, Eq. (3.17) is rewritten as

$$u'' + \left[\frac{a_1^2(a+b)+(d-e)}{a_1} + \left(\frac{2a_1^2C+1}{a_1} \right) u \right] u' + Au + Bu^2 + Cu^3 = 0, \quad (3.18)$$

and the corresponding factorization will be

$$\left[D - \frac{1}{a_1}(d - e + u) \right] [D - a_1(a + b + Cu)] u = 0 \quad (3.19)$$

where from the compatible first order differential equation is obtained

$$u' - a_1(a + b + Cu)u = 0, \quad (3.20)$$

and whose solution is

$$u = \frac{(a+b)\exp[a_1(a+b)(\xi - \xi_0)]}{1 - C\exp[a_1(a+b)(\xi - \xi_0)]} \quad (3.21)$$

where $(a+b) = \frac{B+\sqrt{B^2-4AC}}{2}$.

Let us consider now the following reduction of terms in Eq. (3.17), $B = 0$ and $C = 1$ in order to calculate a particular solution for the so-called autonomous Duffing-van der Pol oscillator equation [25],

$$u'' + (G + Eu^2)u' + Au + u^3 = 0, \quad (3.22)$$

where G and E are arbitrary constant parameters. The polynomial function allows the following factorizing functions

$$f_1(u) = a_1(A + u^2) \quad \text{and} \quad \phi_2(u) = \frac{1}{a_1},$$

then $g(u) = -\left(\frac{a_1^2 A + 1}{a_1} + 3a_1 u^2\right)$. Eq. (3.22) is now rewritten

$$u'' - \left(\frac{a_1^2 A + 1}{a_1} + 3a_1 u^2\right) u' + Au + u^3 = 0. \quad (3.23)$$

The corresponding factorization of Eq. (3.23) is given as follows

$$\left[D - \frac{1}{a_1}\right] [D - a_1(A + u^2)] u = 0, \quad (3.24)$$

and the obtained compatible first order equation

$$u' - a_1(A + u^2)u = 0. \quad (3.25)$$

Integration of Eq. (3.25) gives the particular solution of Eq. (3.23)

$$u = \sqrt{A} \left(\frac{\exp[2a_1 A(\xi - \xi_0)]}{1 - \exp[2a_1 A(\xi - \xi_0)]} \right)^{1/2}. \quad (3.26)$$

Comparing Eqs. (3.22) and (3.23), $a_1 = -\frac{E}{3}$ and $G = \frac{AE^2 + 9}{3E}$ are obtained. Solution (3.26) is now written as a function of A and E ,

$$u = \pm \sqrt{A} \left(\frac{\exp[-\frac{2}{3}AE(\xi - \xi_0)]}{1 - \exp[-\frac{2}{3}AE(\xi - \xi_0)]} \right)^{1/2}. \quad (3.27)$$

This is a more general result for the particular solution than that obtained by Chandrasekar et al. in [25] by other means, in fact, it is recuperated when $E = \beta$ and $A = \frac{3}{\beta^2}$.

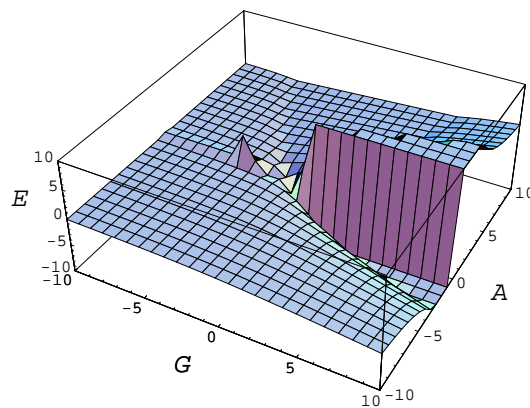


Fig. 3.3: Real part for the factorization curve of the parameter $E_+ = E_+(G, A)$ that allows the factorization of Eq. (3.23). Note that $a_1 = -\frac{E}{3}$; $E \neq 0$. $G \in [-10, 10]$ and $A \in [-10, 10]$.

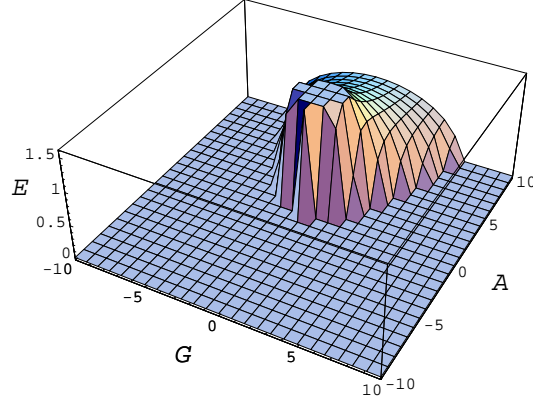


Fig. 3.4: Imaginary part for the factorization curve of the parameter $E_+ = E_+(G, A)$ that allows the factorization of Eq. (3.23). $E \neq 0$. $G \in [-10, 10]$ and $A \in [-10, 10]$.

3.4 Convective Fisher equation

Let us consider the convective Fisher equation given in the following form [26],

$$\frac{\partial u}{\partial t} = \frac{1}{2} \frac{\partial^2 u}{\partial x^2} + u(1-u) - \mu u \frac{\partial u}{\partial x} \quad (3.28)$$

where μ is a positive parameter that serves to tune the relative strength of convection. If the variable transformation $\xi = x - vt$ is performed, then we obtain the following ordinary differential equation

$$u'' + 2(v - \mu u)u' + 2u(1-u) = 0. \quad (3.29)$$

The polynomial function allows the factorizing functions

$$\phi_1(u) = \sqrt{2}a_1(1-u) \quad \text{and} \quad \phi_2(u) = \frac{\sqrt{2}}{a_1},$$

and Eq. (3.5) gives the function $g(u) = -\sqrt{2} \left(\frac{a_1^2+1}{a_1} - 2a_1u \right)$. Eq. (3.29) is rewritten as follows

$$u'' + 2 \left(-\frac{a_1^2+1}{\sqrt{2}a_1} + \sqrt{2}a_1u \right) u' + 2u(1-u) = 0. \quad (3.30)$$

If we set the fitting parameter $a_1 = -\frac{\mu}{\sqrt{2}}$, then we obtain $v = \frac{\mu^2+2}{2\mu}$. Eq. (3.30) is factorized in the following form

$$\left[D - \frac{\sqrt{2}}{a_1} \right] \left[D - \sqrt{2}a_1(1-u) \right] u = 0, \quad (3.31)$$

that provides the compatible first order equation

$$u' - \sqrt{2}a_1u(1-u) = u' + \mu u(1-u) = 0 \quad (3.32)$$

whose integration gives

$$u = \frac{1}{1 \pm \exp[\mu(\xi - \xi_0)]}. \quad (3.33)$$

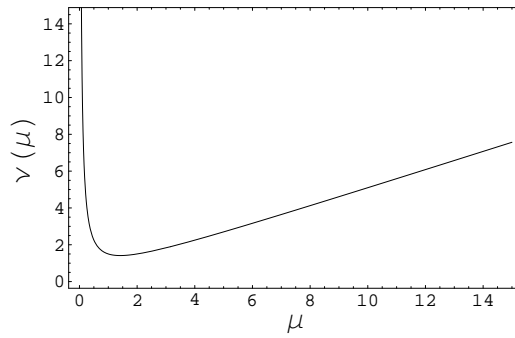


Fig. 3.5: Factorization curve of the parameter $v = v(\mu)$ that allows the factorization of Eq. (3.30). $a_1 = -\frac{\mu}{\sqrt{2}}$.

3.5 Generalized Burgers-Huxley equation

In this section we obtain particular solutions for the generalized Burgers-Huxley equation discussed by Wang et al. in [27]

$$\frac{\partial u}{\partial t} - \alpha u^\delta \frac{\partial u}{\partial x} - \frac{\partial^2 u}{\partial x^2} = \beta u(1-u^\delta)(u^\delta - \gamma). \quad (3.34)$$

If the coordinates transformation $\xi = x - vt$ is performed then Eq. (3.34) is rewritten in the following form

$$u'' + (v + \alpha u^\delta)u' + \beta u(1-u^\delta)(u^\delta - \gamma) = 0, \quad (3.35)$$

and the polynomial function allows the choice for the factorizing terms

$$\phi_1(u) = \sqrt{\beta}a_1(1-u^\delta) \quad \text{and} \quad \phi_2(u) = \frac{\sqrt{\beta}}{a_1}(u^\delta - \gamma).$$

Eq. (3.5) provides $g(u) = \sqrt{\beta} \left(\frac{\gamma - a_1^2}{a_1} + \frac{a_1^2(1+\delta)-1}{a_1} u^\delta \right)$, and we can do the following identification of constant parameters

$$v = \sqrt{\beta} \left(\frac{\gamma - a_1^2}{a_1} \right), \quad \alpha = \sqrt{\beta} \left(\frac{-a_1^2(1+\delta) + 1}{a_1} \right).$$

Writing Eq. (3.35) in factorized form

$$\left[D - \frac{\sqrt{\beta}}{a_1}(u^\delta - \gamma) \right] \left[D - \sqrt{\beta}a_1(1 - u^\delta) \right] u = 0, \quad (3.36)$$

the solution

$$u = \left(\frac{1}{1 \pm \exp[-a_1\sqrt{\beta}\delta(\xi - \xi_0)]} \right)^{1/\delta} \quad (3.37)$$

of the compatible first order equation

$$u' - \sqrt{\beta}a_1u(1 - u^\delta) = 0, \quad (3.38)$$

is also a particular kink solution of Eq. (3.35). Solving the quadratic equation (3.36) for $a_1 = a_1(\alpha, \beta, \delta)$ we obtain

$$a_{1+,-} = \frac{-\alpha \pm \sqrt{\alpha^2 + 4\beta(1 + \delta)}}{2\sqrt{\beta}(1 + \delta)},$$

then Eq. (3.37) becomes a function $u = u(\alpha, \beta, \delta; \tau)$, and $v = v(\alpha, \beta, \gamma, \delta)$. If we set $\delta = 1$ in Eq. (3.34), then we obtain the following particular Burgers-Huxley solution

$$u = \frac{1}{1 \pm \exp[-a_1\sqrt{\beta}(\xi - \xi_0)]}, \quad (3.39)$$

and $a_{1+,-} = \frac{-\alpha \pm \sqrt{\alpha^2 + 8\beta}}{4\sqrt{\beta}}$, $v = v(\alpha, \beta, \gamma)$.

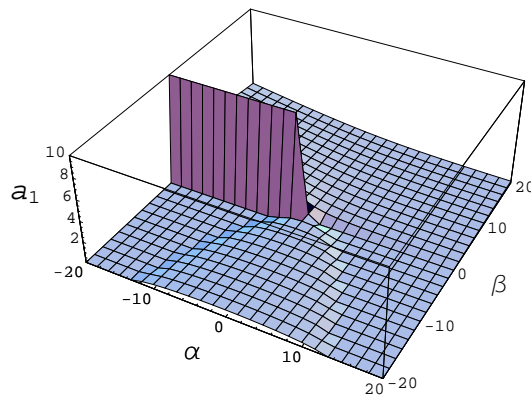


Fig. 3.6: Real part for the factorization curve of the parameter $a_{1+} = a_{1+}(\alpha, \beta, \delta = 1)$ that allows factorization of Eq. (3.35) with $\delta = 1$. $a_1 \neq 0$. $\alpha \in [-20, 20]$ and $\beta \in [-20, 20]$.

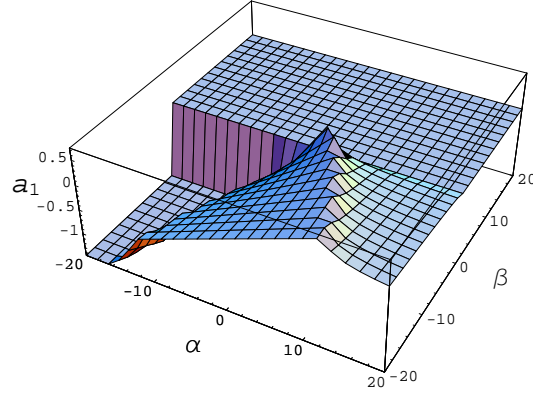


Fig. 3.7: Imaginary part for the factorization curve of the parameter $a_{1+} = a_{1+}(\alpha, \beta, \delta = 1)$ that allows factorization of Eq. (3.35) with $\delta = 1$. $a_1 \neq 0$. $\alpha \in [-20, 20]$ and $\beta \in [-20, 20]$.

If we chose now the factorizing terms as

$$\phi_1(u) = \sqrt{\beta} e_1 (u^\delta - \gamma) \quad \text{and} \quad \phi_2(u) = \frac{\sqrt{\beta}}{e_1} (1 - u^\delta),$$

we obtain $g(u) = \sqrt{\beta} \left(\frac{e_1^2 \gamma - 1}{e_1} + \frac{1 - e_1^2 (1 + \delta)}{e_1} u^\delta \right)$, and the following identification of parameters $v = \sqrt{\beta} \left(\frac{e_1^2 \gamma - 1}{e_1} \right)$ and $\alpha = \sqrt{\beta} \left(\frac{1 - e_1^2 (1 + \delta)}{e_1} \right)$. Eq. (3.35) is then factorized in the different form

$$\left[D - \frac{\sqrt{\beta}}{e_1} (1 - u^\delta) \right] \left[D - \sqrt{\beta} e_1 (u^\delta - \gamma) \right] u = 0. \quad (3.40)$$

The corresponding compatible first order equation is now

$$u' - \sqrt{\beta} e_1 u (u^\delta - \gamma) = 0, \quad (3.41)$$

and its integration gives a different particular solution for Eq. (3.35) from that obtained for the first choice of factorizing terms (3.36), however, we point out that the parameter α has changed for the second choice of factorizing terms. The solution of Eq. (3.41) is given as follows

$$u = \left(\frac{\gamma}{1 \pm \exp[\pm e_1 \sqrt{\beta} \gamma \delta (\xi - \xi_0)]} \right)^{1/\delta}. \quad (3.42)$$

Solving the quadratic equation for $e_1 = e_1(\alpha, \beta, \delta)$ we obtain

$$e_{1+,-} = \frac{\alpha \pm \sqrt{\alpha^2 + 4\beta(1+\delta)}}{2\sqrt{\beta}(1+\delta)},$$

then Eq. (3.42) becomes $u = u(\alpha, \beta, \gamma, \delta; \tau)$, and $v = v(\alpha, \beta, \gamma, \delta)$. If we set $\delta = 1$ in Eq. (3.34), then the following Burgers-Huxley solution is obtained

$$u = \frac{\gamma}{1 \pm \exp[e_1 \sqrt{\beta} \gamma (\xi - \xi_0)]}, \quad (3.43)$$

and $e_{1+,-} = \frac{\alpha \pm \sqrt{\alpha^2 + 8\beta}}{4\sqrt{\beta}}$, $v = v(\alpha, \beta, \gamma)$.

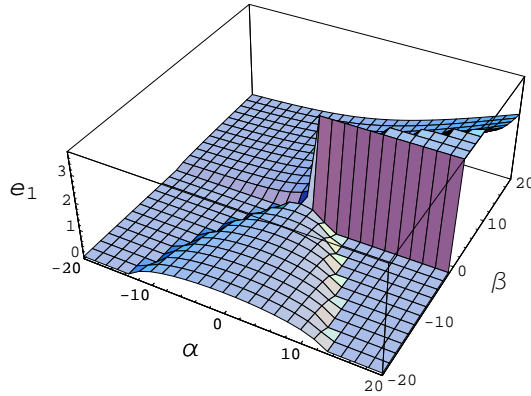


Fig. 3.8: Real part for the factorization curve of the parameter $e_{1+} = e_{1+}(\alpha, \beta, \delta = 1)$ that allows factorization of Eq. (3.35) with $\delta = 1$. $e_1 \neq 0$. $\alpha \in [-20, 20]$ and $\beta \in [-20, 20]$.

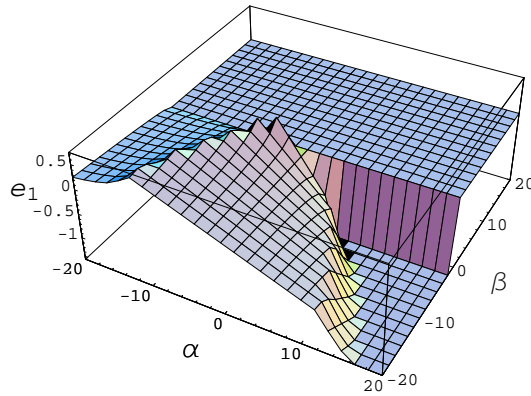


Fig. 3.9: Imaginary part for the factorization curve of the parameter $e_{1+} = e_{1+}(\alpha, \beta, \delta = 1)$ that allows factorization of Eq. (3.35) with $\delta = 1$. $e_1 \neq 0$. $\alpha \in [-20, 20]$ and $\beta \in [-20, 20]$.

Eqs. (3.37) and (3.42) representing particular solutions for the GBHE, are the same as those obtained by Wang et al. [27].

3.6 Conclusion of the chapter

In this chapter, we apply the same factorization scheme for more complicated second order nonlinear differential equations as in Chapter 2. Exact particular solutions have been found for a series of nonlinear differential equations with applications in physics and biology: the modified Emden equation, the generalized Lienard equation, the duffing-van der Pol equation, the convective Fisher equation, and the generalized Burgers-Huxley equation. Also, we display parametric curves along which the differential equations under consideration could be factorized. We find that the proposed factorization procedure is easier and more efficient than other methods used to find particular solutions of second order differential equations.

One-parameter supersymmetry for microtubules

Abstract. The simple supersymmetric model of Caticha [34] as used by Rosu [33] to describe the motion of ferrodistorptive domain walls in microtubules (MTs), is generalized to the case of Mielnik's one-parameter nonrelativistic supersymmetry [11]. By this means, one can introduce Montroll double-well potentials with singularities that move along the positive or negative travelling direction depending on the sign of the free parameter of Mielnik's method. Possible interpretations of the singularity are microtubule associated proteins (motors) or structural discontinuities in the arrangement of the tubulin molecules.

4.1 Introduction

Based on well-established results of Collins, Blumen, Currie and Ross [29] regarding the dynamics of domain walls in ferrodistorptive materials, Tuszyński and collaborators [30, 31] considered MTs to be ferrodistorptive and studied kinks of the Montroll type [32] as excitations responsible for the energy transfer within this highly interesting biological context.

The Euler-Lagrange dimensionless equation of motion of ferrodistorptive domain walls as derived in [29] from a Ginzburg-Landau free energy with driven field and dissipation included is of the travelling reaction-diffusion type

$$\psi'' + \rho\psi' - \psi^3 + \psi + \sigma = 0, \quad (4.1)$$

where the primes are derivatives with respect to a travelling coordinate $\xi = x - vt$, ρ is a friction coefficient and σ is related to the driven field [29].

There may be ferrodistorptive domain walls that can be identified with the Montroll kink solution of Eq. (4.1)

$$M(\xi) = \alpha_1 + \frac{\sqrt{2}\beta}{1 + \exp(\beta\xi)}, \quad (4.2)$$

where $\beta = (\alpha_2 - \alpha_1)/\sqrt{2}$ and the parameters α_1 and α_2 are two nonequal solutions of the cubic equation

$$(\psi - \alpha_1)(\psi - \alpha_2)(\psi - \alpha_3) = \psi^3 - \psi - \sigma. \quad (4.3)$$

4.2 Caticha's supersymmetric model as applied to MTs

Rosu has noted that Montroll's kink can be written as a typical tanh kink [33]

$$M(\xi) = \gamma - \tanh\left(\frac{\beta\xi}{2}\right), \quad (4.4)$$

where $\gamma \equiv \alpha_1 + \alpha_2 = 1 + \frac{\alpha_1\sqrt{2}}{\beta}$. The latter relationship allows one to use a simple construction method of exactly soluble double-well potentials in the Schrödinger equation proposed by Caticha [34]. The scheme is a non-standard application of Witten's supersymmetric quantum mechanics [9] having as the essential assumption the idea of considering the M kink as the switching function between the two lowest eigenstates of the Schrödinger equation with a double-well potential. Thus

$$\phi_1 = M\phi_0, \quad (4.5)$$

where $\phi_{0,1}$ are solutions of $\phi_{0,1}'' + [\varepsilon_{0,1} - u(\xi)]\phi_{0,1}(\xi) = 0$, and $u(\xi)$ is the double-well potential to be found. Substituting Eq. (4.5) into the Schrödinger equation for the subscript 1 and subtracting the same equation multiplied by the switching function for the subscript 0, one obtains

$$\phi_0' + R_M\phi_0 = 0, \quad (4.6)$$

where R_M is given by

$$R_M = \frac{M'' + \varepsilon M}{2M'}, \quad (4.7)$$

and $\varepsilon = \varepsilon_1 - \varepsilon_0$ is the lowest energy splitting in the double-well Schrödinger equation. In addition, notice that Eq. (4.6) is the basic equation introducing the superpotential R in Witten's supersymmetric quantum mechanics, i.e., the Riccati solution. For Montroll's kink the corresponding Riccati solution reads

$$R_M(\xi) = -\frac{\beta}{2}\tanh\left(\frac{\beta}{2}\xi\right) + \frac{\varepsilon}{2\beta}\left[\sinh(\beta\xi) + 2\gamma\cosh^2\left(\frac{\beta}{2}\xi\right)\right] \quad (4.8)$$

and the ground-state Schrödinger function is found by means of Eq. (4.6)

$$\begin{aligned} \phi_{0,M}(\xi) = & \phi_0(0)\cosh\left(\frac{\beta}{2}\xi\right)\exp\left(\frac{\varepsilon}{2\beta^2}\right)\exp\left(-\frac{\varepsilon}{2\beta^2}\left[\cosh(\beta\xi)\right.\right. \\ & \left.\left.-\gamma\beta\xi - \gamma\sinh(\beta\xi)\right]\right), \end{aligned} \quad (4.9)$$

while ϕ_1 is obtained by switching the ground-state wave function by means of M . This ground-state wave function is of supersymmetric type

$$\phi_{0,M}(\xi) = \phi_{0,M}(0)\exp\left[-\int_0^\xi R_M(y)dy\right], \quad (4.10)$$

where $\phi_{0,M}(0)$ is a normalization constant.

The Montroll double well potential is determined up to the additive constant ε_0 by the ‘bosonic’ Riccati equation

$$\begin{aligned} u_M(\xi) = R_M^2 - R_M' + \varepsilon_0 = & \frac{\beta^2}{4} + \frac{(\gamma^2 - 1)\varepsilon^2}{4\beta^2} + \frac{\varepsilon}{2} + \varepsilon_0 \\ & + \frac{\varepsilon}{8\beta^2} \left[(4\gamma^2\varepsilon + 2(\gamma^2 + 1)\varepsilon \cosh(\beta\xi) - 8\beta^2) \cosh(\beta\xi) \right. \\ & \left. - 4\gamma(\varepsilon + \varepsilon \cosh(\beta\xi) - 2\beta^2) \sinh(\beta\xi) \right]. \end{aligned} \quad (4.11)$$

Plots of the asymmetric Montroll potential and ground state wave function are given in Figs. 4.1 and 4.2 for a particular set of the parameters. If, as suggested by Caticha, one chooses the ground state energy to be

$$\varepsilon_0 = -\frac{\beta^2}{4} - \frac{\varepsilon}{2} + \frac{\varepsilon^2}{4\beta^2} (1 - \gamma^2), \quad (4.12)$$

then $u_M(\xi)$ turns into a travelling, asymmetric Morse double-well potential of depths depending on the Montroll parameters β and γ and the splitting ε

$$U_{0,m}^{L,R} = \beta^2 \left[1 \pm \frac{2\varepsilon\gamma}{(2\beta)^2} \right], \quad (4.13)$$

where the subscript m stands for Morse and the superscripts L and R for left and right well, respectively. The difference in depth, the bias, is $\Delta_m \equiv U_0^L - U_0^R = 2\varepsilon\gamma$, while the location of the potential minima on the travelling axis is at

$$\xi_m^{L,R} = \mp \frac{1}{\beta} \ln \left[\frac{(2\beta)^2 \pm 2\varepsilon\gamma}{\varepsilon(\gamma \mp 1)} \right], \quad (4.14)$$

that shows that $\gamma \neq \pm 1$.

4.3 The Mielnik extension

We now discuss shortly in this context the Mielnik extension of these results [11, 3]. The point is that R_M in Eq. (4.8) is only the particular solution of Eq. (4.11). The general solution is a one-parameter function of the form

$$R_M(\xi; \lambda) = R_M(\xi) + \frac{d}{d\xi} \left[\ln(I_M(\xi) + \lambda) \right] \quad (4.15)$$

and the corresponding one-parameter Montroll potential is given by

$$u_M(\xi; \lambda) = u_M(\xi) - 2 \frac{d^2}{d\xi^2} \left[\ln(I_M(\xi) + \lambda) \right]. \quad (4.16)$$

In these formulas, $I_M(\xi) = \int^\xi \phi_{0,M}^2(\xi) d\xi$ and λ is an integration constant that is used as a deforming parameter of the potential and is related to the irregular zero mode. The one-parameter Darboux-deformed ground state wave function can be shown to be

$$\phi_{0,M}(\xi; \lambda) = \sqrt{\lambda(\lambda + 1)} \frac{\phi_{0,M}}{I_M(\xi) + \lambda}, \quad (4.17)$$

where $\sqrt{\lambda(\lambda+1)}$ is the normalization factor implying that $\lambda \notin [0, -1]$. Moreover, the Mielnik parametric potentials and wave functions display singularities at $\lambda_s = -I_M(\xi_s)$. Plots of $u_M(\xi; \lambda)$ and $\phi_{0,M}(\xi; \lambda)$ for $\lambda = 1, 10, 100$ are presented in Figs. 4.3-4.12 and are useful to see the behavior of the singularities and the deformation effect of the λ parameter. For large values of $\pm\lambda$ the singularity moves towards $\mp\infty$ and the potential and ground state wave function recover the shapes of the non-parametric potential and wave function as can be seen in Figs. 4.11 and 4.12, respectively. The one-parameter Morse case corresponds formally to the change of subscript $M \rightarrow m$ in Eqs. (4.15) and (4.16). For the single well Morse potential the one-parameter procedure has been studied by Filho [35] and Bentaiba et al [36].

Mielnik's approach leads to singularities in the double-well potential and the corresponding wave functions. If the parameter λ is positive the singularity is to be found on the negative ξ axis, while for negative λ it is on the positive side. Potentials and wave functions with singularities are not so strange as it seems [37] and could be quite relevant even in nanotechnology [38] where quantum singular interactions of the contact type are appropriate for describing nanoscale quantum devices. We interpret the singularity as representing the effect of an impurity moving along the MT in one direction or the other depending on the sign of the parameter λ . The impurity may represent a protein attached to the MT or a structural discontinuity in the arrangement of the tubulin molecules. This interpretation of impurities has been given by Trpišová and Tuszyński in non-supersymmetric models of nonlinear MT excitations [39].

4.4 Conclusion of the chapter

In conclusion, the supersymmetric approaches allow for a number of interesting *exact* results in this biological framework and point to a direct connection between Schrödinger double-well potentials and nonlinear kinks encountered in nonequilibrium chemical processes. MTs are an important application but the procedures described here can be used in many other applications. Moreover, the supersymmetric constructions can be used as a background for clarifying further details of the exact models. Although it is not so clear why one should take a certain type of kink as switching function between the Schrödinger split modes, it is interesting that proceeding in this way one will be led to some familiar double-well potentials in chemical physics.

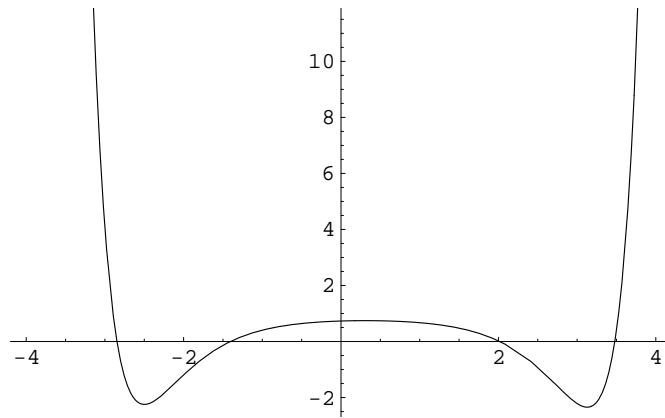


Fig. 4.1: The Montroll asymmetric double-well potential (MDWP) calculated using Eq. (4.11) for $\varepsilon_0 = 0$. In all figures $\alpha_1 = 1$, $\alpha_2 = -1.5$, $\beta = -2.5/\sqrt{2}$, $\gamma = -0.5$, $\varepsilon = 0.1$.

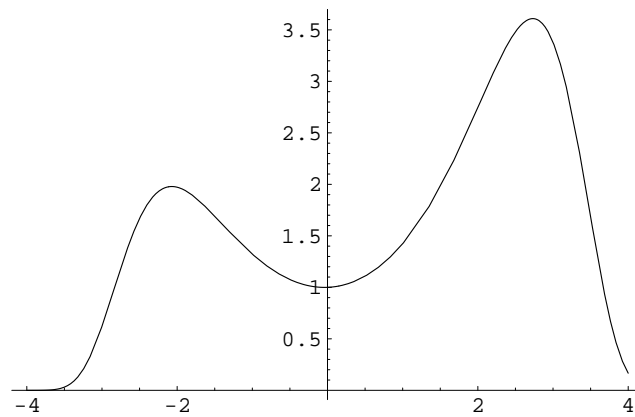


Fig. 4.2: The Montroll ground state wave function of Eq. (4.9) for $\phi_0(0) = 1$.

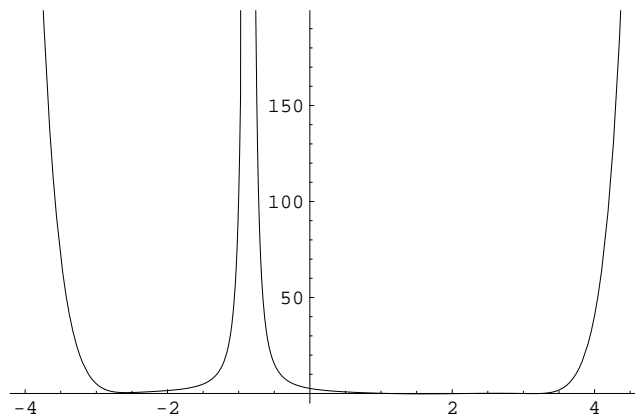


Fig. 4.3: The one-parameter Darboux modified MDWP for $\lambda = 1$.

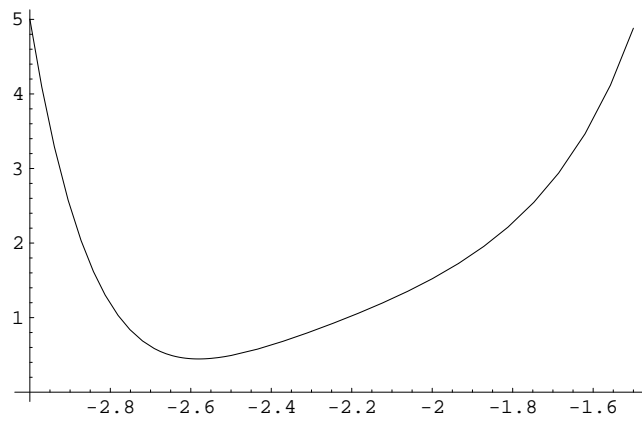


Fig. 4.4: The low-scale left hand side of the singularity.

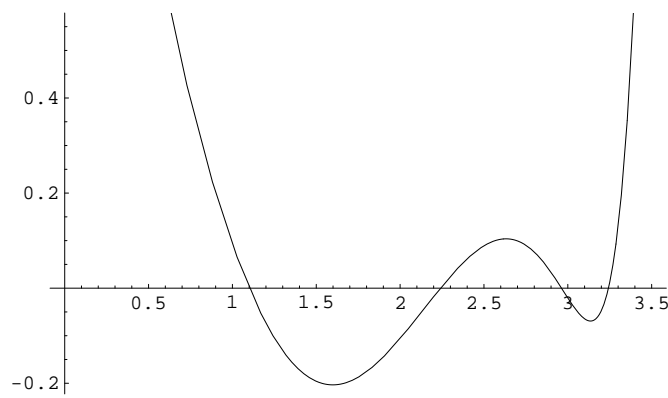
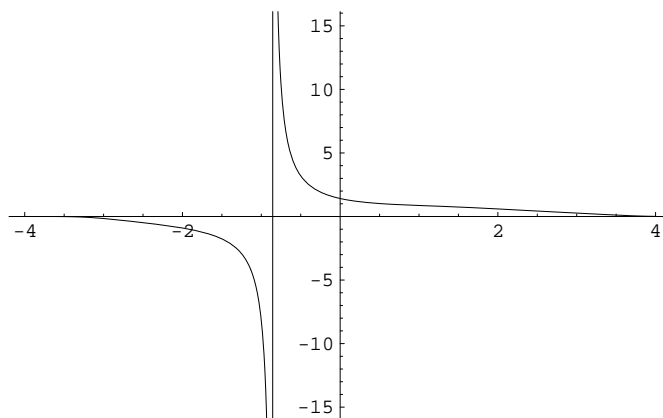


Fig. 4.5: The low-scale right hand side of the singularity.

Fig. 4.6: The wave functions for $\lambda = 1$.

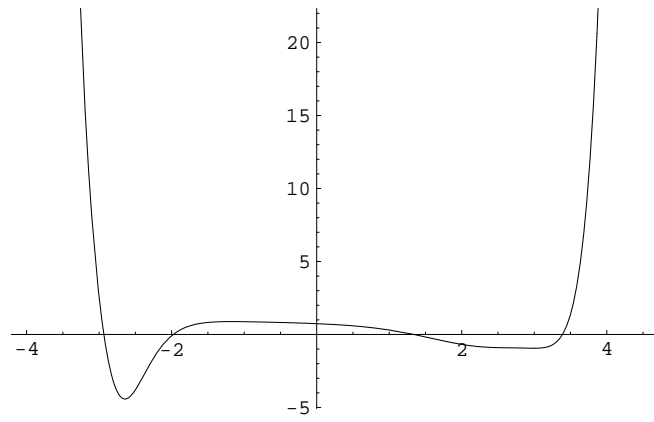


Fig. 4.7: One parameter Darboux-modified MDWP for $\lambda = 10$.

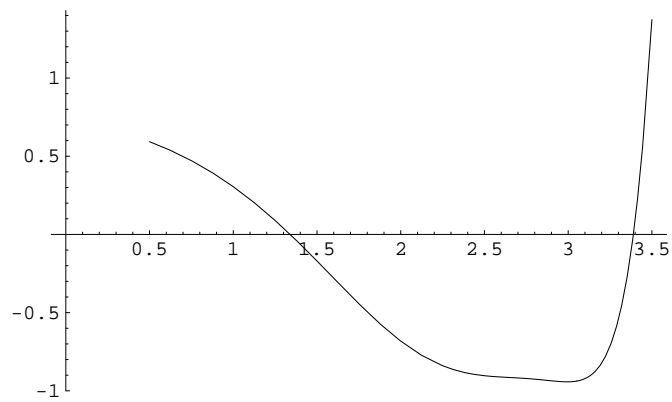


Fig. 4.8: The bottom of the potential at the right hand side.

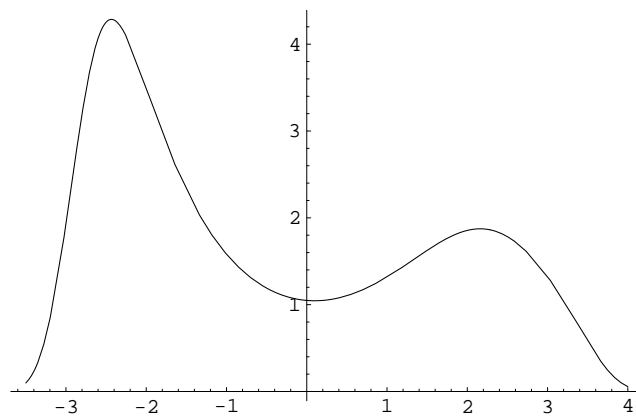


Fig. 4.9: The ground state wave function corresponding to $\lambda = 10$.

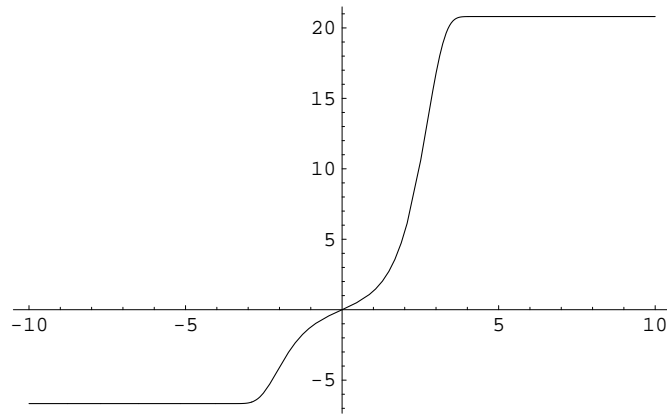


Fig. 4.10: Plot of the integral $I_M(\xi)$ that produces the deformation of the potential and wave functions.

5

Supersymmetric method with Dirac parameters

Abstract. In this chapter we first describe a "supersymmetric" one-dimensional matrix procedure similar to relationships of the same type between Dirac and Schrödinger equations in particle physics that we apply to two problems in classical mechanics and quantum mechanics, respectively. In the first case, we obtain a class of parametric oscillation modes that we call K-modes with damping and absorption that are connected to the classical harmonic oscillator modes through this supersymmetric procedure that is characterized by coupling parameters. When a single coupling parameter, denoted by K , is used, it characterizes both the damping and the dissipative features of these modes. Generalizations to several K parameters are also possible and lead to analytical results. If the problem is passed to the physical optics (and/or acoustics) context by switching from the oscillator equation to the corresponding Helmholtz equation, one may hope to detect the K-modes as waveguide modes of specially designed waveguides and/or cavities. In the second case, the same method is presented in a style appropriate for truly quantum mechanical problems and an application to the Morse potential is performed. We obtain the corresponding nonhermitic Morse problem with possible applications to the diffraction on optical lattices.

5.1 Introduction

Factorizations of differential operators describing simple mechanical motion have been only occasionally used in the past, although in quantum mechanics the procedure led to a vast literature under the name of supersymmetric quantum mechanics initiated by a paper of Witten [9]. However, as shown by Rosu and Reyes [40], for the damped Newtonian free oscillator the factorization method could generate interesting results even in an area settled more than three centuries ago. In this chapter, we apply some of the supersymmetric schemes to the basic classical harmonic oscillator. In particular, we show how a known connection in particle physics between Dirac and Schrödinger equations could lead in the case of harmonic motion to chirped (i.e., time-dependent) frequency oscillator equations whose solutions are a class of oscillatory modes depending on one

more parameter, denoted in the following by K , besides the natural circular frequency ω_0 . The parameter K characterizes both the damping and the losses of these "supersymmetric" partner modes. Moreover, we do not limit this study to one K parameter extending it to several such parameters still getting analytic results. Guided by mathematical equivalence, possible applications in several areas of physics are identified. Moreover, in the final part of the chapter the same supersymmetric scheme is used in the context of exactly solvable quantum problem of the Morse potential. A nonhermitic version of the Morse problem is introduced in this way.

5.2 Classical harmonic oscillator: The Riccati approach

The harmonic oscillator can be described by one of the simplest Riccati equation

$$u' + u^2 + \kappa\omega_0^2 = 0, \quad \kappa = \pm 1, \quad (5.1)$$

where the plus sign is for the normal case whereas the minus sign is for the up side down case. Indeed, employing $u = \frac{w'}{w}$ one gets the harmonic oscillator differential equation

$$w'' + \kappa\omega_0^2 w = 0, \quad (5.2)$$

with the solutions

$$w_b = \begin{cases} W_+ \cos(\omega_0 t + \varphi_+) & \text{if } \kappa = 1 \\ W_- \sinh(\omega_0 t + \varphi_-) & \text{if } \kappa = -1, \end{cases}$$

where W_{\pm} and φ_{\pm} are amplitude and phase parameters, respectively, which can be ignored in the following.

The particular Riccati solution of Eq. (5.1) are

$$u_p = \begin{cases} -\omega_0 \tan(\omega_0 t) & \text{if } \kappa = 1 \\ \omega_0 \coth(\omega_0 t) & \text{if } \kappa = -1. \end{cases}$$

It is well known that the particular Riccati solutions enter as nonoperatorial part in the common factorizations of the second-order linear differential equations that are directly related to the Darboux isospectral transformations [13].

Thus, for Eq. (5.2) one gets ($D_t = \frac{d}{dt}$)

$$(D_t + u_p)(D_t - u_p)w = w'' + (-u_p' - u_p^2)w = 0. \quad (5.3)$$

To fix the ideas, we shall use the terminology of Witten's supersymmetric quantum mechanics and call Eq. (5.3) the bosonic equation. We stress here that the supersymmetric terminology is used only for convenience and should not be taken literally. Thus, the supersymmetric partner (or fermionic) equation of Eq. (5.3) is obtained by reversing the factorization brackets

$$(D_t - u_p)(D_t + u_p)w_f = w'' + (u_p' - u_p^2)w = w'' + \omega_f^2(t)w = 0, \quad (5.4)$$

which is related to the fermionic Riccati equation

$$u' - u^2 - \omega_f^2(t) = 0, \quad (5.5)$$

where the free term ω_f^2 is the following function of time

$$\omega_f^2(t) = u_p' - u_p^2 = \begin{cases} \omega_0^2(-1 - 2\tan^2\omega_0 t) & \text{if } \kappa = 1 \\ \omega_0^2(1 - 2\coth^2\omega_0 t) & \text{if } \kappa = -1 . \end{cases}$$

The solutions (fermionic zero modes) of Eq. (5.4) are given by

$$w_f = \begin{cases} \frac{-\omega_0}{\cos(\omega_0 t)} & \text{if } \kappa = 1 \\ \frac{\omega_0}{\sinh(\omega_0 t)} & \text{if } \kappa = -1 , \end{cases}$$

and thus present strong periodic singularities in the first case and just one singularity at the origin in the second case. These ‘partner’ oscillators, as well as those to be discussed in the following, are parametric oscillators, i.e., of time-dependent frequency. Moreover, their frequencies can become infinite (periodically). In general, signals of this type are known as chirps. “Infinite” chirps could be produced, in principle, in very special astrophysical circumstances, e.g., close to black hole horizons [41].

5.3 Matrix formulation

Using the Pauli matrices $\sigma_y = \begin{pmatrix} 0 & -i \\ i & 0 \end{pmatrix}$ and $\sigma_x = \begin{pmatrix} 0 & 1 \\ 1 & 0 \end{pmatrix}$, we write the matrix equation

$$\hat{\mathcal{D}}_0 W \equiv [\sigma_y D_t + \sigma_x (iu_p)] W = 0 , \quad (5.6)$$

where $W = \begin{pmatrix} w_1 \\ w_2 \end{pmatrix}$ is a two component spinor. Eq. (5.6) is equivalent to the following decoupled equations

$$(iD_t + iu_p)w_1 = 0 \quad (5.7)$$

$$(-iD_t + iu_p)w_2 = 0 . \quad (5.8)$$

Solving these equations one gets $w_1 \propto \omega_0 / \cos(\omega_0 t)$ and $w_2 \propto \omega_0 \cos(\omega_0 t)$ for the $\kappa = 1$ case and $w_1 \propto \omega_0 / \sinh(\omega_0 t)$ and $w_2 \propto \omega_0 \sinh(\omega_0 t)$ for the $\kappa = -1$ case. Thus, we obtain

$$W = \begin{pmatrix} w_1 \\ w_2 \end{pmatrix} = \begin{pmatrix} w_f \\ w_b \end{pmatrix} . \quad (5.9)$$

This shows that the matrix equation is equivalent to the two second-order linear differential equations of bosonic and fermionic type, Eq. (5.2) and Eq. (5.4), respectively, a result quite well known in particle physics. Indeed, a comparison with the true Dirac equation with a Lorentz scalar potential $S(x)$

$$[-i\sigma_y D_x + \sigma_x (m + S(x))] W = E W , \quad (5.10)$$

shows that Eq. (5.6) corresponds to a Dirac spinor of ‘zero mass’ and ‘zero energy’ in an *imaginary* scalar ‘potential’ $iu_p(t)$. We remind that a detailed discussion of the Dirac equation in the supersymmetric approach has been provided by Cooper et al [42] in 1988. They showed that the Dirac equation with a Lorentz scalar potential is associated with a susy pair of Schrödinger Hamiltonians. This result has been used later by many authors in the particle physics context [43].

5.4 Extension through parameter K

We now come to the main issue of this work. Consider the slightly more general Dirac-like equation

$$\hat{\mathcal{D}}_K W \equiv [\sigma_y D_t + \sigma_x (iu_p + K)]W = KW, \quad (5.11)$$

where K is a (not necessarily positive) real constant. On the left hand side of the equation, K stands as an (imaginary) mass parameter of the Dirac spinor, whereas on the right hand side it corresponds to the energy parameter. Thus, we have an equation equivalent to a Dirac equation for a spinor of mass iK at the fixed energy $E = iK$. This equation can be written as the following system of coupled equations

$$iD_t w_1 + (iu_p + K)w_1 = Kw_2 \quad (5.12)$$

$$-iD_t w_2 + (iu_p + K)w_2 = Kw_1. \quad (5.13)$$

The decoupling can be achieved by applying the operator in Eq. (5.12) to Eq. (5.13). For the fermionic spinor component one gets

$$D_t^2 w_1^+ - \omega_0^2 \left[(1 + 2 \tan^2 \omega_0 t) + i \frac{2K}{\omega_0} \tan \omega_0 t \right] w_1^+ = 0 \quad \text{for } \kappa = 1 \quad (5.14)$$

$$D_t^2 w_1^- + \omega_0^2 \left[(1 - 2 \coth^2 \omega_0 t) + i \frac{2K}{\omega_0} \coth \omega_0 t \right] w_1^- = 0 \quad \text{for } \kappa = -1, \quad (5.15)$$

whereas the bosonic component fulfills

$$D_t^2 w_2^+ + \omega_0^2 \left[1 - i \frac{2K}{\omega_0} \tan \omega_0 t \right] w_2^+ = 0 \quad \text{for } \kappa = 1 \quad (5.16)$$

$$D_t^2 w_2^- - \omega_0^2 \left[1 - i \frac{2K}{\omega_0} \coth \omega_0 t \right] w_2^- = 0 \quad \text{for } \kappa = -1. \quad (5.17)$$

The solutions of the bosonic equations are expressed in terms of the Gauss hypergeometric functions ${}_2F_1$

$$\begin{aligned} w_2^+(t; \alpha_+, \beta_+) &= \alpha_+ z_1^{(p-\frac{1}{2})} z_2^{(q-\frac{1}{2})} {}_2F_1 \left[p+q, p+q-1, 2p; -\frac{1}{2} z_1 \right] \\ -\beta_+ e^{-2ip\pi} z_1^{-(p-\frac{1}{2})} z_2^{-(q-\frac{1}{2})} & {}_2F_1 \left[q-p, q-p+1, 2-2p; -\frac{1}{2} z_1 \right] \end{aligned} \quad (5.18)$$

and

$$\begin{aligned} w_2^-(t; \alpha_-, \beta_-) &= \alpha_- z_3^r z_4^s {}_2F_1 \left[r+s, r+s+1, 1+2r; \frac{1}{2} z_3 \right] \\ &+ \beta_- z_3^{-r} z_4^{-s} {}_2F_1 \left[s-r+1, s-r, 1-2r; \frac{1}{2} z_3 \right], \end{aligned} \quad (5.19)$$

where the variables z_i ($i = 1, \dots, 4$) are given in the following form:

$$z_{1,2} = i \tan(\omega_0 t) \mp 1, \quad z_{3,4} = \coth(\omega_0 t) \pm 1,$$

respectively. The parameters are the following:

$$p = \frac{1}{2} \left(1 + \sqrt{1 - \frac{2K}{\omega_0}} \right), \quad q = \frac{1}{2} \left(1 + \sqrt{1 + \frac{2K}{\omega_0}} \right),$$

$$r = \frac{1}{2} \sqrt{1 + i \frac{2K}{\omega_0}}, \quad s = \frac{1}{2} \sqrt{1 - i \frac{2K}{\omega_0}}.$$

The fermionic zero modes can be obtained as the inverse of the bosonic ones. Thus

$$w_1^+ = \frac{1}{w_2^+(t; \alpha_+, \beta_+)}, \quad w_1^- = \frac{1}{w_2^-(t; \alpha_-, \beta_-)}. \quad (5.20)$$

A comparison of w_1^+ with the common $1/\cos t$ fermionic mode is displayed in Figs. 5.3 and 5.4.

In the small K regime, $K \ll \omega_0$, one gets

$$w_2^+(t; \alpha_+, \beta_+) \approx \alpha_+ z_1^{(p-\frac{1}{2})} z_2^{(q-\frac{1}{2})} {}_2F_1 \left[2, 1, 2 - \frac{K}{\omega_0}; -\frac{1}{2} z_1(t) \right] -$$

$$\beta_+ e^{-2ip\pi} 4^{(p-\frac{1}{2})} z_1^{-(p-\frac{1}{2})} z_2^{(q-\frac{1}{2})} {}_2F_1 \left[\frac{K}{\omega_0}, 1 + \frac{K}{\omega_0}, \frac{K}{\omega_0}; -\frac{1}{2} z_1(t) \right] \quad (5.21)$$

and

$$w_2^-(t; \alpha_-, \beta_-) \approx \alpha_- z_3^r z_4^s {}_2F_1 \left[1, 2, 2 + i \frac{K}{\omega_0}; \frac{1}{2} z_3(t) \right] +$$

$$\beta_- 4^r z_3^{-r} z_4^s {}_2F_1 \left[1 - i \frac{K}{\omega_0}, -i \frac{K}{\omega_0}, -i \frac{K}{\omega_0}; \frac{1}{2} z_3(t) \right]. \quad (5.22)$$

Examining the bosonic equations, one can immediately see that the resonant frequencies acquired resistive time-dependent losses whose relative strength is given by the parameter K. The fermionic equations having time-dependent real parts of the frequency can be interpreted as parametric oscillators which are also affected by losses through the imaginary part.

5.5 More K parameters

A more general case in this scheme is to consider the following matrix Dirac-like equation

$$\left[\begin{pmatrix} 0 & -i \\ i & 0 \end{pmatrix} D_t + \begin{pmatrix} 0 & 1 \\ 1 & 0 \end{pmatrix} \begin{pmatrix} iu_p + K_1 & 0 \\ 0 & iu_p + K_2 \end{pmatrix} \right] \begin{pmatrix} w_1 \\ w_2 \end{pmatrix} =$$

$$\begin{pmatrix} K'_1 & 0 \\ 0 & K'_2 \end{pmatrix} \begin{pmatrix} w_1 \\ w_2 \end{pmatrix}. \quad (5.23)$$

The system of coupled first-order differential equations will be now

$$\left[-iD_t + iu_p + K_2 \right] w_2 = K'_1 w_1 \quad (5.24)$$

$$\left[iD_t + iu_p + K_1 \right] w_1 = K'_2 w_2 \quad (5.25)$$

and the equivalent second-order differential equations

$$D_t^2 w_i + \left[-i\Delta K \right] D_t w_i + \left[\pm D_t u_p + i(K_1 + K_2)u_p + (K_1 K_2 - K'_1 K'_2) - u_p^2 \right] w_i = 0, \quad (5.26)$$

where the subindex $i = 1, 2$ and $\Delta K = K_1 - K_2$. Under the gauge transformation

$$w_i = Z_i \exp \left(-\frac{1}{2} \int^t \left[-i\Delta K \right] d\tau \right) = Z_i(t) e^{\frac{1}{2} i t \Delta K}, \quad (5.27)$$

one gets

$$D_t^2 Z_i + Q_i(t) Z_i = 0, \quad (5.28)$$

where the ‘potentials’ have the form

$$Q_i(t) = \left[\pm D_t u_p + i(K_1 + K_2)u_p + (K_1 K_2 - K'_1 K'_2) - u_p^2 \right] - \frac{1}{4} \left[-i\Delta K \right]^2 \quad (5.29)$$

$Q_{1,2}$ are functions that differ from the nonoperatorial parts in Eqs. (5.55)-(5.33) only by constant terms. Indeed, one can obtain easily the following equations.

For the fermionic spinor component one gets

$$D_t^2 Z_1^+ - \omega_0^2 \left[1 + 2 \tan^2 \omega_0 t - \frac{(\Delta K)^2}{4\omega_0^2} - \frac{K_1 K_2 - K'_1 K'_2}{\omega_0^2} + i \frac{K_1 + K_2}{\omega_0} \tan \omega_0 t \right] Z_1^+ = 0 \quad (5.30)$$

for $\kappa = 1$, and

$$D_t^2 Z_1^- + \omega_0^2 \left[1 - 2 \coth^2 \omega_0 t + \frac{(\Delta K)^2}{4\omega_0^2} + \frac{K_1 K_2 - K'_1 K'_2}{\omega_0^2} + i \frac{K_1 + K_2}{\omega_0} \coth \omega_0 t \right] Z_1^- = 0 \quad (5.31)$$

for $\kappa = -1$.

The bosonic component fulfills

$$D_t^2 Z_2^+ + \omega_0^2 \left[1 + \frac{(\Delta K)^2}{4\omega_0^2} + \frac{K_1 K_2 - K'_1 K'_2}{\omega_0^2} - i \frac{K_1 + K_2}{\omega_0} \tan \omega_0 t \right] Z_2^+ = 0, \quad (5.32)$$

for $\kappa = 1$, and

$$D_t^2 Z_2^- - \omega_0^2 \left[1 - \frac{(\Delta K)^2}{4\omega_0^2} - \frac{K_1 K_2 - K'_1 K'_2}{\omega_0^2} - i \frac{K_1 + K_2}{\omega_0} \coth \omega_0 t \right] Z_2^- = 0, \quad (5.33)$$

for $\kappa = -1$. When $K_1 = K_2 = K$ one gets the particular case studied in full detail above.

The more general bosonic modes have the form:

$$\begin{aligned} Z_2^+(t; \alpha_+, \beta_+) &= \alpha_+ [\tan(\omega_0 t) - i]^{\frac{\Omega_1}{4\omega_0}} [\tan(\omega_0 t) + i]^{\frac{\Omega_2}{4\omega_0}} \\ &\times {}_2F_1 \left[\frac{\Omega_1 + \Omega_2}{4\omega_0}, \frac{\Omega_1 + \Omega_2}{4\omega_0} + 1, 1 + \frac{\Omega_1}{2\omega_0}; \frac{1}{2} (\tan(\omega_0 t) - i) \right] \\ &\quad + \beta_+ (-1)^{-\frac{\Omega_1}{2\omega_0}} [\tan(\omega_0 t) - i]^{-\frac{\Omega_1}{4\omega_0}} [\tan(\omega_0 t) + i]^{\frac{\Omega_2}{4\omega_0}} \\ &\times {}_2F_1 \left[\frac{\Omega_2 - \Omega_1}{4\omega_0}, \frac{\Omega_2 - \Omega_1}{4\omega_0} + 1, 1 - \frac{\Omega_1}{2\omega_0}; \frac{1}{2} (\tan(\omega_0 t) - i) \right] \end{aligned} \quad (5.34)$$

and

$$\begin{aligned} Z_2^-(t; \alpha_-, \beta_-) &= \alpha_- [\coth(\omega_0 t) - 1]^{\frac{\Omega_3}{4\omega_0}} [\coth(\omega_0 t) + 1]^{\frac{\Omega_4}{4\omega_0}} \\ &\times {}_2F_1 \left[\frac{\Omega_3 + \Omega_4}{4\omega_0} + 1, \frac{\Omega_3 + \Omega_4}{4\omega_0}, 1 + \frac{\Omega_3}{2\omega_0}; -\frac{1}{2}(\coth(\omega_0 t) - 1) \right] \\ &+ \beta_- (-1)^{-\frac{\Omega_3}{2\omega_0}} 4^{\frac{\Omega_3}{2\omega_0}} [\coth(\omega_0 t) - 1]^{-\frac{\Omega_3}{4\omega_0}} [\coth(\omega_0 t) + 1]^{\frac{\Omega_4}{4\omega_0}} \\ &\times {}_2F_1 \left[\frac{\Omega_3 - \Omega_4}{4\omega_0}, \frac{\Omega_4 - \Omega_3}{4\omega_0} + 1, 1 - \frac{\Omega_3}{2\omega_0}; -\frac{1}{2}(\coth(\omega_0 t) - 1) \right], \end{aligned} \quad (5.35)$$

where

$$\begin{aligned} \Omega_1 &= \left(4\omega_0^2 + (K_1 + K_2)^2 + 4[(K_1 + K_2)\omega_0 - K'_1 K'_2] \right)^{1/2}, \\ \Omega_2 &= \left(4\omega_0^2 + (K_1 + K_2)^2 - 4[(K_1 + K_2)\omega_0 + K'_1 K'_2] \right)^{1/2}, \\ \Omega_3 &= \left(4\omega_0^2 - (K_1 + K_2)^2 - 4[i(K_1 + K_2)\omega_0 - K'_1 K'_2] \right)^{1/2}, \\ \Omega_4 &= \left(4\omega_0^2 - (K_1 + K_2)^2 + 4[i(K_1 + K_2)\omega_0 + K'_1 K'_2] \right)^{1/2}. \end{aligned}$$

5.6 Possible applications of the K-modes

5.6.1 Waveguides.

In view of the correspondence between mechanics and optics, one can also provide an interpretation in terms of the Helmholtz optics for light propagation in waveguides of special profiles. The supersymmetry of the Helmholtz equation has been studied by Wolf and collaborators [44]. To get the waveguide application, one should switch from the temporal independent variable to a spatial variable $t \rightarrow x$ along which we consider the inhomogeneity of the fiber whereas the propagation of beams is along another supplementary spatial coordinate z . Thus, we turn the equations (5.55)-(5.56) into Helmholtz waveguide equations of the type (we take $c = 1$)

$$[\partial_z^2 + \partial_x^2 + \omega_0^2 n^2(x)]\varphi(x, z) = 0, \quad (5.36)$$

where the modes $\varphi(x, z)$ can be written in the form $w_{1,2}(x)e^{-ik_z z}$ for a fixed wavenumber k_z in the propagating coordinate that is common to both wave functions and the index profiles correspond to two pairs of bosonic-fermionic waveguides and are given by

$$n_b^2(x) \sim 1 - i\frac{2K}{k_0} \tan(k_0 x), \quad n_f^2(x) \sim -(1 + 2 \tan^2(\omega_0 x)) - i\frac{2K}{k_0} \tan(k_0 x), \quad (5.37)$$

and

$$n_b^2(x) \sim -1 - i\frac{2K}{k_0} \coth(k_0 x), \quad n_f^2(x) \sim 1 - 2\coth^2(k_0 x) + i\frac{2K}{k_0} \coth(k_0 x), \quad (5.38)$$

respectively. In our units $k_0 = \omega_0$. Eqs. (5.37), (5.38) can be obtained from Riccati equations of the type ($c \neq 1$)

$$\omega_0^2 n_{f,b}^2(x)/c^2 = k^2 \mp R_x - R^2, \quad (5.39)$$

where $R(x)$ are Riccati solutions directly related to the Riccati solutions discussed in the previous sections.

According to Chumakov and Wolf [44] a second waveguide interpretation is possible describing two different Gaussian beams, bosonic and fermionic, whose small difference in frequency is given in terms of a small parameter ε (wavelength/beam width), propagating in the *same* waveguide. In this interpretation, the index profile is the same for both beams. For illustration, let us take the normal oscillator Riccati solution in the space variable x , i.e., $\tan k_0 x$ that we approximate to first order linear Taylor term $k_0 x$. Then, the two beam interpretation leads to the following Riccati equation (for details, see the paper of Chumakov and Wolf)

$$\omega_{1,2}^2 n^2(x) - \omega_0^2 n^2(0) = \mp k_0 - k_0^2 x^2 (1 \mp \varepsilon). \quad (5.40)$$

An almost exact, up to nonlinear corrections of order ε^2 and higher, supersymmetric pairing of the z wavenumbers (propagating constants) occurs, except for the ‘ground state’ one. As noted by Chumakov and Wolf, supersymmetry connects in this case light beams of different frequencies but having the same wavelength in the propagation direction z . This approach is valid only in the paraxial approximation. Therefore, one should know the small x behavior of the K-modes in order to hope to detect them through stable interference patterns along the waveguide axis.

5.6.2 Cavity physics.

Another very interesting application of the K-modes in a radial variable could be Schumann’s resonances, i.e., the resonant frequencies of the spherical cavity provided by the Earth’s surface and the ionosphere plasma layer [45]. The Schumann problem can be approached as a spherical Helmholtz equation $[\nabla_r^2 + k^2]\phi = 0$ with Robin type (mixed) boundary condition $\frac{\partial \phi}{\partial n}|_S = C(\omega)\phi_S$, where $C(\omega)$ is expressed in terms of the skin depth $\delta = \sqrt{2/(\mu_c \sigma \omega)}$ of the conducting wall, μ_c is its permeability and σ is its conductivity. The eigenfrequencies fulfilling such boundary conditions can be written as follows

$$\omega^2 \approx \omega_0^2 [(1 - I) + iI], \quad (5.41)$$

where I is a complicated expression in terms of skin depths and surface and volume integrals of Helmholtz solutions with Neumann boundary conditions $\frac{\partial \phi}{\partial n}|_S = 0$. It is worth noting the similarity between these improved values of Schumann’s eigenfrequencies and the K-eigenfrequencies. Moreover, using the Q parameter of the cavity, one can write Eq. (5.41) in the form

$$\omega^2 \approx \omega_0^2 \left[\left(1 - \frac{1}{Q}\right) + i\frac{1}{Q} \right]. \quad (5.42)$$

This form shows that the modification of the real part of ω leads to a downward shift of the resonant frequencies, while the contribution to the imaginary component changes the rate of decay of the modes.

We point out that Jackson mentions in his textbook that the near equality of the real and imaginary parts of the change in ω^2 is a consequence of the employed boundary condition, which is appropriate for relatively good conductors. Thus, by changing the form of $C(\omega)$ that could result from different surface impedances, the relative magnitude of the real and imaginary parts of the change in ω^2 can be made different. It is this latter case that corresponds better to the K-modes.

5.6.3 Crystal models.

There is also a strong mathematical similarity between the K-modes and the solutions of Scarf's crystal model [46] based on the singular potential $V(x) = -V_0 \operatorname{cosec}^2(\pi x/a)$, where a is an arbitrary lattice parameter. For this model the one-dimensional Schrödinger equation has the form

$$\psi'' + (a/\pi)^2 \left[\lambda^2 + \left(\frac{1}{4} - s^2 \right) \operatorname{cosec}^2(\pi x/a) \right] \psi = 0. \quad (5.43)$$

For $0 < x \leq a/2$, the general solution is

$$\begin{aligned} \psi = & [f(x)]^{\frac{1}{2}+s} {}_2F_1 \left[\frac{1}{4} + \frac{1}{2}(s+\lambda), \frac{1}{4} + \frac{1}{2}(s-\lambda); 1+s; f^2(x) \right] + \\ & [f(x)]^{\frac{1}{2}-s} {}_2F_1 \left[\frac{1}{4} - \frac{1}{2}(s-\lambda), \frac{1}{4} - \frac{1}{2}(s+\lambda); 1-s; f^2(x) \right], \end{aligned} \quad (5.44)$$

where $f(x) = \sin(\pi x/a)$ corresponds to the $z_i(t)$ functions, and s and λ corresponding to $-p$ and $-q$, respectively, are related to the potential amplitude and energy spectral parameter. Thus, by turning the K-oscillator equations into corresponding Schrödinger equations, one could introduce another analytical crystal model with possible applications in photonics crystals.

5.6.4 Cosmology.

Rosu and López-Sandoval apply the K-mode approach to barotropic FRW cosmologies [47]. K- Hubble cosmological parameters have been introduced and expressed as logarithmic derivatives of the K-modes with respect to the conformal time. For $K \rightarrow 0$ the ordinary solutions of the common FRW barotropic fluids have been obtained.

It is also worth noticing the analogy of the nonzero K oscillator case with the phenomenon of diffraction of atomic waves in imaginary crystals of light (crossed laser beams) [48]. In fact, the K parameter is a counterpart of the modulation parameter Q introduced by Berry and O'Dell in their study of imaginary optical gratings. Roughly speaking, the nonzero K modes could occur in an *imaginary crystal of time* that could occur in some exotic astrophysical conditions.

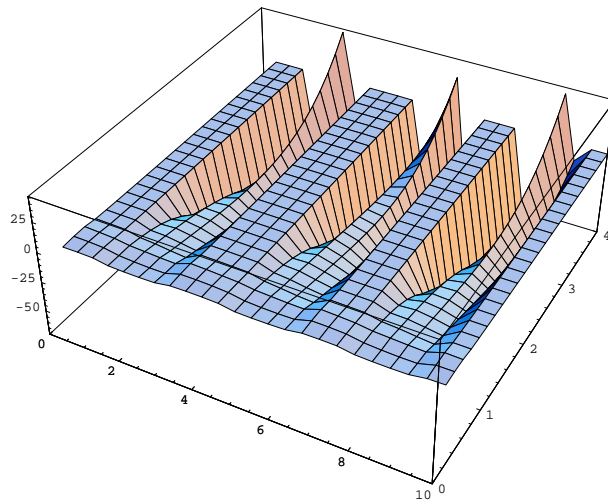


Fig. 5.1: The real part of the bosonic mode $w_2^+(y; \frac{1}{2}, \frac{1}{2})$ for $t \in [0, 10]$ and $K \in [0, 4]$.

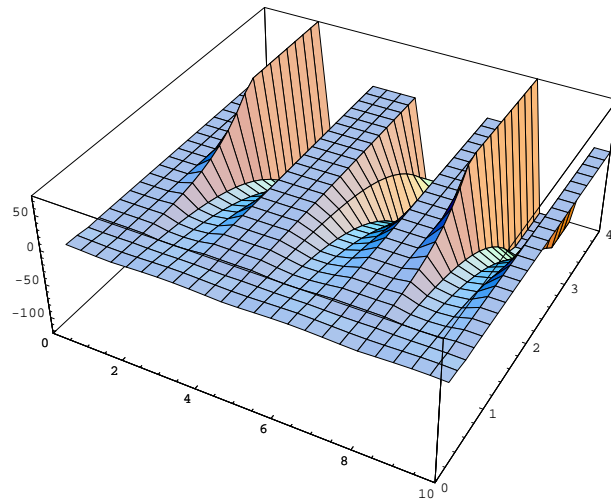


Fig. 5.2: The imaginary part of the bosonic mode $w_2^+(y; \frac{1}{2}, \frac{1}{2})$ for $t \in [0, 10]$ and $K \in [0, 4]$.

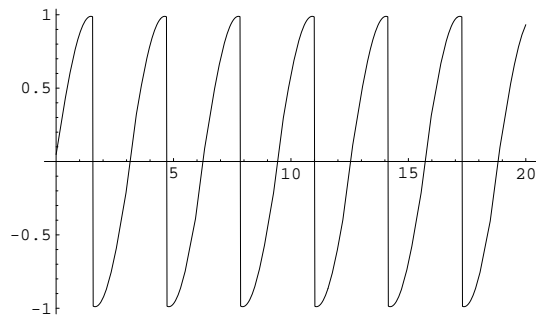


Fig. 5.3: The real part of the bosonic mode $w_2^+(y; \frac{1}{2}, \frac{1}{2})$ for $t \in [0, 20]$ and $K = 0.01$.

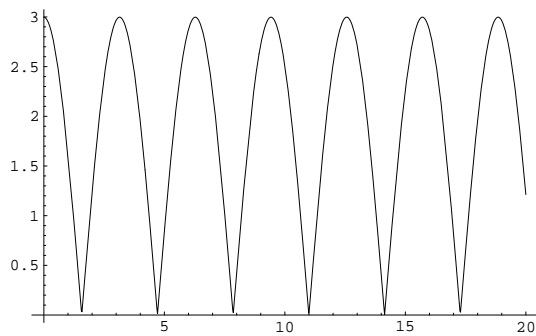


Fig. 5.4: The imaginary part of the bosonic mode $w_2^+(y; \frac{1}{2}, \frac{1}{2})$ for $t \in [0, 20]$ and $K = 0.01$.

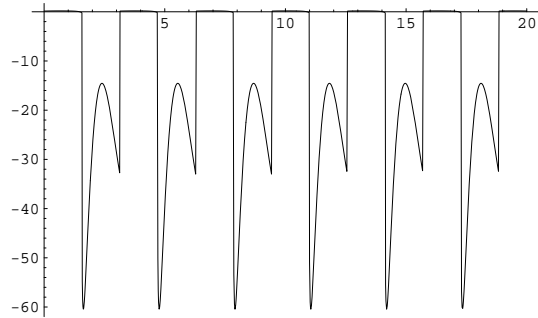


Fig. 5.5: The real part of the bosonic mode $w_2^+(y; \frac{1}{2}, \frac{1}{2})$ for $t \in [0, 20]$ and $K = 2$.

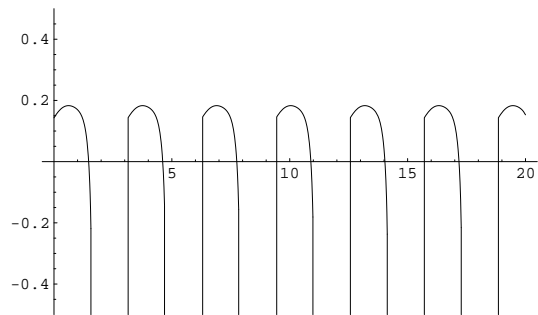


Fig. 5.6: The real part of the bosonic mode $w_2^+(y; \frac{1}{2}, \frac{1}{2})$ for $t \in [0, 20]$ and $K = 2$ in the vertical strip $[-0.5, 0.5]$.

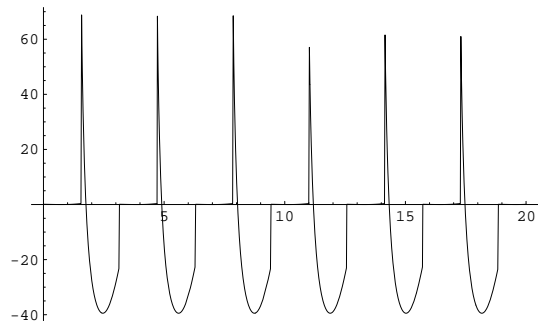


Fig. 5.7: The imaginary part of the bosonic mode $w_2^+(y; \frac{1}{2}, \frac{1}{2})$ for $t \in [0, 20]$ and $K = 2$.

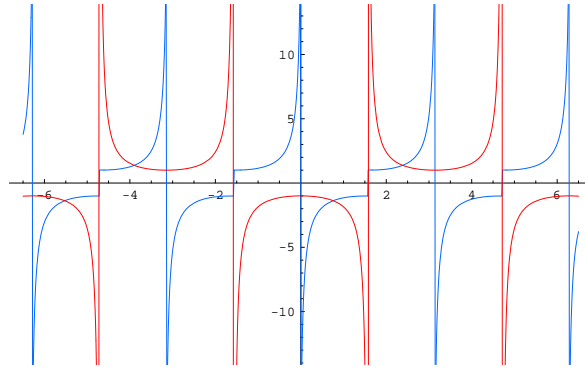


Fig. 5.8: The fermionic zero mode $-1/\text{cost}$, (red curve), and the real part of $-1/w_2^+$, (blue curve), for $K = 0.01$.

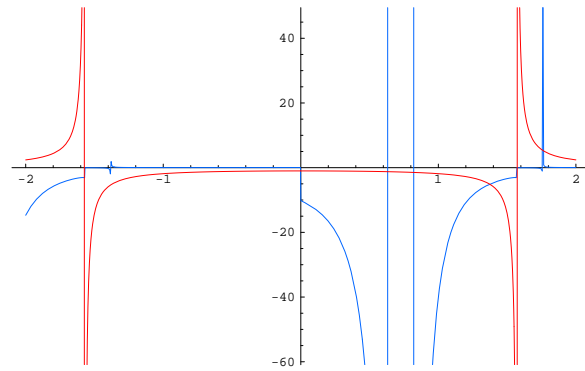


Fig. 5.9: The fermionic zero mode $-1/\text{cost}$, (red curve), and the imaginary part of $-1/w_2^+$, (blue curve), for $K = 2$.

5.7 Quantum mechanics with Riccati nonhermiticity

We have elaborated in the previous sections on an interesting way of introducing imaginary parts (nonhermiticities) in second order differential equations starting from a Dirac-like matrix equation [47, 49]. The procedure is a complex extension of the known supersymmetric connection between the Dirac matrix equation and the Schrödinger equation. A detailed discussion of the Dirac equation in the supersymmetric approach has been provided by Cooper et al. [42, 43] in 1988, who showed that the Dirac equation with a Lorentz scalar potential is associated with a susy pair of Schrödinger Hamiltonians. In the supersymmetric approach one uses the fact that the Dirac potential, that we denote by S , is the solution of a Riccati equation with the free term related to the potential function U in the second order linear differential equations of the Schrödinger type.

Indeed, writing the one-dimensional Dirac equation in the form

$$[\alpha p + \beta m + \beta R(x)]\psi(x) = E\psi(x) \quad (5.45)$$

where $c = \hbar = 1$, $p = -id/dx$, $m (> 0)$ is the fermion mass, and $R(x)$ is a Lorentz scalar. The wave function ψ is a two-component spinor $\begin{pmatrix} \psi_1 \\ \psi_2 \end{pmatrix}$ and the Pauli matrices α and β are the following

$$\sigma_y = \begin{pmatrix} 0 & -i \\ i & 0 \end{pmatrix} \quad \text{and} \quad \sigma_x = \begin{pmatrix} 0 & 1 \\ 1 & 0 \end{pmatrix}$$

Writing the matrix Dirac equation in coupled system form leads to

$$[D_x + m + R]\psi_1 = E\psi_2 \quad (5.46)$$

$$[-D_x + m + R]\psi_2 = E\psi_1 \quad (5.47)$$

By decoupling one gets two Schrödinger equations for each spinor component, respectively

$$H_i\psi_i \equiv [-D_x^2 + U_i]\psi_i = \varepsilon\psi_i, \quad \varepsilon = E^2 - m^2, \quad (5.48)$$

where $i = 1, 2$, and

$$U_i(x) = (R^2 + 2mR \mp dR/dx).$$

One can also write factorizing operators for Eqs. (5.48)

$$A^\pm = \pm D_x + m + R \quad (5.49)$$

such that

$$H_1 = A^-A^+ - \frac{m}{2}, \quad H_2 = A^+A^- - \frac{m}{2} \quad (5.50)$$

However, we have employed the method for the case of the classical harmonic oscillator, which is the very specific situation in which the Dirac mass parameter that we denoted by K was treated as a free parameter *equal* to the Dirac eigenvalue parameter E . This is equivalent to Schrödinger equations at zero energy, $\varepsilon = 0$. On the other hand, it is interesting to see how the method works for negative energies, i.e., for a bound spectrum in quantum mechanics. Here we briefly describe the method and next apply it to the case of Morse potential.

5.8 Complex extension with a single K parameter

We consider the slightly different Dirac-like equation with respect to Eq. (5.45)

$$\hat{\mathcal{D}}_K W \equiv [\sigma_y D_x + \sigma_x (iR + K)]W = KW, \quad (5.51)$$

where K is a (not necessarily positive) real constant. In the left hand side of the equation, K stands as a mass parameter of the Dirac spinor, whereas on the right hand side it corresponds to the energy parameter. R is an arbitrary solution of the Riccati equation of the Witten type [9]

$$R' \pm R^2 = u, \quad (5.52)$$

where u is the real part of the nonhermitic potential in the Schrödinger equations we get.

Thus, we have an equation equivalent to a Dirac equation for a spinor $W = \begin{pmatrix} \phi_1 \\ \phi_0 \end{pmatrix} \equiv$

$\begin{pmatrix} w_f \\ w_b \end{pmatrix}$ of mass K at the fixed energy $E = K$ but in a purely imaginary potential (optical lattices). This equation can be written as the following system of coupled equations

$$iD_x \phi_1 + (iR + K)\phi_1 = K\phi_0 \quad (5.53)$$

$$-iD_x \phi_0 + (iR + K)\phi_0 = K\phi_1 . \quad (5.54)$$

The decoupling of these two equations can be achieved by applying the operator in Eq. (5.54) to Eq. (5.53) . For the fermionic spinor component one gets

$$D_x^2 \phi_1 - [R^2 - D_x R - i2KR] \phi_1 = 0 \quad (5.55)$$

whereas the bosonic component fulfills

$$D_x^2 \phi_0 - [R^2 + D_x R - i2KR] \phi_0 = 0 . \quad (5.56)$$

This is a very simple mathematical scheme for introducing a special type of nonhermiticity directly proportional to the Riccati solution.

5.9 Complex extension with parameters K and K' .

A more general case in this scheme is to consider the following matrix Dirac-like equation

$$\left[\begin{pmatrix} 0 & -i \\ i & 0 \end{pmatrix} D_x + \begin{pmatrix} 0 & 1 \\ 1 & 0 \end{pmatrix} \begin{pmatrix} iR + K & 0 \\ 0 & iR + K \end{pmatrix} \right] \begin{pmatrix} w_1 \\ w_2 \end{pmatrix} = \begin{pmatrix} K' & 0 \\ 0 & K' \end{pmatrix} \begin{pmatrix} w_1 \\ w_2 \end{pmatrix} . \quad (5.57)$$

The system of coupled first-order differential equations will be now

$$[-iD_x + iR + K] w_2 = K' w_1 \quad (5.58)$$

$$[iD_x + iR + K] w_1 = K' w_2 \quad (5.59)$$

and the equivalent second-order differential equations

$$D_x^2 w_i + [\pm D_x R + 2iKR + (K^2 - K'^2) - R^2] w_i = 0 , \quad (5.60)$$

where the subindex $i = 1, 2$ refers to the fermionic and bosonic components, respectively.

5.10 Application to the Morse potential

This potential is frequently used in molecular physics in connection with the disassociation of diatomic molecules. In this case, the Riccati solution is of the type

$$R = A - Be^{-ax} , \quad (5.61)$$

Therefore, the second-order fermionic differential equation will be

$$D_x^2 w_1 + \left[-(\bar{B}e^{-2ax} - \bar{C}_1 e^{-ax}) + (K^2 - K'^2) - A^2 + 2iK(A - Be^{-ax}) \right] w_1 = 0 \quad (5.62)$$

where $\bar{B} = B^2$, and $\bar{C}_1 = B(2A + a)$.

The solution is expressed as a superposition of Whittaker functions

$$w_1 = \alpha_1 e^{ax/2} M_{\kappa_1, \mu} \left(\frac{2B}{a} e^{-ax} \right) + \beta_1 e^{ax/2} W_{\kappa_1, \mu} \left(\frac{2B}{a} e^{-ax} \right) \quad (5.63)$$

$\kappa_1 = \frac{A}{2a} \left(2 + \frac{a}{A} - i\frac{2K}{A} \right)$ and $\mu = \frac{A}{a} \left(\frac{K'^2 - K^2}{A^2} - i\frac{2K}{A} \right)^{1/2}$.

The bosonic equation reads

$$D_x^2 w_2 + \left[-(\bar{B}e^{-2ax} - \bar{C}_2 e^{-ax}) + (K^2 - K'^2) - A^2 + 2iK(A - Be^{-ax}) \right] w_2 = 0 \quad (5.64)$$

where $\bar{B} = B^2$, and $\bar{C}_2 = B(2A - a)$.

The solution is a superposition of the following Whittaker functions

$$w_2 = \alpha_2 e^{ax/2} M_{\kappa_2, \mu} \left(\frac{2B}{a} e^{-ax} \right) + \beta_2 e^{ax/2} W_{\kappa_2, \mu} \left(\frac{2B}{a} e^{-ax} \right) \quad (5.65)$$

where $\kappa_2 = \frac{A}{2a} \left(2 - \frac{a}{A} - i\frac{2K}{A} \right)$ and the μ subindex is unchanged.

If we now place ourselves within the quantum mechanical (hermitic) Morse problem we should take $\beta_2 = 0$ and $K = 0$ in order to achieve the exact correspondence with the bound spectrum problem and eliminate the nonhermiticity. Moreover, the following well-known connection with the associated Laguerre polynomials

$$M_{\frac{p}{2} + n + \frac{1}{2}, \frac{p}{2}}(y) = y^{\frac{p+1}{2}} e^{-y/2} L_n^p(y), \quad y = \frac{2B}{a} e^{-ax} \quad (5.66)$$

can be used in our case with the following identifications

$$\frac{p}{2} = \frac{K'}{a}, \quad K' = (A - an)$$

i.e.,

$$p = 2 \left(\frac{A}{a} - n \right).$$

Then we can write the solution of the hermitic bosonic problem in the well-known form

$$w_{2,n}(y) = \alpha_2 \left(\frac{2B}{a} \right)^{\frac{1}{2}} y^{\frac{A-n}{a}} e^{-y/2} L_n^{2(A-n)}(y). \quad (5.67)$$

If we want to approach the nonhermitic problem we define by analogy with Eq. (5.66)

$$M_{\kappa_2, \mu}(y) = y^{\mu + \frac{1}{2}} e^{-y/2} L_{\kappa_2 - \mu - \frac{1}{2}}^{2\mu}(y), \quad (5.68)$$

where κ_2 and μ are the complex parameters mentioned before and the symbol corresponding to the associated Laguerre polynomial representing now a Laguerre-like

function introduced by definition through Eq. (5.68). The wave function of the nonhermitic problem can be written as follows

$$w_{2,nonherm}(y) = \alpha_2 \left(\frac{2B}{a} \right)^{\frac{1}{2}} y^\mu e^{-y/2} L_{\kappa_2 - \mu - \frac{1}{2}}^{2\mu}(y). \quad (5.69)$$

For the nonhermitic fermionic problem, the formulas are similar with the replacement of κ_2 by κ_1 .

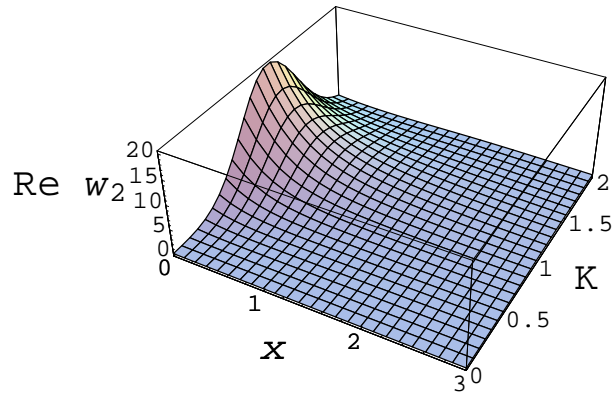


Fig. 5.10: Real part of the bosonic wave function w_2 in the range $x \in [0, 3]$ and $K \in [0, 2]$.

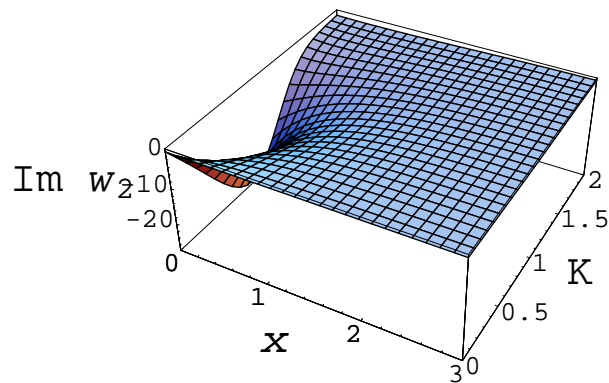


Fig. 5.11: Imaginary part of the bosonic wave function w_2 in the range $x \in [0, 3]$ and $K \in [0, 2]$.

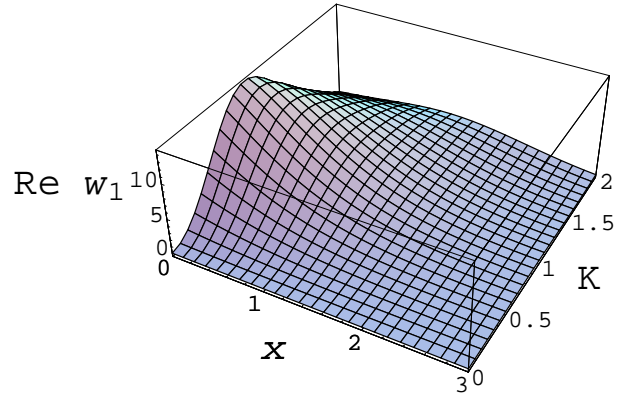


Fig. 5.12: Real part of the fermionic wave function w_1 in the range $x \in [0, 3]$ and $K \in [0, 2]$.

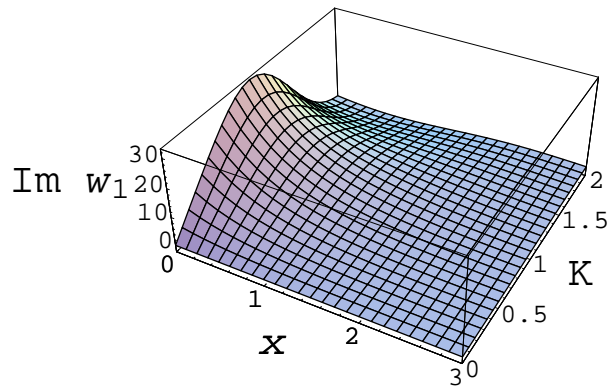


Fig. 5.13: Imaginary part of the fermionic wave function w_1 in the range $x \in [0, 3]$ and $K \in [0, 2]$.

5.11 Conclusion of the chapter

By a procedure involving the factorization connection between the Dirac-like equations and the simple second-order linear differential equations of harmonic oscillator type, a class of classical modes with a Dirac-like parameter describing their damping and absorption (dissipation) has been introduced in this chapter. While for zero values of the

Dirac parameters the highly singular fermionic modes are decoupled from their normal bosonic harmonic modes, at nonzero values a coupling between the two types of modes is introduced at the level of the matrix equation. These interesting modes are given by the solutions of the Eqs. (5.55)-(5.33) and in a more general way by Eqs. (5.27), (5.34)-(5.35) and are expressed in terms of hypergeometric functions. Several possible applications in different fields of physics are mentioned as well. Finally, similar to the fact that the PT quantum mechanics can be considered as a complex extension of standard quantum mechanics, we notice that what we have done here is a particular type of complex extension of the classical harmonic oscillator. The complex supersymmetric extension introduced in the first sections has been applied to exactly solvable quantum Morse problem. The bosonic and fermionic wave functions have been obtained in explicit form. This complex extension could have applications to the diffraction of diatomic molecules on optical lattices (systems of laser beams).

Part II

**SYNCHRONIZATION
METHODS**

6

Preliminary remarks on Part II

The following remarks are pointed out in order to describe the relationship between Part I and Part II of the thesis work, where factorization methods for nonlinear ODE and synchronization of a neuronal ensemble through feedback methods, respectively, have been developed. The study of many biological systems from a mathematical point of view is very stimulating because of the possibilities to forecast the dynamic behavior of such biological systems. An important example is the neuronal dynamics that governs many living organisms. The neuronal dynamics performs the processing of biological information by means of transmitted signals. The pulse propagation along a nerve axon as described by the FitzHugh-Nagumo equation that was solved in Section 2.4 through factorization methods is given by a travelling signal of the kink type. The kink solution represents the transition between two stable equilibrium states, and the "level change" travelling waves are transmitted along the neuron axon [50]. It is a very interesting challenge to study the synchronization dynamics for a minimal ensemble of two neurons. However, the kink type solutions that have been considered by us could not describe the most realistic dynamical behavior for the neuronal ensemble. In fact, the FitzHugh-Nagumo neuron model can be shown to be an approximation (see, e.g. [50]) of the widely known Hodgkin-Huxley (HH) neuron model [69]. Therefore, the problem of neurons synchronization has been addressed in the more realistic case of the HH neuron model. Although theoretical attempts have been made to obtain analytical solutions of the travelling wave type for the HH systems (see, e.g. [51, 52]), it is an easier task to achieve numerical results to study the synchronization dynamics. That is why we do not pay attention to the HH travelling waves in the second part. The nonlinear control theory is a very suitable way to study and search for the intrinsic mechanisms underlying the synchronization phenomena. In the next Chapters 7 and 8, the problem of synchronizing a minimal ensemble of two HH neurons is stated, and results on its synchronized dynamics are achieved by implementing adequate feedback schemes.



Synchronization of chaotic dynamics and neuronal systems

Abstract. In this chapter, the synchronization phenomena and the concept of chaos, their importance in natural process and engineering systems are reviewed. A brief overview of synchronization methods for the control of chaos and its applications in biological systems is presented. Neuronal synchronization activity and its role on brain dynamics is also discussed in order to state the problem of neuronal synchronization employing nonlinear control theory tools. In addition, the dynamical model for the Hodgkin-Huxley (HH) neurons is described.

7.1 Introduction

Synchronization phenomena are very important processes occurring in nature and often produced as a desired behavior in engineering systems. In very general terms, the synchronization of coupled systems means "to share time or events". It refers to the way in which networked elements, due to their dynamics, communicate and exhibit collective behavior [53]. Some examples are the observed synchronized flashing of fireflies, synchronization of cells in a beating heart, the quantum synchronization in superfluidity and superconductivity, in the phenomena related to Josephson tunneling. Other important examples are the generated synchronization in computer chips, communication systems and global positioning systems.

On the other hand, the disquieting question about the exact forecast of the evolution in time of diverse systems produced the discovery of the existence of *chaos*. The concept of chaos usually refers to the issue of whether or not it is possible to make long-term predictions about the behavior of a system. There exist several mathematical definitions of chaos, however, all of them express the property of high sensitivity to the initial conditions. Such a characteristic implies that two even arbitrarily close trajectories, separate exponentially in the course of time. A deterministic system is said to be chaotic if necessary requirements of nonlinearity and dimensionality (of at least three) are characteristic for that system [54].

During the last fifteen years there have been an increased interest in studying chaotic systems, since the proved fact that chaos "cannot be forecasted but it can be controlled" [55]. The issue of the control of chaos is of interest for both theorist and control engineers. Interest arises because of many observations show that the chaotic behavior is common in nature, for instance, chaotic dynamics can be found in meteorology, plasma physics, heart and brain of living organisms; and experimental results dealing with the control of chaotic systems lead us to practically an unlimited amount of technical applications in mechanical and space engineering, electrical and electronic systems, communication and information systems, etc. [56].

Two applications of the control of chaos have been widely studied for the past few year: the control and use of chaos for communication systems, and the synchronization (and suppression) of chaotic dynamics for several communication schemes [54, 57].

In the following section a review of synchronization methods concerning the control of chaotic dynamics and its applications in biological systems is presented. Then we focus on synchronization of a neuronal system comprised of two isolated HH neurons, whose dynamical model is also described in final section. In Chapter 8, the obtained results employing the mathematical tools provided by the nonlinear control theory [58], that can be applied in order to show the way the HH neurons can synchronize are presented. We find that isolated neurons unidirectionally couple and synchronize through feedback action. In addition, robust synchronization dynamics is obtained by implementing a dynamic compensator.

7.2 Synchronization methods for the control of chaos

Many approaches have been proposed to control chaotic dynamics of systems. Open loop or non feedback methods and closed loop or feedback methods [54, 55, 56] have been developed in order to produce the desired behavior in chaotic systems. Two basic problems concerning the control of chaotic dynamics through feedback methods are identified: synchronization and suppression of chaos. Suppression of chaos consists in stabilization of the system around regular orbits or equilibrium points. The chaos synchronization problem has the characteristic that the receiver (slave) system must track in some sense the trajectories of the sender (master) system [59]. Because of uncertainties may appear in the chaos control problem, adaptive schemes are implemented in order to achieve robust synchronization dynamics. Synchronization can be achieved for identical chaotic systems with (obviously) different initial conditions [60], however, researchers have found that non identical systems synchronize when adequate developed feedback schemes are applied [59, 61, 86].

From the standpoint of the geometrical control theory, the synchronization problem can be seen as a stabilization problem. For a defined synchronization error $x_e = x_{e,M} - x_{e,S}$, where x_e represents the difference between the master and slave system states, and $x \in R^d$, $e = 1, 2, \dots, d$, there exists a synchronization error system [61] whose trajectories exponentially converge to zero under a feedback control action; consequently, the master and slave systems unidirectionally couple.

In the following chapter, the statement of the synchronization problem and its solution using the geometrical control theory for a proposed chaotic neuronal system is explained in detail. Also, because of appearing uncertain system states, i.e., non accurately measured states, an adaptive scheme is implemented via construction of a state observer or uncertainty estimator that guarantees robust synchronization.

7.3 Applications of synchronization methods in biological systems

Synchronization methods for the control of chaos where feedback action is implemented have a wide variety of technical and scientific applications. Among the main technical applications of chaos synchronization can be found a diversity of schemes for communication systems. The scientific applications are directed to study properties, regularities, and mechanisms of the behavior of physical, chemical and biological systems. Moreover, very interesting results are obtained when the control methods are applied to experimental systems. Examples of suppression and synchronization of chaos can be found in biomechanical systems, medicine, biology and ecology: design of feedback pacemakers, suppression of oscillating epileptiform activity in neural networks, control of population dynamics in plankton and other biological species, etc.

The main interest in Part II is to apply feedback synchronization methods to a chaotic neuronal system. Two HH neurons are regarded as a system of two dynamical subsystems, with the aim to show that synchronized dynamics is achieved through feedback strategies. Synchronization and suppression of chaos, using the tools of control theory, could provide insights to understand and show their relevance in the processing of biological information in neural networks.

7.4 Synchronized dynamics of neurons

Synchronization of neuronal activity patterns (action potentials) is a fundamental topic in the modern research of brain dynamics. Experimental evidence reveals that synchronization phenomena are basic for the processing of biological information. It has been demonstrated [62] that large ensembles of neurons whose functionality is related to visual perception synchronize their oscillatory activity (in the gamma frequency range, 40-60 Hz) when stimulated. Some researchers consider that neuronal synchronization allows the brain to solve the so-called binding problem [63]. Take for example a car: it may be characterized by its shape, color, emitted noise, and so on. All these features are processed in different parts of the brain, however we conceive the car as a single entity because of still unknown binding procedures. More recent studies suggest that synchronization is a basic mechanism for consciousness [64, 65, 66]. Also, Parkinsonian tremor and epileptic seizures are closely related with this mechanism [63, 67].

Recently, it was shown that two coupled living neurons synchronize their activity patterns when depolarized by an external current [68]. However, the whole underlying mechanisms are not completely understood. From a theoretical point of view, neurons are considered as nonlinear oscillators. A lot of theoretical studies have been carried out to investigate the dynamics of single neurons and neural networks. The most employed and realistic neuron models are the Hodgkin-Huxley and the FitzHugh-Nagumo systems [63], that have been used in detailed studies of neuron behavior under external forcing. Moreover, within these models one can consider the change of dynamical parameters and implications on the neuronal activity, for instance, the strength of synaptic conductance, and intrinsic or added noise. The neuronal synchronization problem is addressed regarding diffusive coupling, or modelling unidirectionally coupled master-slave systems. Many people believe that control theory could be very useful to address the problem of synchronization in ensembles of neurons. The mathematical tools provided by the nonlinear control theory, can suitably be applied to the mathematical model of a system comprised of two noiseless HH neurons.

7.5 The Hodgkin-Huxley model of the neuron

The brain is the most complex system known to us. Understanding the way it works and its structure has been a very interesting research issue during many decades. The basic units which integrate the brain tissue and, in general, any nervous system, are the nerve cells or neurons. The transmission of signals and the processing of biological information are carried out through complicated interactions between large ensembles of neurons. External and internal stimuli generate the biological information which propagates from the sensory sites to specific areas of the brain, for instance, the visual, olfactory and auditive perception, and the conscious sensory-motor activity.

Most of the nerve cells generate a series of voltage spiking sequences called the membrane action potential, in response to external stimuli performing the information processing. These pulses of the action potential originate at the cell body and propagate down the axon at constant amplitude and velocity. They can be transmitted via synaptic coupling to another nerve cell which is stimulated by the corresponding current. The electric behavior of the cell axon membrane is described by the net ion flux through a great amount of potassium and sodium ionic channels; each ion passing from the inner (outer) to the outer (inner) side of the cell. It is known that potassium and sodium channels are composed of four independent *gates*, which can be in a permissive or non permissive state. The potassium ions cross the membrane only through channels that are specific for potassium. If the four gates of a potassium channel are in permissive state, then the channel is open and potassium ions flow through it. The sodium ions cross the membrane only through channels that are specific for sodium. Three of the gates for a sodium channel are activation gates, and one is inactivation gate. All of them must be in permissive state to allow sodium ions to cross the sodium channel.

Several neuron models have been proposed to describe the dynamics of the action potentials. However, the most widely used is still the realistic HH neuron model [69]. In the early 1950's, Hodgkin and Huxley developed and published a series of investigations where they studied the electrophysiology of the squid giant axon. Their results allow them to calculate the total membrane current as the sum of the potassium and calcium ionic channels currents and the capacitive current,

$$I_m(t) = I_{ionic}(t) + C_m \frac{dV(t)}{dt}. \quad (7.1)$$

In addition, based on the large number of realized experiments they postulated a phenomenological model that turned itself into a paradigm for the generation of the action potential in the squid axon. We follow next the recent discussion in the book of C. Koch [70] for a compact presentation of the main statements of the HH model:

1. The action potential involves two major voltage-dependent ionic conductances, a sodium conductance g_{Na} and a potassium conductance g_K . They are independent from each other. A third, smaller "leak" conductance g_l does not depend on the membrane potential. The total ionic current flowing is given by the following equation

$$I_{ionic}(t) = I_{Na} + I_K + I_{leak}. \quad (7.2)$$

2. The individual ionic currents $I_i(t)$ are linearly related to driving potential via Ohm's law,

$$I_i(t) = g_i(V(t), t)(V(t) - E_i) \quad (7.3)$$

where the ionic reversal potential E_i is given by Nernst's equation for the appropriate ionic species. Depending on the balance between the concentration difference of the ions and the electrical field across the membrane separating the intracellular cytoplasm from the extracellular milieu, each ionic species has an associated "ionic battery". Conceptually, there exist an equivalent electrical circuit to describe the axonal membrane.

3. Each of the two ionic conductances is expressed as a maximum conductance, g_{Na} and g_K , multiplied by a numerical coefficient representing the fraction of the maximum conductance actually open. These numbers are functions of one or more fictive gating particles Hodgkin and Huxley introduced to describe the dynamics of the conductances. In their original model, they talked about activating and inactivating gating particles. Each gating particle can be in one of two possible states, open or close, depending on time and on the membrane potential. In order for the conductance to open, all of these gating particles must be open simultaneously. The entire kinetic properties of their model are contained in these variables.

The gating particles, also known as gating variables, Hodgkin and Huxley presented are usually denoted by n , m and h . They are the same as the currently known ion channel gates. The following set of four coupled nonlinear differential equations represents the complete HH neuron dynamical model [69]:

$$C_m \frac{dV}{dt} = I_{ext} - g_K n^4 (V - V_K) - g_{Na} m^3 h (V - V_{Na}) - g_l (V - V_{Na}), \quad (7.4)$$

$$\frac{dn}{dt} = \alpha_n(V)(1-n) - \beta_n(V)n, \quad (7.5)$$

$$\frac{dm}{dt} = \alpha_m(V)(1-m) - \beta_m(V)m, \quad (7.6)$$

$$\frac{dh}{dt} = \alpha_h(V)(1-h) - \beta_h(V)h, \quad (7.7)$$

where V represents the membrane potential, n is the probability of any given potassium channel gate being in the permissive state (activation of the potassium flow current), m is the probability of any given activation sodium channel gate being in the permissive state (activation of the sodium flow current), and h is the probability of any given inactivation sodium channel gate being in the permissive state (inactivation of the sodium flow current). Gating variables are dimensionless and within the range $[0,1]$. C_m is the membrane capacitance, g_K , g_{Na} and g_l are the maximum ionic and leak conductances, while V_K , V_{Na} and V_l stand for the ionic and leak reversal potentials. The external stimulus current can be modelled by the term I_{ext} , usually a tonic or periodic forcing. The respective differential equations for n , m and h , describe the transition from open to closed states for the gating variables. The explicit form of the functions $\alpha_j(V)$ and $\beta_j(V)$ ($j = n, m, h$) in Eqs. (7.5)-(7.7) is given as follows [69, 70],

$$\alpha_n = \frac{0.01(V+10)}{\{\exp[(V+10)/10] - 1\}}, \quad \beta_n = 0.125 \exp(V/80); \quad (7.8)$$

$$\alpha_m = \frac{0.1(V+25)}{\{\exp[(V+25)/10] - 1\}}, \quad \beta_m = 4 \exp(V/18); \quad (7.9)$$

$$\alpha_h = 0.07 \exp(V/20), \quad \beta_h = \frac{1}{\{\exp[(V+30)/10] + 1\}}. \quad (7.10)$$

Also, nominal values for the system parameters can be found in [69, 70].



Unidirectional synchronization of Hodgkin-Huxley neurons

Abstract. Synchronization dynamics of two noiseless Hodgkin-Huxley (HH) neurons under the action of feedback control is studied. The spiking patterns of the action potentials evoked by periodic external modulations attain synchronization states under the feedback action. Numerical simulations for the synchronization dynamics of regular-irregular desynchronized spiking sequences are displayed. The results are discussed in context of generalized synchronization. It is also shown that the HH neurons can be synchronized in face of unmeasured states.

8.1 Introduction

For several decades many attempts have been addressed to understand the processing of biological information in single neurons and neural networks. Experimental reports [71, 72, 73] suggest that the synchronization plays a very important role in the processing of information by large ensembles of neurons. Recently, it has been demonstrated that a minimal ensemble of two coupled living neurons fire synchronized spiking activity when depolarized by an external DC current [74]. However, total neural mechanisms underlying synchronization are not well understood yet. The Hodgkin-Huxley neurons are usually used as realistic models of neuronal systems, for studying neuronal synchronization. Some theoretical approaches investigate the synchronization phenomena considering diffusive coupling and the influence of intrinsic noise as a promoter of neuronal activity [75, 76], and studying the synchronization dynamics related to the rhythmic oscillations phenomena (theta and gamma frequency rhythms) in neurons of localized areas of the brain [77, 78, 79]. In addition, the forcing of HH neurons by external stimulus has been widely studied [80, 81, 82, 83, 84] for tonic or periodic currents that trigger the action potential displaying spike activity and refractory dynamics.

On the other hand, synchronization of chaotic systems is a relatively recent phenomena [60] which can be understood from nonlinear geometrical control theory [59, 61]. In this chapter we study the synchronized behavior of two silent (i.e., the autonomous HH systems exhibit fixed point dynamics) [81] HH neurons, proposing an unidirectionally coupled

synchronization system. In the chaos synchronization problem the trajectories of a slave system must track, in some sense, the trajectories of a master system even though slave and master systems may be different. The obtained results contribute in the theoretical framework of neurons synchronization, and relates the phenomena to the well-posed concept of generalized synchronization (GS) [85]. Because of uncertain states cannot be accurately measured in practice, they are not available to do control, for instance, the ionic channels activation. Then, an approach for robust synchronization via construction of an uncertainty estimator, is implemented.

The organization of this chapter is as follows. In Section 8.2 the HH neuronal systems are described. The statement of the problem for unidirectionally coupling synchronization of HH neurons is given in Section 8.3. The HH neuronal synchronization dynamics obtained through a stabilizing control law is studied in Section 8.4. In Section 8.5 the generalized and robust synchronization are discussed, and a final conclusion section is given.

8.2 The Hodgkin-Huxley system redefined

We redefine the HH system of equations in order to state the synchronization problem of two HH neurons. Let $x_{i,M}$ and $x_{i,S}$ ($i = 1, 2, 3, 4$ and subscripts M, S stand for the master and slave system, respectively) be the four variables V , n , m and h in each system. As the meaning of synchronous behavior is "to share time or events", we shall consider two HH neurons modelled by Eqs. (7.4)-(7.7). Thus, the master system is represented by the following set of equations:

$$\dot{x}_{1,M} = 1/C_{mM} [I_{extM}(t) - g_{K_M} x_{2,M}^4 (x_{1,M} - V_{K_M}) - g_{NaM} x_{3,M}^3 x_{4,M} (x_{1,M} - V_{NaM}) - g_{lM} (x_{1,M} - V_{lM})], \quad (8.1)$$

$$\dot{x}_{2,M} = \alpha_n(x_{1,M}) (1 - x_{2,M}) - \beta_n(x_{1,M}) x_{2,M}, \quad (8.2)$$

$$\dot{x}_{3,M} = \alpha_m(x_{1,M}) (1 - x_{3,M}) - \beta_m(x_{1,M}) x_{3,M}, \quad (8.3)$$

$$\dot{x}_{4,M} = \alpha_h(x_{1,M}) (1 - x_{4,M}) - \beta_h(x_{1,M}) x_{4,M}, \quad (8.4)$$

and the slave system is proposed to be governed by the equations:

$$\dot{x}_{1,S} = 1/C_{mS} [I_{extS}(t) - g_{K_S} x_{2,S}^4 (x_{1,S} - V_{K_S}) - g_{NaS} x_{3,S}^3 x_{4,S} (x_{1,S} - V_{NaS}) - g_{lS} (x_{1,S} - V_{lS})] + u, \quad (8.5)$$

$$\dot{x}_{2,S} = \alpha_n(x_{1,S}) (1 - x_{2,S}) - \beta_n(x_{1,S}) x_{2,S}, \quad (8.6)$$

$$\dot{x}_{3,S} = \alpha_m(x_{1,S}) (1 - x_{3,S}) - \beta_m(x_{1,S}) x_{3,S}, \quad (8.7)$$

$$\dot{x}_{4,S} = \alpha_h(x_{1,S}) (1 - x_{4,S}) - \beta_h(x_{1,S}) x_{4,S}, \quad (8.8)$$

where the added term u in Eq. (8.5) represents a feedback synchronization force. Nominal values are considered for parameters of the master system: $C_{mM} = 1 \mu F/cm^2$, $g_{K_M} = 36 m\Omega^{-1}/cm^2$, $g_{NaM} = 120 m\Omega^{-1}/cm^2$, $g_{lM} = 0.3 m\Omega^{-1}/cm^2$, $V_{K_M} = 12 mV$, $V_{NaM} = -115 mV$ and $V_{lM} = -10.613 mV$, and parameters for the slave system are chosen with a difference of 10 % from the nominal values: $C_{mS} = 0.9 \mu F/cm^2$, $g_{K_S} = 32.4 m\Omega^{-1}/cm^2$, $g_{NaS} = 108 m\Omega^{-1}/cm^2$, $g_{lS} = 0.27 m\Omega^{-1}/cm^2$, $V_{K_S} = 10.8 mV$, $V_{NaS} = -103.5 mV$ and $V_{lS} = -9.5517 mV$. Under such a parameters both neurons shall not "share time solutions", then they cannot be synchronous.

8.3 Synchronization problem statement

In the nonlinear control theory a synchronization problem can be stated as a feedback stabilization one [61, 86]. It has been established that for a defined synchronization error, $x_e = x_{e,M} - x_{e,S}$ (where $x \in R^d$, $e = 1, 2, \dots, d$), there exists a synchronization error (dynamical) system [61] whose trajectories exponentially converge to zero under a feedback control u . Hence, it can be said that the master and slave systems (unidirectionally) couple and attain a synchronization dynamical state under the action of the control command u . The following definition of Exact Synchronization is presented in [59]:

Definition 1. It is said that two chaotic systems are exactly synchronized if the synchronization error, $x_e = x_{e,M} - x_{e,S}$, exponentially converges to the origin. This implies that at a finite time $x_{e,S} = x_{e,M}$.

In this section, a proof for the Exact Synchronization of two HH neurons is provided.

Lemma 1. Consider the two HH neuronal systems represented in Eqs. (8.1)-(8.8). Such two silent HH neurons attain dynamical states of Exact Synchronization for all $t > t_0 \geq 0$ under the action of a nonlinear feedback control despite parametric differences for any initial condition $x_i(0) = x_{i,M}(0) - x_{i,S}(0)$ in the domain physically realizable.

Proof. Let us define the following synchronization error system for the HH neuronal systems:

$$\dot{x} = F(x, t) + G(x)u = \Delta f(x) + \Delta I(t) - Bu, \quad y = h(x) = x_1, \quad (8.9)$$

where

$$\Delta f(x) = \begin{pmatrix} \{-1/C_{mM} [g_{KM}x_{2,M}^4(x_{1,M} - V_{KM}) + g_{NaM}x_{3,M}^3x_{4,M}(x_{1,M} - V_{NaM}) + g_{lM}(x_{1,M} - V_{lM})] + 1/C_{mS} [g_{KS}x_{2,S}^4(x_{1,S} - V_{KS}) + g_{NaS}x_{3,S}^3x_{4,S}(x_{1,S} - V_{NaS}) + g_{lS}(x_{1,S} - V_{lS})]\} \\ \{\alpha_n(x_{1,M})(1 - x_{2,M}) - \beta_n(x_{1,M})x_{2,M} \\ - \alpha_n(x_{1,S})(1 - x_{2,S}) + \beta_n(x_{1,S})x_{2,S}\} \\ \{\alpha_m(x_{1,M})(1 - x_{3,M}) - \beta_m(x_{1,M})x_{3,M} \\ - \alpha_m(x_{1,S})(1 - x_{3,S}) + \beta_m(x_{1,S})x_{3,S}\} \\ \{\alpha_h(x_{1,M})(1 - x_{4,M}) - \beta_h(x_{1,M})x_{4,M} \\ - \alpha_h(x_{1,S})(1 - x_{4,S}) + \beta_h(x_{1,S})x_{4,S}\} \end{pmatrix},$$

$$\Delta I(t) = \left(\frac{I_{extM}(t)}{C_{mM}} - \frac{I_{extS}(t)}{C_{mS}}, 0, 0, 0 \right)^T, \quad B = (1, 0, 0, 0)^T,$$

$\Delta f(x)$ is a smooth vector field, $\Delta I(t)$ is the difference between the external exciting forces and $y \in R$ represents the measured state of the system. The relative degree of a system is defined as the number of times one has to differentiate the output $y(t)$ before the control action u explicitly appears [58]. It can be easily shown that the relative degree for the system (8.9) is $\rho = 1$. Let us consider now the **Proposition 4.4.2** given in [58]. The following stabilizing control law is proposed,

$$u = \frac{1}{L_g L_f^{\rho-1} h(x)} \left(-L_f^\rho h(x) - c_0 h(x) - c_1 L_f h(x) - \dots - c_{\rho-1} L_f^{\rho-1} h(x) \right) \quad (8.10)$$

where $L_f h(x)$ stands for the Lie derivative of the function $h(x)$ along the vector field f , and the constant parameters $c_0, c_1, \dots, c_{\rho-1}$, belong to the polynomial $p(s) = c_0 + c_1 s + \dots +$

$c_{\rho-1}s^{\rho-1} + s^{\rho}$ with all its eigenvalues having negative real part. Then, the synchronization error system (8.9) is stabilized by the control law $u = [-L_F h(x) - C_0 h(x)]/L_G h(x)$, and C_0 is a positive real constant that represents the convergence rate. Under the control action given by

$$\begin{aligned} u = & 1/C_{m_M} [I_{ext_M}(t) - g_{K_M} x_{2,M}^4 (x_{1,M} - V_{K_M}) - g_{Na_M} x_{3,M}^3 x_{4,M} (x_{1,M} - V_{Na_M}) \\ & - g_{l_M} (x_{1,M} - V_{l_M})] - 1/C_{m_S} [I_{ext_S}(t) - g_{K_S} x_{2,S}^4 (x_{1,S} - V_{K_S}) \\ & - g_{Na_S} x_{3,S}^3 x_{4,S} (x_{1,S} - V_{Na_S}) - g_{l_S} (x_{1,S} - V_{l_S})] + C_0 (x_{1,M} - x_{1,S}) \end{aligned} \quad (8.11)$$

Eq. (8.9) becomes

$$\dot{x}_1 = -C_0 x_1, \quad (8.12)$$

$$\begin{aligned} \dot{x}_2 = & \alpha_n(x_{1,M}) - \alpha_n(x_{1,M}, x_1) - [\alpha_n(x_{1,M}) + \beta_n(x_{1,M}) - \alpha_n(x_{1,M}, x_1) \\ & - \beta_n(x_{1,M}, x_1)] x_{2,M} - [\alpha_n(x_{1,M}, x_1) + \beta_n(x_{1,M}, x_1)] x_2, \end{aligned} \quad (8.13)$$

$$\begin{aligned} \dot{x}_3 = & \alpha_m(x_{1,M}) - \alpha_m(x_{1,M}, x_1) - [\alpha_m(x_{1,M}) + \beta_m(x_{1,M}) - \alpha_m(x_{1,M}, x_1) \\ & - \beta_m(x_{1,M}, x_1)] x_{3,M} - [\alpha_m(x_{1,M}, x_1) + \beta_m(x_{1,M}, x_1)] x_3, \end{aligned} \quad (8.14)$$

$$\begin{aligned} \dot{x}_4 = & \alpha_h(x_{1,M}) - \alpha_h(x_{1,M}, x_1) - [\alpha_h(x_{1,M}) + \beta_h(x_{1,M}) - \alpha_h(x_{1,M}, x_1) \\ & - \beta_h(x_{1,M}, x_1)] x_{4,M} - [\alpha_h(x_{1,M}, x_1) + \beta_h(x_{1,M}, x_1)] x_4. \end{aligned} \quad (8.15)$$

Because of the system (8.12)-(8.15) is minimum-phase (see Appendix A at the end of the chapter), the obtained control law u leads the trajectories of the synchronization error system to asymptotically converge to zero in a finite time. \square

Remark 1. It should be noted that, by definition, Exact Synchronization implies that $x_M \equiv x_S$ for any time $t > t_0 \geq 0$ and $x(0) = x_M(0) - x_S(0)$ in a given domain. Now, also by definition, GS corresponds to the state where the states of slave systems can be written as a function of the master states (i.e., $x_S = \psi(x_M)$). Thus, as we shall see below, the unidirectional synchronization of noiseless HH neurons is exact and $x_S = I x_M$, where I stands for the identity matrix.

In order to establish the GS between the neurons (8.1)-(8.8), the following results state the conditions to derive an expression for $x_S = \psi(x_M)$. Thus, we depart from the Fact 1.

The following definitions are useful concepts presented in [58]. For two vector fields f and g , both defined on an open subset U of R^n (i.e., $U \subset R^n$), the *Lie bracket* $[f, g]$ is a third vector field defined by $[f, g](x) = \frac{\partial g}{\partial x} f(x) - \frac{\partial f}{\partial x} g(x)$, where $\frac{\partial g}{\partial x}$ and $\frac{\partial f}{\partial x}$ are Jacobian matrices.

For a given set of d vector fields f_1, \dots, f_d , all defined on the same open set U , let $\Delta(x) = \text{span}\{f_1(x), \dots, f_d(x)\}$ be a subspace of R^n spanned by the vectors f_1, \dots, f_d , at any fixed point x in U . The subspace $\Delta(x)$ of R^n , for $x \in U$, is called a *distribution*. A distribution Δ is *involutive* if $\tau_1 \in \Delta$, $\tau_2 \in \Delta \Rightarrow [\tau_1, \tau_2] \in \Delta$, where τ_1 and τ_2 are any pair of vector fields belonging to Δ .

Fact 1 [58]. Consider an affine nonlinear system $\dot{x} = f(x) + g(x)u$; where $x \in \Omega \subseteq R^n$, $u \in R$, $g, f: R^n \rightarrow R^n$ are smooth vector fields. Besides, let us consider that $y = h(x)$ for any smooth function $h(x)$. If involutivity condition is satisfied, then the mappings $\Phi_1: R^n \rightarrow R^p$, $x \mapsto z$ and $\Phi_2: R^n \rightarrow R^{n-p}$, $x \mapsto (z, v)$ are such that the affine nonlinear

system can be written in the canonical form

$$\begin{aligned}\dot{z}_i &= z_{i+1}, \quad i = 1, 2, \dots, \rho - 1, \\ \dot{z}_\rho &= \alpha(z, v) + \beta(z, v)u, \\ \dot{v} &= \zeta(z, v),\end{aligned}\quad (8.16)$$

and can be derived from Lie derivatives of the output function $h(x)$ along the vector fields $f(x)$ and $g(x)$ as follows

$$z = \Phi_1(x) = \begin{pmatrix} h(x) \\ L_f h(x) \\ \vdots \\ L_f^{\rho-1} h(x) \end{pmatrix}\quad (8.17)$$

and

$$v = \Phi_2(x) = \begin{pmatrix} \phi_{\rho+1}(x) \\ \phi_{\rho+2}(x) \\ \vdots \\ \phi_n(x) \end{pmatrix},\quad (8.18)$$

moreover, it is always possible to chose $\phi_{\rho+1}, \dots, \phi_n$ in such a way that

$$L_g \phi_j(x) = 0, \quad \rho + 1 \leq j \leq n.\quad (8.19)$$

□

The Fact 1 is well known in nonlinear control theory. Here it is included for clarity in presentation and exploited in neuronal synchronization towards robust feedback synchronization of HH neurons.

Fact 2 [58]. If exists the map $\Phi = (\Phi_1, \Phi_2) : R^n \rightarrow R^n$, $x \mapsto (z, v)$ derived from (8.17) and (8.18), then there exists the inverse $\Phi^{-1}(\Phi(x)) = x \in \Omega \subset R^n$. This fact is proved since $h(x), L_f h(x), \dots, L_f^{\rho-1} h(x)$ and $\phi_{\rho+1}(x), \dots, \phi_n(x)$ are linearly independent at any x in the neighborhood $U \subset \Omega \subseteq R^n$ of the point x^0 in Ω .

8.4 Synchronizing the Hodgkin-Huxley neurons

Once obtained the control action (8.11), it can be directly implemented in Eq. (8.5) for the slave system leading to the following set of coupled nonlinear differential equations,

$$\begin{aligned}\dot{x}_{1,M} &= 1/C_{mM} [I_{extM}(t) - g_{KM} x_{2,M}^4 (x_{1,M} - V_{KM}) \\ &\quad - g_{NaM} x_{3,M}^3 x_{4,M} (x_{1,M} - V_{NaM}) - g_{lM} (x_{1,M} - V_{lM})],\end{aligned}\quad (8.20)$$

$$\dot{x}_{2,M} = \alpha_n(x_{1,M}) (1 - x_{2,M}) - \beta_n(x_{1,M}) x_{2,M},\quad (8.21)$$

$$\dot{x}_{3,M} = \alpha_m(x_{1,M}) (1 - x_{3,M}) - \beta_m(x_{1,M}) x_{3,M},\quad (8.22)$$

$$\dot{x}_{4,M} = \alpha_h(x_{1,M}) (1 - x_{4,M}) - \beta_h(x_{1,M}) x_{4,M},\quad (8.23)$$

$$\begin{aligned}\dot{x}_{1,S} &= 1/C_{mM} [I_{extM}(t) - g_{KM} x_{2,M}^4 (x_{1,M} - V_{KM}) \\ &\quad - g_{NaM} x_{3,M}^3 x_{4,M} (x_{1,M} - V_{NaM}) - g_{lM} (x_{1,M} - V_{lM})] \\ &\quad + C_0 (x_{1,M} - x_{1,S}),\end{aligned}\quad (8.24)$$

$$\dot{x}_{2,S} = \alpha_n(x_{1,S}) (1 - x_{2,S}) - \beta_n(x_{1,S}) x_{2,S},\quad (8.25)$$

$$\dot{x}_{3,S} = \alpha_m(x_{1,S}) (1 - x_{3,S}) - \beta_m(x_{1,S}) x_{3,S},\quad (8.26)$$

$$\dot{x}_{4,S} = \alpha_h(x_{1,S}) (1 - x_{4,S}) - \beta_h(x_{1,S}) x_{4,S}.\quad (8.27)$$

The above set of equations represents the dynamics of the HH neuronal synchronization when the control action u is implemented. The right-hand side of Eq. (8.24) describes the new induced dynamics of the slave system. The master and slave systems unidirectionally couple through u ; also parametric differences have been subtracted. The term containing the convergence rate C_0 can be interpreted as a synaptic-like control current (divided by a constant capacitance) being $C_0 C_{mM}$ a constant synaptic conductance. In the framework of geometrical control and its applications on communicating systems, the synchronization of chaotic dynamics for the HH neurons could be understood as synchronization of a transmitter (master)-receiver (slave) system. Interpretation of HH neurons as chaotic systems in context of communicating systems, which transmit information, could provide insight to understand the way the biological information is processed in neuronal ensembles.

Numerical simulations were carried out for the HH neuronal synchronization system. Sinusoidal exciting modulations are considered, and the amplitude and frequency parameters are chosen within the U -shaped curve shown in Fig. 1.(b) of reference [81]. This curve encapsulates the region of parameter space (in amplitude and frequency domain) where the exciting modulations trigger spike trains of the action potential in the model system of single silent HH neurons.

Fig. 8.1 shows desynchronized regular (master system) and irregular (slave system) spiking patterns and the transition to a regular synchronized state of the action potentials. The applied forcing functions are $I_{extM}(t) = -2.58\sin(.245t)$ and $I_{extS}(t) = -3.15\sin(.715t)$. Initial conditions were chosen as $x_{i,M}(0) = (10\text{mV}, 0, 0, 0)$ and $x_{i,S}(0) = (0, 0, 0, 0)$, and the control action was implemented at time $t_0 = 180\text{ms}$. A choice for $C_0 = 0.3$ leads to rapid synchronization convergence for the refractory period. The activation and inactivation dynamics for the ionic channels also attains synchronization state. Fig. 8.2 shows the evolution in time of voltage per second which is supplied to the neuronal system to achieve the synchronization. Fig. 8.3 shows the phase locking of the action potentials in synchronized state of Fig. 8.1.

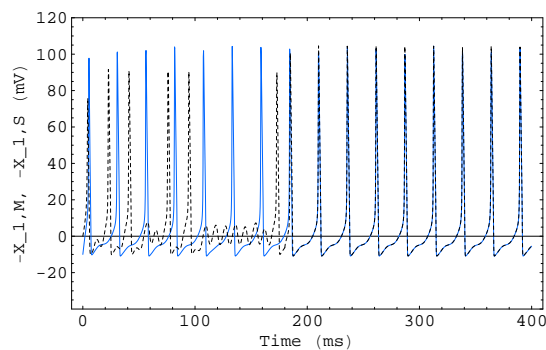


Fig. 8.1: Spiking patterns of the master (solid line) and slave (dashed line) systems for the action potentials in desynchronized and synchronized states. The forcing functions amplitude and frequency parameters as specified in the text: $I_{extM}(t) = -2.58\sin(.245t)$, $I_{extS}(t) = -3.15\sin(.715t)$.

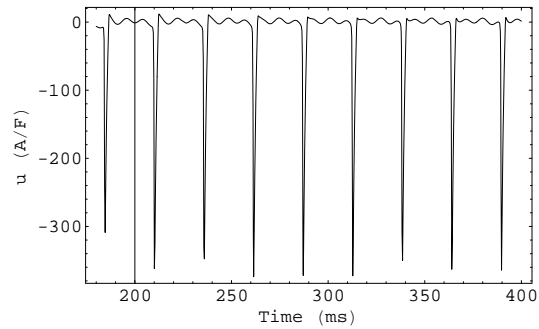


Fig. 8.2: Dynamical response of the implemented control action of Fig 8.1.

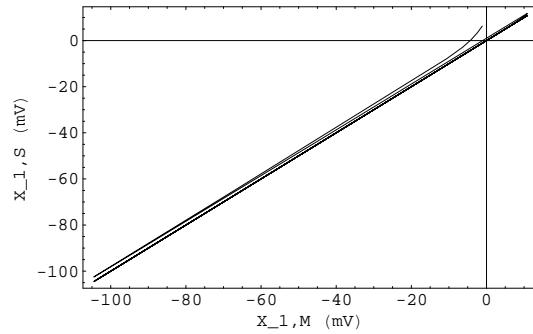


Fig. 8.3: Phase locking of the synchronized action potentials of Fig 8.1.

Note that the nonlinear feedback (8.11) requires information about currents flowing through the membrane and the ionic channels of the master and slave neurons. Such a coupling cannot be implemented in practice on real neurons. However, as we shall see below, the controller (8.11) allows to discuss the robust synchronization in context of GS, which is the most significant phenomenon in chaotic synchronization. Thus, once neuron synchronization is discussed in terms of GS, the robust synchronization is proposed by relaxing the nonlinear controller (8.11) towards a linear approach. This linear approach is robust in the sense that synchronization is induced in face of parameter mismatches and differences between amplitude and frequency parameters in external current entering into master and slave neurons.

8.5 Generalized and robust synchronization

8.5.1 Generalized synchronization

In this subsection, we derive the mappings $\Phi_1 : R^n \rightarrow R^\rho$, $x \mapsto z$ and $\Phi_2 : R^n \rightarrow R^{n-\rho}$, $x \mapsto (z, v)$, and write the HH model of neurons in canonical form (8.16) towards generalized synchronization (GS).

Dynamical models for each HH neuron can be written in nonlinear affine form $\dot{x} = f(x) + g(x)u$, with

$$f(x) = \begin{pmatrix} \{1/C_m[I_{ext} - g_K x_2^4(x_1 - V_K) - g_{Na} x_3^3 x_4(x_1 - V_{Na}) - g_l(x_1 - V_{Na})]\} \\ \alpha_n(x_1)(1 - x_2) - \beta_n(x_1)x_2 \\ \alpha_m(x_1)(1 - x_3) - \beta_m(x_1)x_3 \\ \alpha_h(x_1)(1 - x_4) - \beta_h(x_1)x_4 \end{pmatrix}, \quad g(x) = \begin{pmatrix} 1 \\ 0 \\ 0 \\ 0 \end{pmatrix}, \quad (8.28)$$

and the output $y = h(x)$ is given by the membrane potential, i.e., $h(x) = x_1$. By computing the Lie derivatives of the output function along the vector fields (8.28), we obtain

$$z = \Phi_1(x) = h(x) = x_1 \quad (8.29)$$

and

$$v = \Phi_2(x) = \begin{pmatrix} \phi_1(x) \\ \phi_2(x) \\ \phi_3(x) \end{pmatrix}, \quad (8.30)$$

then according to Eqs. (8.18) and (8.19) v can be chosen as

$$v = \begin{pmatrix} v_1 \\ v_2 \\ v_3 \end{pmatrix} = \begin{pmatrix} x_2 \\ x_3 \\ x_4 \end{pmatrix}. \quad (8.31)$$

Consequently, the previous HH model (7.4)-(7.7) is transformed into

$$\dot{z}_1 = 1/C_m[I_{ext} - g_K v_1^4(z_1 - V_K) - g_{Na} v_2^3 v_3(z_1 - V_{Na}) - g_l(z_1 - V_{Na})] + u, \quad (8.32)$$

$$\dot{v}_1 = \alpha_n(z_1)(1 - v_1) - \beta_n(z_1)v_1, \quad (8.33)$$

$$\dot{v}_2 = \alpha_m(z_1)(1 - v_2) - \beta_m(z_1)v_2, \quad (8.34)$$

$$\dot{v}_3 = \alpha_h(z_1)(1 - v_3) - \beta_h(z_1)v_3. \quad (8.35)$$

In what follows we show how the GS can be studied in HH neurons by departing from Lemma 1 and Fact 1. To this end, we can separately transform both master and slave neurons. In this manner, we shall derive the maps $\Phi_M(x_M)$ and $\Phi_S(x_S)$ to get

$$\begin{pmatrix} z_M \\ v_M \end{pmatrix} = \begin{pmatrix} \Phi_{1M}(x_M) \\ \Phi_{2M}(x_M) \end{pmatrix} \quad \text{and} \quad \begin{pmatrix} z_S \\ v_S \end{pmatrix} = \begin{pmatrix} \Phi_{1S}(x_S) \\ \Phi_{2S}(x_S) \end{pmatrix}, \quad (8.36)$$

from where each HH neuron can be transformed into (8.16) and driving signal (8.10) induces the master behavior onto slave neuron. Then, if stability holds and neurons are minimum-phase systems, $(z_S, v_S) \rightarrow (z_M, v_S^*)$ for $t > t_0 \geq 0$, for any initial conditions $(z(0), v(0)) = (\Phi_1(x(0)), \Phi_2(x(0)))$ in physical domain. Note that v_S^* is a stable manifold

which can correspond to the stable manifold of the master neuron v_M^* . In this case complete synchronization is achieved. In case $v_S^* \neq v_M^*$, the partial state synchronization is attained [59]. Anyway, the composition $\Phi_S^{-1}(\Phi_1(x_M); v_S^*) = x_S \in \Omega \subset R^n$, where Ω denotes the physical domain. In particular, if $v_S^* \equiv v_M^*$ for all time $t > t_0 \geq 0$, where t_0 stands for time of turning on the control, then $x_S = \Phi_S^{-1}(\Phi_{1M}(x_M), \Phi_{2M}(x_M))$. Since HH neurons (7.4)-(7.7) are minimum-phase systems (see Appendix A at the end of the chapter), the GS yields the following relation

$$x_S = \begin{pmatrix} h_S^{-1}(h_M(x_M)) \\ x_{2S}^* \\ x_{3S}^* \\ x_{4S}^* \end{pmatrix}. \quad (8.37)$$

Now, it should be pointed out that driving signal (8.10) has full information about states of both master and slave neurons. This situation cannot be physically realizable (for example, currents due to the ionic channels activity cannot be available for feedback). In next paragraphs, a robust approach is taken from open literature to show how the HH neurons can be synchronized.

8.5.2 Robust synchronization

The nonlinear controller (8.11) allows to obtain states of Exact Synchronization for the silent HH neurons represented by systems (8.1)-(8.8). However, because of measurements for activation and inactivation of the ionic channels cannot be physically carried out, implementation of the control action (8.11) would be unpractical. Then, an adaptive scheme to yield robust synchronization is realized by using a modified feedback control law. The synchronization error system (8.9) can be represented in the following extended form [61],

$$\dot{z}_1 = \eta + \beta_E(z)u, \quad \dot{\eta} = \Gamma(z_1, \eta, v, u), \quad \dot{v} = \zeta(z_1, v), \quad y = z_1, \quad (8.38)$$

where the invertible coordinates change $x = (z_1, v)$ has been developed; $\eta = \Delta f_1(z_1, v) + \Delta I_1(t)$, represents an augmented state which lumps the uncertain terms (the ionic channels activation and inactivation variables for the master and slave systems) contained in Δf_1 , v is the state vector for the internal dynamics and $\beta_E(z) = -1$. In order to stabilize the synchronization error system, we consider the nonlinear controller (8.11) and observe that it can be written in the following (linearizing-like) form

$$u = [\eta + kz_1] \quad (8.39)$$

where $k \in R_+$ represents a control gain value. However, since the control law (8.39) depends on the uncertain state η , it is not physically realizable. The problem of estimating (z_1, η) is solved by using a high-gain observer (dynamic compensator) [61],

$$\dot{\hat{z}}_1 = \hat{\eta} - u + L_0 \kappa_1^* (z_1 - \hat{z}_1), \quad (8.40)$$

$$\dot{\hat{\eta}} = L_0^2 \kappa_2^* (z_1 - \hat{z}_1), \quad (8.41)$$

where $(\hat{z}_1, \hat{\eta})$ are the estimated values of (z_1, η) ; L_0 is the unique tuning parameter, and represents a high-gain estimation parameter that can be interpreted as the uncertainties estimation rate. The parameters $\kappa_{1,2}$ are chosen for the polynomial $P(s) = s^2 + \kappa_2 s + \kappa_1 = 0$ with all its eigenvalues in the left-half complex plane.

The linearizing control law with uncertainty estimation that, together with the dynamic compensator (8.40)-(8.41), stabilizes the synchronization error at the origin and, consequently, synchronizes the HH neuronal systems now becomes

$$u = [\hat{\eta} + k\hat{z}_1]. \quad (8.42)$$

A stability analysis for the closed loop system (8.38), (8.40)-(8.42) is provided in Appendix B at the end of the chapter. A tuning algorithm for stability and duration time is also provided in [87]. Thus, controller (8.40)-(8.42) is a general approach to synchronization of HH neurons despite it lacks knowledge about the states of activation and/or inactivation of the potassium and sodium ionic channels.

It is pointed out that the modified feedback control law (8.40)-(8.42) yields Complete Practical Synchronization [59], i.e., the trajectories of the synchronization error system converge around the origin within a ball of radius L_0^{-1} .

Once obtained the modified control law, it can be implemented in systems (8.1)-(8.8). Then, we are led to the following extended system of differential equations that guarantees the robust synchronization of HH neurons,

$$\begin{aligned} \dot{x}_{1,M} &= 1/C_{m_M} [I_{ext_M}(t) - g_{K_M}x_{2,M}^4(x_{1,M} - V_{K_M}) \\ &\quad - g_{Na_M}x_{3,M}^3x_{4,M}(x_{1,M} - V_{Na_M}) - g_{l_M}(x_{1,M} - V_{l_M})], \end{aligned} \quad (8.43)$$

$$\dot{x}_{2,M} = \alpha_n(x_{1,M})(1 - x_{2,M}) - \beta_n(x_{1,M})x_{2,M}, \quad (8.44)$$

$$\dot{x}_{3,M} = \alpha_m(x_{1,M})(1 - x_{3,M}) - \beta_m(x_{1,M})x_{3,M}, \quad (8.45)$$

$$\dot{x}_{4,M} = \alpha_h(x_{1,M})(1 - x_{4,M}) - \beta_h(x_{1,M})x_{4,M}, \quad (8.46)$$

$$\begin{aligned} \dot{x}_{1,S} &= 1/C_{m_S} [I_{ext_S}(t) - g_{K_S}x_{2,S}^4(x_{1,S} - V_{K_S}) \\ &\quad - g_{Na_S}x_{3,S}^3x_{4,S}(x_{1,S} - V_{Na_S}) - g_{l_S}(x_{1,S} - V_{l_S})] + (\hat{\eta} + k\hat{z}_1), \end{aligned} \quad (8.47)$$

$$\dot{x}_{2,S} = \alpha_n(x_{1,S})(1 - x_{2,S}) - \beta_n(x_{1,S})x_{2,S}, \quad (8.48)$$

$$\dot{x}_{3,S} = \alpha_m(x_{1,S})(1 - x_{3,S}) - \beta_m(x_{1,S})x_{3,S}, \quad (8.49)$$

$$\dot{x}_{4,S} = \alpha_h(x_{1,S})(1 - x_{4,S}) - \beta_h(x_{1,S})x_{4,S}, \quad (8.50)$$

$$\dot{\hat{z}}_1 = -k\hat{z}_1 + L_0\kappa_1^*((x_{1,M} - x_{1,S}) - \hat{z}_1), \quad (8.51)$$

$$\dot{\hat{\eta}} = L_0^2\kappa_2^*((x_{1,M} - x_{1,S}) - \hat{z}_1), \quad (8.52)$$

Fig. 8.4 shows the attained robust synchronization dynamics for the master (solid line) and slave (dashed line) systems when the modified feedback control law has been implemented. The control gain value was chosen as $k = 1$, the $\kappa_{1,2}$ parameters were chosen for the polynomial $P(s)$ with its eigenvalues located at $s = -20$, and the high-gain parameter is $L_0 = 50$. The applied forcing functions are taken as in Section 8.4, $I_{ext_M}(t) = -2.58\sin(.245t)$ and $I_{ext_S}(t) = -3.15\sin(.715t)$. Initial conditions were chosen as $x_{i,M}(0) = (10mV, 0, 0, 0)$ and $x_{i,S}(0) = (0, 0, 0, 0)$, and the modified control law was implemented at time $t_0 = 200$ ms. Dynamics of the ionic channels is also synchronized by the modified control law. Fig. 8.5 shows the evolution in time of voltage per second which is supplied to the neuronal system to achieve the robust synchronization. Fig. 8.6 shows the phase locking of the action potentials for the robust synchronization state of Fig. 8.4.

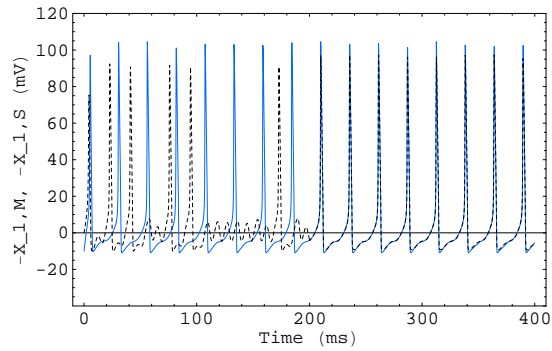


Fig. 8.4: Spiking patterns of the master (solid line) and slave (dashed line) systems for the action potentials in desynchronized state and the transition to a robust synchronization state when the modified feedback control law is implemented. The forcing functions are

$$I_{ext_M}(t) = -2.58\sin(.245t), I_{ext_S}(t) = -3.15\sin(.715t).$$

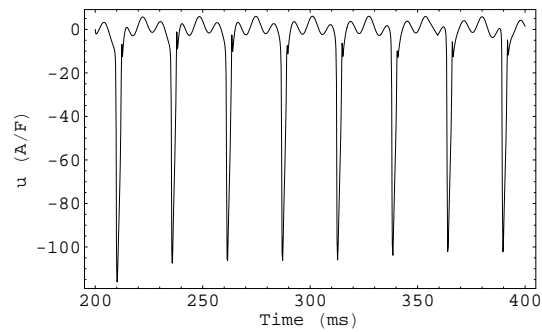


Fig. 8.5: Dynamical response of the implemented modified control law of Fig 8.4.

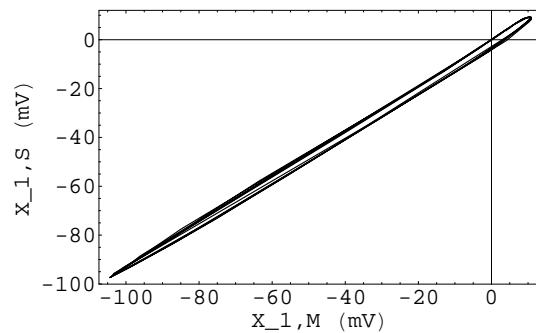


Fig. 8.6: Phase locking of the action potentials in robust synchronization state of Fig 8.4.

8.6 Conclusion of the chapter

In this chapter, we have shown that there exists a nonlinear unidirectional coupling such that two silent HH neurons attain synchronized states in spite of parametric discrepancies. Results show that synchronized spiking patterns of the action potentials are displayed by the unidirectionally coupled system of HH neurons. The synchronization coupling via the control action (8.11) yields a synaptic-like control current term containing as control parameter the convergence rate. Increases on the control parameter have the effect to allow faster synchronization convergence for the refractory dynamics. Regular spiking patterns in synchronized state can be achieved for regular-irregular desynchronized spiking sequences as shown in Fig. 8.1. Because of measurements for the ionic channels activation and inactivation are not physically realizable, a robust adaptive scheme has been developed to yield the synchronization dynamics of the HH neurons. A modified feedback control law composed of a dynamic compensator and a linearizing control law with uncertainties estimation has been implemented. The adaptive scheme leads to robust synchronization dynamical states of the action potentials as shown in Fig. 8.4. The ionic channels activity is also synchronized. The dynamic compensator allows to reconstruct the dynamics of the states (z_1, η) from measurements of the action potentials, and it requires only one tuning parameter, L_0 . Artificial devices experimentally implemented in neuronal systems [74] are elucidating in the unveiling of mechanisms underlying synchronization and control parameters perform a very important role. The nonlinear control theory could provide useful methods in studying synchronization phenomena in single neurons and neural networks, even though natural properties like intrinsic noise and synaptic conductances must be regarded.

Appendix A: Internal dynamics of the synchronization error system

The synchronization error system (8.12)-(8.15) is already in canonical form. This means that the closed-loop system has two subsystems: the first one, given by Eq. (8.12), is controllable while second one, given by Eqs. (8.13)-(8.15), is not affected by the unidirectionally synchronization force u . Hence, to assure asymptotic stability it is necessary to study the dynamics of subsystem (8.13)-(8.15). If subsystem (8.13)-(8.15) is (asymptotically) stable at origin, then the closed-loop is said minimum-phase and, as a consequence, the synchronization force u leads the trajectories of system (8.9) to zero. Thus, we have that, for any time $t > t_0 \geq 0$, $x_M \equiv x_S$ and GS via Exact Synchronization is achieved. The zero dynamics can be obtained by setting $x_1 = 0$ [58] and considering the master system dynamics,

$$\begin{aligned}
 \dot{x}_2 &= -[\alpha_n(x_{1,M}) + \beta_n(x_{1,M})]x_2, \\
 \dot{x}_3 &= -[\alpha_m(x_{1,M}) + \beta_m(x_{1,M})]x_3, \\
 \dot{x}_4 &= -[\alpha_h(x_{1,M}) + \beta_h(x_{1,M})]x_4, \\
 \dot{x}_{1,M} &= 1/C_{mM} [I_{extM}(t) - g_{KM}x_{2,M}^4(x_{1,M} - V_{KM}) \\
 &\quad - g_{NaM}x_{3,M}^3x_{4,M}(x_{1,M} - V_{NaM}) - g_{lM}(x_{1,M} - V_{lM})], \\
 \dot{x}_{2,M} &= \alpha_n(x_{1,M})(1 - x_{2,M}) - \beta_n(x_{1,M})x_{2,M}, \\
 \dot{x}_{3,M} &= \alpha_m(x_{1,M})(1 - x_{3,M}) - \beta_m(x_{1,M})x_{3,M}, \\
 \dot{x}_{4,M} &= \alpha_h(x_{1,M})(1 - x_{4,M}) - \beta_h(x_{1,M})x_{4,M}.
 \end{aligned} \tag{A.1}$$

Calculation of a linear approximation for the zero dynamics (A.1) allows to obtain the corresponding eigenvalues in order to determine the stability of the system. Let $\dot{x}_z = f_z(x_z, t)$ be the zero dynamics system where x_z is the state vector and $f_z(x_z, t)$ is a smooth vector field. The linear approximation $\dot{x}_z = Ax_z$ where A is the Jacobian matrix of the mapping f_z evaluated at $x_z = 0$, yields the following result for the matrix A ,

$$A = \begin{pmatrix} -0.183 & 0 & 0 & 0 & 0 & 0 & 0 \\ 0 & -4.224 & 0 & 0 & 0 & 0 & 0 \\ 0 & 0 & -0.117 & 0 & 0 & 0 & 0 \\ 0 & 0 & 0 & -0.3 & 0 & 0 & 0 \\ 0 & 0 & 0 & -0.0034 & -0.183 & 0 & 0 \\ 0 & 0 & 0 & -0.0154 & 0 & -4.224 & 0 \\ 0 & 0 & 0 & 0.0035 & 0 & 0 & -0.117 \end{pmatrix} \tag{A.2}$$

Due to the system (A.1) has all its eigenvalues in the left-half complex plane the internal dynamics is locally asymptotically stable and system (8.12)-(8.15) is minimum-phase.

Appendix B: Stability analysis for the synchronization error system under the modified feedback control law

Let $e \in R^2$ be the estimation error vector [61] with states given by $e_1 = z_1 - \hat{z}_1$ and $e_2 = \eta - \hat{\eta}$. Then, the dynamics of the estimation error is represented by the following system,

$$\dot{e} = De + (0, \Gamma(z_1, \eta, v, u))^T = \begin{pmatrix} -L_0\kappa_1^* & 1 \\ -L_0^2\kappa_2^* & 0 \end{pmatrix} e + \begin{pmatrix} 0 \\ \Gamma(z_1, \eta, v, u) \end{pmatrix} \quad (\text{B.1})$$

Because of the trajectories of the synchronization error system are contained in a chaotic attractor, the uncertain terms $\eta(t)$ and $\Gamma(z_1, \eta, v, u)$ are bounded functions. Moreover, the matrix D has all its eigenvalues in the left-half complex plane, consequently, the dynamics of the estimation error converges asymptotically to zero for any $L_0 > L_0^* > 0$, and $(\hat{z}_1, \hat{\eta}) \rightarrow (z_1, \eta)$. Therefore, the closed loop system (8.38), (8.40)-(8.42) is asymptotically stable for $L_0 > L_0^* > 0$.

Part III

CONCLUSION

Final conclusion

For the first part of this thesis the main original result is an efficient factorization method for second order ordinary differential equations (ODE) with polynomial nonlinearities. This method allows us to find kink particular solutions for reaction-diffusion (RD) equations and anharmonic oscillator equations. In addition, application of SUSYQM-type factorization techniques allows to find a pair of travelling wave solutions for different RD equations with the same wave velocity. The method is also applied to more complicated second order nonlinear equations with interesting results. We believe that this factorization scheme is easier and more efficient than other employed methods to find exact particular solutions of second order ODE. Exact solutions have been found for differential equations with applications in nonlinear physics and biology, for instance, the generalized and convective Fisher equations, the Duffing-van der Pol oscillator equation and the generalized Burgers-Huxley equation. An application to the biological dynamics of microtubules (MTs) has been developed as a byproduct of supersymmetric procedures. Possible interpretation of our results may be related to the motion of impurities along the MTs or to the structural discontinuities in the arrangement of tubulin molecules. Another interesting result, in the context of applications of supersymmetric factorization procedures in physical systems, is a complex parametric extension of the classical harmonic oscillator. This extension is based on a SUSYQM procedure that has been previously used for Dirac equation in relativistic particle physics. This result may have applications in dissipative (absorptive) processes in physical optics as well as in the physics of cavities. Also, an application to the chemical physics of diatomic molecules using the same supersymmetric factorization scheme is included. As a result an exactly solvable nonhermitic quantum Morse problem is obtained.

In the second part of the thesis it was shown that two noiseless Hodgkin-Huxley (HH) neurons attain synchronized dynamical states when a feedback action is implemented. Because there exist uncertain states that cannot be accurately measured in practice (for instance, the ionic channels activity), a robust approach that guarantees the synchronization of the HH neurons is implemented. Numerical results describing the synchronized behavior of the membrane action potentials of the two neurons are displayed.

Part IV

BIBLIOGRAPHY

Bibliography

- [1] E. Schrödinger, *A method of determining quantum-mechanical eigenvalues and eigenfunctions*, Proc. Roy. Irish Acad. **A 46**, 9 (1940); *Further studies on solving eigenvalue problems by factorization*, Proc. Roy. Irish Acad. **A 46**, 183 (1940).
- [2] B. Mielnik, O. Rosas-Ortiz, *Factorization: little or great algorithm?*, J. Phys. A **37**, 10007 (2004).
- [3] H.C. Rosu, *Short survey of Darboux transformations*, in *Symmetries in Quantum Mechanics and Quantum Optics*, Eds. F.J. Herranz, A. Ballesteros, L.M. Nieto, J. Negro, C.M. Pereña, Servicio de Publicaciones de la Universidad de Burgos, Burgos, Spain, 1999, pp. 301-315 (available on-line, <http://lanl.arXiv.org/quant-ph/9809056>).
- [4] E. Schrödinger, *The factorization of the hypergeometric equation*, Proc. Roy. Irish Acad. **A 47**, 53 (1941) (available at <http://lanl.arXiv.org/physics9910003>).
- [5] P.A.M. Dirac, *Principles of Quantum Mechanics* (Clarendon Press, Oxford, Second Ed., 1935).
- [6] W. Pauli, *On the spectrum of the hydrogen from the standpoint of the new Quantum Mechanics*, Z. Phys. **36**, 336 (1926).
- [7] H. Weyl, *The Theory of Groups and Quantum Mechanics* (E.P. Dotton and Company, Inc., New York, 2nd Ed., 1931), p. 231.
- [8] L. Infeld, T.E. Hull, *The factorization method*, Rev. Mod. Phys. **23**, 21 (1951).
- [9] E. Witten, *Dynamical breaking of supersymmetry*, Nucl. Phys. B **185**, 513 (1981).
- [10] L.E. Gendenshtein, *Derivation of exact spectra of the Schrödinger equation by means of SUSY*, JETP Lett. **38**, 356 (1983).
- [11] B. Mielnik, *Factorization method and new potentials with the oscillator spectrum* J. Math. Phys. **25**, 3387 (1984); D. Fernández, *New hydrogen-like potentials*, Lett. Math. Phys. **8**, 337 (1984); M.M. Nieto, *Relation between SUSY and the inverse method in Quantum Mechanics*, Phys. Lett. B **145**, 208 (1984).

- [12] A.A. Andrianov, N.V. Borisov, M.V. Ioffe, *SUSY mechanics: A new look at the equivalence of quantum systems*, *Theor. Math. Phys.* **61**, 965 (1984).
- [13] V. Matveev, M. Salle, *Darboux Transformations and Solitons* (Springer, 1991).
- [14] J. Delsarte, *On some functional transformations relative to linear PDE's of second order*, *Comp. Rend. Acad. Sci. (Paris)* **206**, 1780 (1938) (available on-line at <http://lanl.arXiv.org/physics/9909061>).
- [15] Yu F. Smirnov, *Factorization method: new aspects*, *Rev. Mex. Fís.* **45** (S2), 1 (1999).
- [16] J.A. Tuszynski, M. Otwinowski, J.M. Dixon, *Spiral-pattern formation and multistability in Landau-Ginzburg systems*, *Phys. Rev. B* **44**, 9201 (1991).
- [17] L.M. Berkovich, *Factorization as a method of finding exact invariant solutions of the Kolmogorov-Petrovskii-Piskunov equation and the related Semenov and Zel'dovich equations*, *Sov. Math. Dokl.* **45**, 162 (1992).
- [18] X.Y. Wang, *Exact and explicit solitary wave solutions for the generalized Fisher equations*, *Phys. Lett. A* **131**, 277 (1988); P. Kaliappan, *An exact solution for travelling waves of $u_t = Du_{xx} + u - u^k$* , *Physica D* **11**, 368 (1984).
- [19] W. Hereman, M. Takaoka, *Solitary wave solutions of nonlinear evolution and wave equations using a direct method and MACSYMA*, *J. Phys. A* **23**, 4805 (1990).
- [20] S. Portet, J.A. Tuszynski, J.M. Dixon, *Models of spatial and orientational self-organization of microtubules under the influence of gravitational fields*, *Phys. Rev. E* **68**, 021903 (2003); J. Tabony, *Morphological bifurcations involving reaction-diffusion processes during microtubule formation*, *Science* **264**, 245 (1994).
- [21] M. Ablowitz, A. Zeppetella, *Explicit solutions of Fisher's equation for special wave speed*, *Bull. Math. Biol.* **41**, 835 (1979).
- [22] J.M. Dixon, J.A. Tuszynski, M. Otwinowski, *Special analytical solutions of the damped-anharmonic-oscillator equation*, *Phys. Rev. A* **44**, 3484 (1991).
- [23] P.C. Bressloff, G. Rowlands, *Exact travelling wave solutions of an "integrable" discrete reaction-diffusion equation*, *Physica D* **106**, 255 (1997); J.C. Comte, P. Marquié, M. Remoissenet, *Dissipative lattice model with exact travelling discrete kink-soliton solutions: Discrete breather generation and reaction-diffusion regime*, *Phys. Rev. E* **60**, 7484 (1999).
- [24] H.C. Rosu, O. Cornejo-Pérez, *Supersymmetric pairing of kinks for polynomial nonlinearities*, *Phys. Rev. E* **71**, 046607 (2005).
- [25] V.K. Chandrasekar, M. Senthilvelan, M. Lakshmanan, *New aspects of integrability of force-free Duffing-van der Pol oscillator and related nonlinear systems*, *J. Phys. A* **37**, 4527 (2004).
- [26] O. Schönborn, R.C. Desai, D. Stauffer, *Nonlinear bias and the convective Fisher equation*, *J. Phys. A* **27**, L251 (1994); O. Schönborn, S. Puri, R.C. Desai, *Singular perturbation analysis for unstable systems with convective nonlinearity*, *Phys. Rev. E* **49**, 3480 (1994).
- [27] X.Y. Wang, Z.S. Zhu, Y.K. Lu, *Solitary wave solutions of the generalized Burgers-Huxley equation*, *J. Phys. A* **23**, 271 (1990).

- [28] See, e.g., N.E. Mavromatos, A. Mershin, D.V. Nanopoulos, *QED-Cavity model of microtubules implies dissipationless energy transfer and biological quantum teleportation*, Int. J. Mod. Phys. B **16**, 3623 (2002).
- [29] M.A. Collins, A. Blumen, J.F. Currie, J. Ross, *Dynamics of domain walls in ferrodistorive materials. I. Theory*, Phys. Rev. B **19**, 3630 (1979).
- [30] M.V. Satarić, J.A. Tuszyński, R.B. Žakula, *Kinklike excitations as an energy-transfer mechanism in microtubules*, Phys. Rev. E **48**, 589 (1993).
- [31] J.A. Tuszyński, S. Hameroff, M.V. Satarić, B. Trpišová, M.L.A. Nip, *Ferroelectric behavior in microtubule dipole lattices: implications for information processing, signaling and assembly/disassembly*, J. Theor. Biol. **174**, 371 (1995).
- [32] E.W. Montroll, in *Statistical Mechanics*, ed. by S.A. Rice, K.F. Freed, J.C. Light (Univ. of Chicago, Chicago, 1972).
- [33] H.C. Rosu, *Microtubules: Montroll's kink and Morse vibrations*, Phys. Rev. E **55**, 2038 (1997).
- [34] A. Caticha, *Construction of exactly soluble double-well potentials*, Phys. Rev. A **51**, 4264 (1995).
- [35] E.D. Filho, *The Morse oscillator generalized from supersymmetry*, J. Phys. A **21**, L1025 (1988).
- [36] M. Bentaiba, L. Chetouni, T.F. Hammann, *Feynman-Kleinert treatment of the supersymmetric generalization of the Morse potential*, Phys. Lett. A **189**, 433 (1994).
- [37] T. Cheon and T. Shigehara, *Realizing discontinuous wave functions with generalized short-range potentials*, Phys. Lett. A **243**, 111 (1998). I. Tsutsui, T. Fülöp, T. Cheon, *Connection conditions and the spectral family under singular potentials*, J. Phys. A **36**, 275 (2003). T. Cheon, *Quantum contact interactions*, Pramana J. Phys. **59**, 311 (2002).
- [38] T. Fülöp, I. Tsutsui, T. Cheon, *Spectral properties on a circle with a singularity*, J. Phys. Soc. Jpn. **72**, 2737 (2003).
- [39] B. Trpišová and J.A. Tuszyński, *Possible link between guanosine 5' triphosphate hydrolysis and solitary waves in microtubules*, Phys. Rev. E **55**, 3288 (1997).
- [40] H.C. Rosu, M.A. Reyes, *Riccati parameter modes from Newtonian free damping motion by supersymmetry*, Phys. Rev. E **57**, 4850 (1998).
- [41] T. Jacobson, *On the origin of the outgoing black-holes modes*, Phys. Rev. D **53**, 7082 (1996).
- [42] F. Cooper, A. Khare, R. Musto, A. Wipf, *Supersymmetry and the Dirac equation*, Ann. Phys. **187**, 1 (1988). See also, C.V. Sukumar, *SUSY and the Dirac equation for a central Coulomb field*, J. Phys. A **18**, L697 (1985); R.J. Hughes, V.A. Kostelecký, M.M. Nieto, *SUSY quantum mechanics in a first-order Dirac equation*, Phys. Rev. D **34**, 1100 (1986).
- [43] Y. Nogami, F.M. Toyama, *Supersymmetry aspects of the Dirac equation in one dimension with a Lorentz scalar potential*, Phys. Rev. A **47**, 1708 (1993); M. Bellini, R.R. Deza, R. Montemayor, *Maqueo en una mecánica cuántica SUSY para la ecuación de Dirac en $D=1+1$* , Rev. Mex. Fís. **42**, 209 (1996); B. Goodman, S.R. Ignjatović, A

- simpler solution of the Dirac equation in a Coulomb potential*, Am. J. Phys. **65**, 214 (1997) and references therein.
- [44] S.M. Chumakov, K.B. Wolf, *Supersymmetry in Helmholtz optics*, Phys. Lett. A **193**, 51 (1994); E.V. Kurmyshev, K.B. Wolf, "Squeezed states" in *Helmholtz optics*, Phys. Rev. A **47**, 3365 (1993); See also, A. Angelow, *Light propagation in nonlinear waveguide and classical two-dimension oscillator*, Physica A **256**, 485 (1998).
- [45] J.D. Jackson, *Classical Electrodynamics*, Section 8.9, 3d Edition (Wiley & Sons, 1999); M.F. Ciappina, M. Febbo, *Schumann's resonances: A particular example of a spherical resonant cavity*, Am. J. Phys. **72**, 704 (2004).
- [46] F.L. Scarf, *New soluble energy band problem*, Phys. Rev. **112**, 1137 (1958).
- [47] H.C. Rosu, R. López-Sandoval, *Barotropic FRW cosmologies with a Dirac-like parameter*, Mod. Phys. Lett. A **19**, 1529 (2004).
- [48] M.V. Berry, D.H.J. O'Dell, *Diffraction by volume gratings with imaginary potentials*, J. Phys. A **31**, 2093 (1998); M.K. Oberthaler et al., *Dynamical diffraction of atomic matter waves by crystals of light*, Phys. Rev. A **60**, 456 (1999).
- [49] H.C. Rosu, O. Cornejo-Pérez, R. López-Sandoval, *Classical harmonic oscillator with Dirac-like parameters and possible applications*, J. Phys. A **37**, 11699 (2004).
- [50] A.C. Scoot, *Electrophysics of a nerve fiber*, Rev. Mod. Phys. **47**, 487 (1975). pp. 509-514.
- [51] V.A. Simpao, *Travelling-wave solutions of a modified Hodgkin-Huxley type neural model via novel analytical results for nonlinear transmission lines with arbitrary $I(V)$ characteristics*, Electronic J. of Diff. Eq., Conference 02, 133 (1999). Also available at <http://ejde.math.swt.edu>
- [52] C.B. Muratov, *A quantitative approximation scheme for the travelling wave solutions in the Hodgkin-Huxley model*, Biophys. J. **79**, 2893 (2000).
- [53] N. Goldenfeld, Phys. Today **57**, 59 (2004). S. Strogatz, *Sync: The Emerging Science of Spontaneous Order* (Hyperion, New York, 2003).
- [54] S. Boccaletti, C. Grebogi, Y.-C. Lai, H. Mancini, D. Maza, *The control of chaos: Theory and applications*, Phys. Rep. **329**, 103 (2000).
- [55] B.R. Andrievskii, A.L. Fradkov, *Control of chaos: Methods and applications. I. Methods*, Aut. Rem. Control **64**, 673 (2003).
- [56] B.R. Andrievskii, A.L. Fradkov, *Control of chaos: Methods and applications. II. Applications*, Aut. Rem. Control **64**, 673 (2003).
- [57] R. Femat, R. Jauregui-Ortiz, G. Solís-Perales, *A chaos-based communication scheme via robust asymptotic feedback*, IEEE Trans. Circuits Syst. I, **48**, 1161 (2001).
- [58] A. Isidori, *Nonlinear Control Systems* (Springer-Verlag, London, UK, 1995).
- [59] R. Femat, G. Solís-Perales, *On the chaos synchronization phenomena*, Phys. Lett. A **262**, 50 (1999).
- [60] L.M. Pecora, T.L. Carrol, *Synchronization in chaotic systems*, Phys. Rev. Lett. **64**, 821 (1990).

- [61] R. Femat, J. Alvarez-Ramírez, G. Fernández-Anaya, *Adaptive synchronization of high-order chaotic systems: a feedback with low-order parametrization*, *Physica D* **139**, 231 (2000).
- [62] C.M. Gray, W. Singer, *Stimulus-specific neuronal oscillations in the cat visual cortex: a cortical functional unit*, *Soc. Neurosci. Abstr.* **404**, 3 (1987). C.M. Gray, P. Konig, A.K. Engel, W. Singer, *Oscillatory responses in cat visual cortex exhibit intercolumnar synchronization which reflects global stimulus properties*, *Nature* **338**, 334 (1989).
- [63] H. Haken, *Brain Dynamics, Synchronization and Activity Patterns in Pulse-Coupled Neural Nets with Delays and Noise* (Springer-Verlag, Berlin, 2002), and references therein.
- [64] J. Wakefield, *A mind for consciousness*, *Sci. American* **285**, 26 (2001).
- [65] G.M. Edelman, G. Tononi, *El Universo de la Conciencia* (Ed. Crítica, Barcelona, 2002).
- [66] E. Rodriguez, N. George, J.P. Lachaux, J. Martinerie, B. Renault, F.J. Varela, *Perception's shadows: long-distance synchronization of human brain activity*, *Nature* **397**, 430 (1999).
- [67] T.I. Netoff, *Decreased neuronal synchronization during experimental seizures*, *J. Neurosci.* **22**, 7297 (2002).
- [68] R.C. Elson, A.I. Selverston, R. Huerta, N.F. Rulkov, M.I. Rabinovich, H.D. Abarbanel, *Synchronous behavior of two coupled biological neurons*, *Phys. Rev. Lett.* **87**, 5692 (1999).
- [69] A.L. Hodgkin, A.F. Huxley, *A quantitative description of membrane current and its application to conduction and excitation in nerve*, *J. Physiol. (London)* **117**, 500 (1952).
- [70] C. Koch, *Biophysics of Computation: Information Processing in Single Neurons* (Oxford University Press, New York, 1998).
- [71] C.M. Gray, P. Konig, A.K. Engel, W. Singer, *Oscillatory responses in cat visual cortex exhibit intercolumnar synchronization which reflects global stimulus properties*, *Nature* **338**, 334 (1989).
- [72] M. Meister, R.O.L. Wong, D.A. Baylor, C.J. Shatz, *Synchronous bursts of action potentials in ganglion cells of the developing mammalian retina*, *Science* **252**, 939 (1991).
- [73] A.K. Kreiter, W. Singer, *Stimulus-dependent synchronization of neuronal responses in the visual cortex of the awake macaque monkey*, *J. Neurosci.* **16**, 2381 (1996).
- [74] R.C. Elson, A.I. Selverston, R. Huerta, N.F. Rulkov, M.I. Rabinovich, H.D. Abarbanel, *Synchronous behavior of two coupled biological neurons*, *Phys. Rev. Lett.* **87**, 5692 (1999).
- [75] J.M. Casado, *Synchronization of two Hodgkin-Huxley neurons due to internal noise*, *Phys. Lett. A* **310**, 400 (2003).
- [76] J.M. Casado, J.P. Baltanás, *Phase switching in a system of two noisy Hodgkin-Huxley neurons coupled by a diffusive interaction*, *Phys. Rev. E* **68**, 061917 (2003).

- [77] X.J. Wang, *Pacemaker neurons for the theta rhythm and their synchronization in the septohippocampal reciprocal loop*, J. Neurophysiol. **87**, 889 (2002).
- [78] C.D. Acker, N. Kopell, J.A. White, *Synchronization of strongly coupled excitatory neurons: Relating network behavior to biophysics*, J. Comput. Neurosci. **15**, 71 (2003).
- [79] G.B. Ermentrout, N. Kopell, *Fine structure of neural spiking and synchronization in the presence of conduction delays*, Proc. Natl. Acad. Sci. **95**, 1259 (1998).
- [80] Y. Yu, W. Wang, J. Wang, F. Liu, *Resonance-enhanced signal detection and transduction in the Hodgkin-Huxley neuronal systems*, Phys. Rev. E **63**, 21907 (2001).
- [81] P. Parmananda, C.H. Mena, G. Baier, *Resonant forcing of a silent Hodgkin-Huxley neuron*, Phys. Rev. E **66**, 47202 (2002).
- [82] W. Wang, Y. Wang, Z.D. Wang, W. Wang, *Firing and signal transduction associated with an intrinsic oscillation in neuronal systems*, Phys. Rev. E **57**, 2527 (1998).
- [83] S. Lee, A. Neiman, A. Kim, *Coherence resonance in a Hodgkin-Huxley neuron*, Phys. Rev. E **57**, 3292 (1998).
- [84] S. Tanabe, S. Sato, K. Pakdaman, *Response of an ensemble of noisy neuron models to a single input*, Phys. Rev. E **60**, 7235 (1999).
- [85] U. Parlitz, L. Junge, L. Kocarev, *Subharmonic entrainment of unstable period orbits and generalized synchronization*, Phys. Rev. Lett. **79**, 3158 (1997).
- [86] R. Femat, J. Alvarez-Ramírez, *Synchronization of a class of strictly different chaotic oscillators*, Phys. Lett. A **236**, 307 (1997).
- [87] S. Bowong, F.M.M. Kakmeni, *Chaos control and duration time of a class of uncertain chaotic systems*, Phys. Lett. A **316**, 196 (2003).